

this document downloaded from

# vulcanhammer.info

the website about  
Vulcan Iron Works  
Inc. and the pile  
driving equipment it  
manufactured

Visit our companion site  
<http://www.vulcanhammer.org>

## Terms and Conditions of Use:

All of the information, data and computer software ("information") presented on this web site is for general information only. While every effort will be made to insure its accuracy, this information should not be used or relied on for any specific application without independent, competent professional examination and verification of its accuracy, suitability and applicability by a licensed professional. Anyone making use of this information does so at his or her own risk and assumes any and all liability resulting from such use. The entire risk as to quality or usability of the information contained within is with the reader. In no event will this web page or webmaster be held liable, nor does this web page or its webmaster provide insurance against liability, for any damages including lost profits, lost savings or any other incidental or consequential damages arising from the use or inability to use the information contained within.

This site is not an official site of Prentice-Hall, Pile Buck, or Vulcan Foundation Equipment. All references to sources of software, equipment, parts, service or repairs do not constitute an endorsement.

**RECALIBRATION OF THE  
GRLWEAP LRFD RESISTANCE  
FACTOR FOR OREGON DOT**

**Final Report**

**SPR 683**



**RECALIBRATION OF THE GRLWEAP LRFD RESISTANCE  
FACTOR FOR OREGON DOT**

**Final Report**

**SPR 683**

by

Trevor Smith, Ph.D., P.E., Andrew Banas, Max Gummer, and Jaesup Jin  
Civil and Environmental Engineering  
Portland State University  
Portland, OR 97207

for

Oregon Department of Transportation  
Research Section  
200 Hawthorne Ave. SE, Suite B-240  
Salem OR 97301-5192

and

Federal Highway Administration  
400 Seventh Street, SW  
Washington, DC 20590-0003

**February 2011**



1. Report No. FHWA-OR-RD-11-08		2. Government Accession No.		3. Recipient's Catalog No.	
4. Title and Subtitle Recalibration of the GRLWEAP LRFD Resistance Factor for Oregon DOT				5. Report Date February 2011	
				6. Performing Organization Code	
7. Author(s) Trevor D. Smith, PhD. PE, Andrew Banas, Max Gummer, Jaesup Jin				8. Performing Organization Report No.	
9. Performing Organization Name and Address Department of Civil and Environmental Engineering Portland State University PO Box 751 Portland, OR 97207				10. Work Unit No. (TRAIS)	
				11. Contract or Grant No. SPR 683	
12. Sponsoring Agency Name and Address Oregon Department of Transportation Research Section 200 Hawthorne Ave. SE, Suite B-240 Salem, OR 97301-5192 and Federal Highway Administration 400 Seventh Street, SW Washington, DC 20590-0003				13. Type of Report and Period Covered Final Report	
				14. Sponsoring Agency Code	
15. Supplementary Notes					
16. Abstract  <p>The Bridge Section of the Oregon Department of Transportation (ODOT) is responsible for the design of all bridge structures and routinely uses GRLWEAP for controlling pile driving stresses and establishing capacity from the bearing graph. The LRFD resistance factor, <math>\phi</math>, for GRLWEAP sets the factored amount of nominal capacity in the LRFD inequality. Foundation conditions throughout Oregon's Willamette Valley and the Portland metropolitan area are predominantly sand, silt, and clay. Steel pipe and H section foundation piles typically are of sufficient length to be friction piles and exhibit set-up after the end of initial driving (EOID). The two objectives of this study were to build an extensive database of driven pile case histories to include restrike conditions from the present available sources that reflect ODOT's diverse soils and piles, and to establish <math>\phi</math> factors for EOID and beginning of restrike (BOR) conditions using GRLWEAP to match ODOT practice.</p> <p>A diverse group of existing databases, including the FHWA-built <i>DFLTD</i> and NCHRP 507 <i>PDLT2000</i>, were accessed and merged with new cases from the literature to build a comprehensive database, called the <i>Full PSU Master</i>. Neither of these two national databases proved always correct for the large amount of source input required, with the largest source of anomalies and missing data being the blow count, especially at the BOR condition. Over 150 new cases were added to establish the <i>Full PSU Master</i> database containing 322 piles, with each case placed into one of three input tiers for statistical profiling to assist in preserving quality for the <math>\phi</math> calibration. The <i>Full PSU Master</i> database then supplied 179 cases analyzed by FHWA static capacity software DRIVEN and by GRLWEAP for capacity prediction by the bearing graph. These predictions generated bias mean <math>\lambda</math> and COV statistics for a range of ODOT selected scenarios. The 322 piles ranged up to 40 inches in diameter, and up to 197 ft in embedment length. The 179 analyzed piles ranged up to 36 inches in diameter and 167 ft in embedment length and had driving blow counts up to 100 BPI. This research showed similar trends for GRLWEAP capacity as that reported in NCHRP 507 for CAPWAP capacity on the statistical effects from variables such as blow count ranges. Sub-grouping <math>\lambda</math> by blow count revealed a clear decay in easy driving mean <math>\lambda</math> and COV parameters when blow counts were <math>\leq 2</math> BPI. Above 2 BPI, little difference was found in these parameters, and no upper limit of statistical accuracy was identified. A clear difference in statistical sample characteristics existed between piles supported in predominately cohesive soils to those in cohesionless soils, and also between pile types.</p> <p>For the ODOT case of redundant piles in groups, a reliability index <math>\beta</math> at 2.33 was used to establish <math>\phi</math> resistance factors and <math>\phi/\lambda</math> efficiency measures. Statistics for an initial ten scenarios were generated, and the First Order Second Moment (FOSM) resistance factor at EOID and BOR was reported, based on lognormal fits to the <math>\lambda</math> distribution. The final five ODOT selected scenarios to permit comparison to NCHRP 507 and to form a basis to design implementation measures underwent advanced Monte Carlo based probabilistic procedures using random number generation and the <math>\lambda</math> lognormal tail fits to provide EOID and BOR <math>\phi</math> factors. Recommended resistance factors from the visual tail fit procedure on the likely best fit to ODOT practice scenario containing all soil and pile types were 0.55 and 0.4 for EOID and BOR respectively. Recommendations were made for a separate implementation activity, including additional <math>\phi</math> calibration work based on the <i>Full PSU Master</i> including use of field measured hammer performance, CAPWAP based soil input parameters, and pile type.</p>					
17. Key Words Driven piles, GRLWEAP, LRFD, resistance factor, database, calibration, soil, DFLTD, NCHRP507, pile blow counts			18. Distribution Statement Copies available from NTIS, and online at <a href="http://www.oregon.gov/ODOT/TD/TP_RES/">http://www.oregon.gov/ODOT/TD/TP_RES/</a>		
19. Security Classification (of this report) Unclassified		20. Security Classification (of this page) Unclassified		21. No. of Pages 92 + appendices	
				22. Price	

## SI\* (MODERN METRIC) CONVERSION FACTORS

### APPROXIMATE CONVERSIONS TO SI UNITS

Symbol	When You Know	Multiply By	To Find	Symbol
<b><u>LENGTH</u></b>				
in	inches	25.4	millimeters	mm
ft	feet	0.305	meters	m
yd	yards	0.914	meters	m
mi	miles	1.61	kilometers	km
<b><u>AREA</u></b>				
in <sup>2</sup>	square inches	645.2	millimeters squared	mm <sup>2</sup>
ft <sup>2</sup>	square feet	0.093	meters squared	m <sup>2</sup>
yd <sup>2</sup>	square yards	0.836	meters squared	m <sup>2</sup>
ac	acres	0.405	hectares	ha
mi <sup>2</sup>	square miles	2.59	kilometers squared	km <sup>2</sup>
<b><u>VOLUME</u></b>				
fl oz	fluid ounces	29.57	milliliters	ml
gal	gallons	3.785	liters	L
ft <sup>3</sup>	cubic feet	0.028	meters cubed	m <sup>3</sup>
yd <sup>3</sup>	cubic yards	0.765	meters cubed	m <sup>3</sup>
NOTE: Volumes greater than 1000 L shall be shown in m <sup>3</sup> .				
<b><u>MASS</u></b>				
oz	ounces	28.35	grams	g
lb	pounds	0.454	kilograms	kg
T	short tons (2000 lb)	0.907	megagrams	Mg
<b><u>TEMPERATURE (exact)</u></b>				
°F	Fahrenheit	(F-32)/1.8	Celsius	°C

### APPROXIMATE CONVERSIONS FROM SI UNITS

Symbol	When You Know	Multiply By	To Find	Symbol
<b><u>LENGTH</u></b>				
mm	millimeters	0.039	inches	in
m	meters	3.28	feet	ft
m	meters	1.09	yards	yd
km	kilometers	0.621	miles	mi
<b><u>AREA</u></b>				
mm <sup>2</sup>	millimeters squared	0.0016	square inches	in <sup>2</sup>
m <sup>2</sup>	meters squared	10.764	square feet	ft <sup>2</sup>
m <sup>2</sup>	meters squared	1.196	square yards	yd <sup>2</sup>
ha	hectares	2.47	acres	ac
km <sup>2</sup>	kilometers squared	0.386	square miles	mi <sup>2</sup>
<b><u>VOLUME</u></b>				
ml	milliliters	0.034	fluid ounces	fl oz
L	liters	0.264	gallons	gal
m <sup>3</sup>	meters cubed	35.315	cubic feet	ft <sup>3</sup>
m <sup>3</sup>	meters cubed	1.308	cubic yards	yd <sup>3</sup>
<b><u>MASS</u></b>				
g	grams	0.035	ounces	oz
kg	kilograms	2.205	pounds	lb
Mg	megagrams	1.102	short tons (2000 lb)	T
<b><u>TEMPERATURE (exact)</u></b>				
°C	Celsius	1.8C+32	Fahrenheit	°F

\*SI is the symbol for the International System of Measurement

## **ACKNOWLEDGEMENTS**

The authors of this report wish to thank all those individuals and agencies that have generously shared data, expertise, and time during the course of this research. The contributions of undergraduate students Jane Wallis and Jaclyn Schaefer were invaluable on the research team. Special thanks go to the members of the Technical Advisory Committee: Jan Six, Thomas Braibish, and Steve Soltesz of ODOT, Tony Allen of WSDOT, Robert Miner of Robert Miner Dynamic Testing, Inc., and Dr. Naser Abu-Hejleh of FHWA. Their collective input, experience, and willingness to review the research progress and results contributed greatly to its success.

A debt of thanks goes to all of those who assisted by providing new case histories and/or by supplying data to resolve case history anomalies, including: Eric Thibodeau (NHDOT), Jay Wang (LADOT), Mark Morvant (LADOT), Jeffrey Sizemore (SCDOT), Tom Shantz (CALTRANS), Jeffrey Horsfell (WISDOT), Larry Jones (FLDOT), Darrin Beckett (KYDOT), Dave Dundas (Ontario Ministry of Transportation), Lynn C. Doyle (Geotechnical Engineering Testing, Inc.), Houston Walker (TNDOT), Jim Scott (URS CORP), Erik Tørum (Multiconsult) and Denise Whelan (MMSD). Special thanks are owed to those contributors who unselfishly shared valuable databases: Prof. James Long (Univ. of Illinois), Prof. Mike McVay (Univ. of Florida), and Prof. Roy Olson (Univ. of Texas). Also thanks to Professors Kyle Rollins and Steve Bartlett, Dr. Mike Hollaway, and Dr. Bengt Fellenius.

Finally, much praise is due to Judy Fox and Beth Richardson at GRL, Inc. for their help in supplying biannually the correct versions of GRLWEAP. And to Elise Smith for her diligence, fortitude, and attention to detail above and beyond the call in editing and proofing.

## **DISCLAIMER**

This document is disseminated under the sponsorship of the Oregon Department of Transportation and the United States Department of Transportation in the interest of information exchange. The State of Oregon and the United States Government assume no liability of its contents or use thereof.

The contents of this report reflect the view of the authors who are solely responsible for the facts and accuracy of the material presented. The contents do not necessarily reflect the official views of the Oregon Department of Transportation or the United States Department of Transportation.

The State of Oregon and the United States Government do not endorse products of manufacturers. Trademarks or manufacturers' names appear herein only because they are considered essential to the object of this document.

This report does not constitute a standard, specification, or regulation.





# RECALIBRATION OF THE GRLWEAP LRFD RESISTANCE FACTOR FOR OREGON DOT

## TABLE OF CONTENTS

<b>1.0 INTRODUCTION.....</b>	<b>1</b>
1.1 OVERVIEW AND NCHRP 507 .....	1
1.1.1 Overview .....	1
1.1.2 The NCHRP 507 Report.....	3
1.2 BACKGROUND AND PHASE 1 STUDY .....	4
1.2.1 GRLWEAP.....	6
1.3 ODOT LRFD ISSUES IN PRACTICE .....	8
1.4 FIRST ORDER SECOND MOMENT AND MONTE CARLO METHODS.....	9
<b>2.0 DRIVEN AND GRLWEAP SOFTWARE.....</b>	<b>13</b>
2.1 DRIVEN APPLICATION RULES.....	13
2.2 GRLWEAP APPLICATION PROCEDURES .....	15
2.2.1 Overview .....	15
2.2.2 GRLWEAP application.....	15
<b>3.0 PSU DATABASE DEVELOPMENT .....</b>	<b>21</b>
3.1 SOURCES.....	21
3.1.1 The PDLT2000.....	21
3.1.2 The FHWA DFLTD Database.....	22
3.1.3 Other Databases.....	23
3.1.4 Other Sources .....	24
3.2 FULL PSU MASTER DATABASE.....	24
3.2.1 Input Quality Tier.....	25
3.2.2 Case Histories Overview .....	28
3.3 CASE HISTORY ANOMALIES AND ERRORS .....	30
3.4 SUBSURFACE INFORMATION, QUALITY, AND INTERPRETATION.....	33
<b>4.0 BEARING CAPACITY METHODOLOGY .....</b>	<b>35</b>
4.1 EOID AND BOR MODELING AND BLOW COUNTS.....	35
4.2 OUTPUT RANKING .....	36
4.3 GENERAL SENSITIVITY COMMENTS.....	37
4.4 PILE BLOW COUNTS .....	38
<b>5.0 STATISTICAL PROFILING OF RESULTS .....</b>	<b>41</b>
5.1 REANALYSES OF NCHRP 507 CASE HISTORY SET.....	41
5.2 FULL POPULATION SAMPLE ANALYSIS.....	42
5.3 SCENARIO DEVELOPMENT .....	47
5.4 DISTRIBUTION TESTING.....	49

<b>6.0 OUTLIER EXAMINATION .....</b>	<b>51</b>
6.1 INPUT TIER AND OUTPUT RANK .....	51
6.2 BLOW COUNT INVESTIGATION .....	53
6.3 TIME TO RESTRIKE AND TIME TO LOAD TEST INVESTIGATIONS.....	56
<b>7.0 RESISTANCE FACTOR DEVELOPMENT .....</b>	<b>59</b>
7.1 FIRST ORDER SECOND MOMENT (FOSM) $\Phi$ .....	59
7.2 ODOT SCENARIOS AND MONTE CARLO RELIABILITY $\Phi$ .....	62
7.3 LRFD FACTORED CAPACITY OPTIMIZATION.....	67
<b>8.0 CONCLUSIONS AND RECOMMENDATIONS.....</b>	<b>71</b>
8.1 CONCLUSIONS.....	71
8.2 RECOMMENDATIONS AND FUTURE WORK.....	75
<b>9.0 REFERENCES.....</b>	<b>79</b>

**APPENDICES**

APPENDIX A: <i>FULL PSU MASTER DATABASE</i>	
APPENDIX B: LOGNORMAL DISTRIBUTION EOID/BOR STATISTICAL CHECKS FOR SCENARIO A, F, G, AND I (BOR)	
APPENDIX C: SCENARIO A STATISTICAL EOID/BOR PDF AND CDF PLOTS	
APPENDIX D: SCENARIO F STATISTICAL EOID/BOR PDF AND CDF PLOTS	
APPENDIX E: SCENARIO G STATISTICAL EOID/BOR PDF AND CDF PLOTS	
APPENDIX F: SCENARIO I STATISTICAL EOID/BOR PDF AND CDF PLOTS	

**List of Tables**

Table 1.1: Recommended resistance factors from NCHRP 507.....	2
Table 2.1: Acceptable damping factors for variable soil layers .....	17
Table 3.1: Pile case histories in PDLT2000 by pile type and driving time .....	22
Table 3.2: Source of data for pile case histories for resolution of errors and anomalies .....	25
Table 3.3: Summary of the input tier rubric utilized for analysis .....	26
Table 3.4: Geographic distribution of Full PSU Master pile case histories .....	28
Table 3.5: Breakdown of all 322 piles in the Full PSU Master by pile and soil type.....	30
Table 3.6: Number of piles and anomalies found in the 156 from <i>PSU PDLT2000 Master</i> .....	31
Table 4.1: Summary of output ranking requirements .....	36
Table 5.1: Comparison between NCHRP 507, PSU matched piles, and all analyzed 179 piles in the Full PSU Master.....	41
Table 5.2: Statistical characteristics for GRLWEAP based capacity of the 175 qualified cases by soil and pile type* .....	45
Table 5.3: Base statistics for Scenarios A-H compared to NCHRP 507* .....	48
Table 6.1: Statistical breakdown of Tier 1, Tiers 1 & 2a, and Tiers 1 & 2 for EOID and BOR .....	51
Table 6.2: Top input Tier 1 & 2a statistical breakdown by soil and pile type* .....	52
Table 6.3: Top output ranks 1 & 2 statistical breakdown by soil and pile type* .....	53
Table 6.4: Blow count ranges for EOID and BOR in Full PSU Master .....	55
Table 6.5: Pile counts complying with current AASHTO and ODOT TR and TST times .....	56
Table 7.1: Statistical load parameters used for calibration .....	60
Table 7.2: FOSM resistance values and efficiencies for $\beta=2.33$ and $\beta=3.0$ .....	61

## List of Figures

Figure 1.1: Example of a GRLWEAP bearing graph.....	7
Figure 1.2: Probability of failure and reliability index ( <i>William, et al. 1998</i> ).....	10
Figure 2.1: Example of DRIVEN provided soil resistance to GRLWEAP.....	16
Figure 3.1: Growth of cases in the Full PSU Master by input tier.....	27
Figure 3.2: Distribution of Full PSU Master pile case histories worldwide.....	28
Figure 3.3: Number of pile case histories in <i>Full PSU Master</i> by state.....	29
Figure 3.4: Source of <i>Full PSU Master</i> pile case histories by region.....	29
Figure 3.5: Source of anomalies between databases for <i>Full PSU Master</i> .....	32
Figure 4.1: PSU Case History #293 - effects to the bearing graph of stiffer restrrike cushion.....	35
Figure 4.2: Illustration of <i>DFLTD</i> presentation in digital feet for restrrike.....	39
Figure 5.1: Predicted BOR capacity to predicted EOID capacity from GRLWEAP.....	42
Figure 5.2: Frequency of set-up ratio in the Full PSU Master.....	44
Figure 5.3: EOID $\lambda$ histogram.....	46
Figure 5.4: BOR $\lambda$ histogram.....	46
Figure 5.5: Lognormal distribution fit to Scenario A at EOID.....	50
Figure 6.1: All EOID and BOR qualified 175 $\lambda$ values plotted to blow count by soil type.....	54
Figure 6.2: All EOID and BOR qualified 175 $\lambda$ values plotted to blow count in 2 BPI intervals.....	55
Figure 6.3: Restrike and load test time ratios by soil type.....	57
Figure 6.4: Restrike and load test time ratios by pile type.....	57
Figure 7.1: Scenario A Monte Carlo reliability method CDF fits at EOID.....	64
Figure 7.2: Factored BOR plotted to factored EOID for Scenario A.....	68
Figure 7.3: Factored BOR plotted to factored EOID for Scenario F.....	68
Figure 7.4: Factored BOR plotted to factored EOID for Scenario G.....	69
Figure 7.5: Set-up implementation on cohesive soils factored BOR Scenario I to factored EOID for Scenario G.....	70
Figure 7.6: Set-up implementation on cohesionless soil factored BOR Scenario J to factored EOID for Scenario G.....	70



# 1.0 INTRODUCTION

## 1.1 OVERVIEW AND NCHRP 507

### 1.1.1 Overview

In Oregon, the Bridge Section of the Oregon Department of Transportation (ODOT) is responsible for satisfactory design, based on current standards of practice, of all bridge structures, including bridge foundations, within the state's highway system. The Bridge Section also plays a significant leadership role in the distribution and implementation of new and emerging bridge technologies. For implementation of Load Resistance Factor Design (LRFD) reliability-based principles for bridge foundations, the American Association of State Highway and Transportation Officials (AASHTO) and the Federal Highway Administration (FHWA) require LRFD adoption through the AASHTO bridge design code. The LRFD reliability-based principles created a precedent in the areas of driven pile foundation policy and implementation from national load test databases to fit highly regionalized "standards of practice." The widespread adoption by the nation's departments of transportation (DOTs) of geotechnical LRFD principles, specified in the AASHTO code, has been difficult in the case of deep foundations. Difficulty around LRFD principles for driven pile design, including resistance reduction factors (called  $\phi$  resistance factors) for dynamic methods, has caused multiple and local implementation concerns. These have led to successive revisions to the AASHTO code, and a fourth edition was subsequently released (*AASHTO 2007*). The AASHTO Bridge Design Specification, 2006 Interim Revision drew heavily from the work performed for both drilled shafts and driven pile foundations by the National Cooperative Highway Research Program (NCHRP), referred to hereafter as NCHRP 507 (*Paikowsky 2004*).

The well-known Wave Equation of Pile driving (GRLWEAP<sup>1</sup>) software (*Pile Dynamics, Inc. 2005*) calculates the induced stress and displacement waves traveling along the pile for a single hammer blow. The program computes the pile blow count, axial stresses in the pile and transferred energy from the hammer for each capacity analyzed. The program then allows the user to indirectly determine bearing capacity at the time of driving or restrrike using observed blow count. In the most recent version, GRLWEAP features include improved set-up models, as well as use of the pile static capacity DRIVEN software code (*Mathias and Cribbs 1998*) for soil resistance distribution. The Phase 1 portion of this research effort for ODOT (*Smith and Dusicka 2009*), included a survey of Northwest state DOT's current pile field acceptance practice relating to GRLWEAP. The survey's objective was to assess both the overall use of GRLWEAP in Northwest practice and the effects of applying the AASHTO resistance factors using GRLWEAP to bridge designs in the Northwest. The survey's results showed a strong opinion among DOT practitioners to support increasing the AASHTO reported GRLWEAP

---

<sup>1</sup> Only GRLWEAP version of the wave equation of pile driving was used in this research and no other code is either endorsed or approved.

resistance factors,  $\phi$ , in the code when used on both initial driving and restrike to capture pile capacity. The objective of this study is to provide new calibrated resistance  $\phi$  factors for ODOT field practice for the end of initial driving (EOID) and the beginning of restrike (BOR) driving conditions.

ODOT typically uses the GRLWEAP method for verifying the predicted nominal resistance of driven pile deep foundations. According to the Pacific Northwest DOT survey for the resistance factor of GRLWEAP in AASHTO codes, approximately 80% of respondents believed the  $\phi$  value of 0.4 (Table 1.1) for redundant piles with a 1% probability of failure is too conservative, and 37.5% of those surveyed do not use 0.4, but have set separate and higher values (*Smith and Dusicka 2009*). The purpose of this research was to determine the appropriate resistance factors for the GRLWEAP method using an extended high-quality pile load test database, including data from the NCHRP 507 study, the FHWA DFLTD (*Raghavendra, et al. 2001*) database, and other sources. For completeness, the GRLWEAP method is discussed in Section 1.2.1 and Section 2.

**Table 1.1: Recommended resistance factors from NCHRP 507**

Method		Time of Driving	# of Cases	Mean	S. D.	COV	Resistance Factor, $\phi$	
							$P_f=1.0\%$ , $\beta=2.33$	$P_f=0.1\%$ , $\beta=3.0$
Dynamic Measurement	CAPWAP	EOID	125	1.626	0.797	0.49	0.65	0.45
		BOR	162	1.158	0.393	0.339	0.65	0.50
	Energy Approach	EOID	128	1.084	0.431	0.398	0.55	0.40
		BOR	153	0.785	0.29	0.369	0.40	0.30
Dynamic Equation	ENR	general	384	1.602	1.458	0.91	0.25	0.15
	Gates	general	384	1.787	0.848	0.475	0.75	0.55
	FHWA Modified	general	384	0.94	0.472	0.502	0.40	0.25
GRLWEAP		EOID	99	1.656	1.199	0.724	0.40	0.25

The Phase 2 effort described in this report had two primary objectives: to build an extensive database from the present sources that reflects ODOT diverse soils, and to calibrate the resistance factors for the GRLWEAP method for use with EOID and BOR conditions. To achieve the primary objectives, the tasks described below for this Phase 2 were performed:

- Searched and reviewed current national DOT LRFD recalibration efforts and the available published procedures discussing LRFD calibration, as well as the references adopted in AASHTO Bridge Design Specification (*AASHTO 2006*) for the resistance factors.
- Reviewed and recompiled the static and dynamic tested pile case histories from the existing databases made available by ODOT, and generated a new Portland State University (PSU) database for this study.
- Performed static analysis with the DRIVEN software program and the bearing graph evaluation of capacity with the GRLWEAP software program.

- Searched and expanded the database with new documented cases. Conducted a statistical analysis to profile the database and design practice scenarios.
- Recalibrated the resistance factor by using the reliability-based methods for the wave equation analysis and recommended resistance factors for approved scenarios.

FHWA has collected extensive deep foundation load test information and compiled a database with entries up to 2004, primarily drawn from state DOT load tests. The database offered more than 1,000 load test entries from 1985 to 2004 and was obtained by the research group in preparation for this Phase 2 recalibration study. The information collected included soil boring logs, laboratory data, and the field load test results for both driven pile and drilled shaft deep foundations, including pile driving logs up to the EOID, as well as the restrike-driving log when a pile is re-driven after some delay, referred to as BOR driving. J. Long (*Long, et al. 2009*) accessed five independent databases to identify statistical means and standard deviations for seven capacity predictive methods. Some of these databases included EOID and BOR driving data that permitted examination of the GRLWEAP produced bearing graph, as well as CAsE Pile Wave Analysis Program (CAPWAP) predictions of nominal capacity. For both these methods, Long illustrated the improvement in predictive ability achieved by moving from EOID to BOR blow counts, something NCHRP 507 did not illustrate for the GRLWEAP bearing graph. The improvement in both mean and standard deviation reported by Long when comparing EOID to BOR was statistically better for GRLWEAP than for CAPWAP.

### **1.1.2 The NCHRP 507 Report**

The NCHRP 507 project was performed to provide updated resistance factors for a new AASHTO LRFD Bridge Design Specification edition that would reflect current practice in geotechnical design and construction (*Paikowsky 2004*). The resistance values and methodology in codes existing at that time were thought to be significantly conservative and would increase foundation costs. As the first step of the NCHRP 507 project, high quality databases containing case histories of piles tested to failure were compiled and reliability-based methods were used for the calibration of the resistance factors. Then statistical analyses were performed for all acceptable methods including the static analysis by  $\alpha$ -method, Nordlund's method, and dynamic analysis for six different methods: CAPWAP, Energy Approach, ENR, Gates, FHWA modified Gates, and the GRLWEAP method.

For the reliability-based method, the target reliability index was recommended according to the condition of pile redundancy. NCHRP 507 recommended resistance values from the First Order Reliability Method (FORM) rather than the First Order Second Moment (FOSM). The former is called the advanced FOSM method for the case of a lognormal distribution of the variables and a non-linear limit state function.

The NCHRP 507 work statistically established  $\phi$  resistance factors by setting dead load to live load ratios, site variability, pile redundancy, soil types, and the quality of dynamic testing; all of which are, in fact, regional factors. The AASHTO code was an attempt to provide a basis for uniform implementation of LRFD. The NCHRP 507 report recommended resistance factors for static and dynamic analyses methods and recommended the number of dynamic tests according to the site variability. Table 1.1 presented the recommended resistance factors for dynamic



analysis extracted from NCHRP 507. Resistance factors,  $\phi$ , at BOR condition in GRLWEAP method were not shown in the NCHRP 507 main report text but can be located in the appendix of the report. It appears likely that the values originated with the earlier FHWA report using GRLWEAP at both EOID and BOR (*Rausche, et al. 1997*). ODOT obtained the NCHRP 507 database with modifications, including quality metrics and pile selection strategy, from the Washington State Department of Transportation (WSDOT) that was employed in its own resistance factor calibration of the pile driving dynamic formula. The Phase 1 study for ODOT (*Smith and Dusicka 2009*) revealed that considerable information was missing for approximately two-thirds of the NCHRP 507 pile load test database on restrrike.

## 1.2 BACKGROUND AND PHASE 1 STUDY

The LRFD methodology at the ultimate limit state calls for the load to be factored up by load factors ( $\gamma$ ) assigned to the load source (e.g. dead, live, wind) and compared to a reduced nominal resistance,  $R_{nk}$ , employing a resistance factor,  $\phi$ . The inequality to be satisfied in LRFD based design is set out in the equation below:

$$\sum \gamma_{ij} Q_{ij} \leq \phi_k R_{nk} \quad (1-1)$$

where:  $Q_{ij}$  = Structural load from each source condition  
 $\gamma_{ij}$  = Magnification load factor set by the code  
 $R_{nk}$  = Nominal strength-based resistance established by a *defined* method  
 $\phi_k$  = Resistance factor for the defined resistance method

$Q_{ij}$  and  $R_{nk}$  are not deterministic but are random variables; therefore, the calibration of  $\gamma_{ij}$  and  $\phi_k$  to foundation design employs a fixed Reliability Index value,  $\beta$ , quantifying risk for the foundation. Deep foundations with a high redundancy in a group have a 1/100 probability of “failure,” which sets the target  $\beta$  at 2.3. The NCHRP 507 required low redundancy foundation groups ( $\leq 4$  piles) to have a stricter 1/1000 probability of exceedance with  $\beta$  at 3 as the target reliability. The calibration reported here for ODOT driven piles uses the pile redundancy target  $\beta$  of 2.33 and AASHTO approved  $\gamma_{ij}$  load factors. The “calibration” by matching to Allowable Stress Design (ASD) is only a mathematical based design equivalency to calculate the same number of piles. It uses no reliability theory and should not be used as a valid calibration for  $\phi$ . The appropriate resistance value (determined by any method) to satisfy the inequality of Equation 1-1 is a function of the structure’s proportion of live load (LL) and dead load (DL) and the AASHTO code load factors,  $\gamma_{ij}$ .

Given the mandated October 1, 2007 implementation date for adoption of the AASHTO bridge code, the number of individual state DOTs making efforts to implement the code with load modifications has increased. Continued research efforts to meet local needs, as well as bridge code changes, are occurring. The concerns of state foundation engineering practitioners caused major revisions to the code, resulting in the subsequent release of a fourth edition of the code (*AASHTO 2007*). In parallel to the AASHTO/FHWA effort, the last five years have seen a growth in LRFD research material published in foundation engineering journals and conference

proceedings. It is evident that LRFD implementation is proceeding slowly. Better recognition of the need for regional and local standards of practice, together with improvements in statistical competency to assist local implementation of the AASHTO recommendations, is beginning to gain momentum.

Tony Allen (*Allen 2005a*) provided a clear presentation of axial capacity, load, and resistance factor historical development, as well as the difficulties relating to driven pile foundations. In addition, a calibration of the resistance factor was undertaken by WSDOT (*Allen 2005b*) for the Modified Gates pile driving formulae based on reinterpretation of the same pile driving databases accessed by NCHRP 507. Both of these reports were identified by ODOT as key reference studies in the recalibration effort. However, ODOT had extensive experience and successful application of GRLWEAP. The evaluation of the nominal static capacity by ODOT for each pile was most often performed in the field using GRLWEAP models, while the AASHTO code presented resistance factors for this technique in its LRFD methodology. GRLWEAP models of the pile driving hammer, driving accessories, pile, and soil by a viscous mass-spring system is widespread and constitutes the industry standard internationally.

The Phase 1 study identified the current trends in recalibration, key resources to assist in designing implementation procedures, and the role played by GRLWEAP in assessing nominal capacity. In reality, piles are often driven at locations for which no borehole exists at that position to provide concise subsurface conditions. Subsurface conditions, together with pile size and type, dictate the axial capacity. This limits the direct application and reliability of static methods derived from borehole testing of samples to those physical locations coinciding with borehole locations. In all calibration efforts, the basis for statistical comparison between different prediction methods is the static load test capacity using Davisson's interpretation. Recall that predicting Davisson's capacity is not the intent of either the static capacity analytical methods or the dynamic methods. (AASHTO 2009 mandates a different interpretation for piles with diameters in the range 24 to 36 in.) Therefore, in addition to analytical modeling errors, a "bias" to Davisson's capacity is introduced and statistically reported from any database studies.

In addition to NCHRP 507, significant documentation of correct consistent design procedures for pile foundations had recently appeared from FHWA (*Hannigan, et al. 2006*). This two-volume report offered a comprehensive exploration of pile design and analysis in Volume I and field testing quality control and field dynamic testing in Volume II. The key communication connections to the structural engineer, bridge engineer, and contractor were well presented, as were the decisions concerning construction capacity verification testing. Both volumes were directed toward ASD and did not directly incorporate LRFD principles. A simple LRFD example was presented in Volume I of Appendix G, following the discussion of the LRFD structural origins.

A series of studies in the Phase 1 effort reported the full effect of switching design methodologies from ASD to LRFD linked to ODOT's design and field procedure. The first study of Phase 1 surveyed the U.S. Northwest States' DOTs to determine each DOT's standard of practice GRLWEAP recommended  $\phi$  value. The survey results found strong support for a LRFD resistance factor recalibration effort of GRLWEAP. Summary findings included:

- 60% of the surveyed Northwest DOTs utilized GRLWEAP.

- 80% of the surveyed Northwest DOTs considered a  $\phi_n$  at 0.4 to be conservative.
- 750 bridges were expected to be designed for the Northwest in the next 10 years.
- 60% of the surveyed Northwest DOTs were willing to assist in a recalibration effort.

The second part of the Phase 1 effort studied the economic impact to ODOT via the cost difference between bridge foundations designed with ASD vs LRFD utilizing ODOT's standard of practice. The study concluded that with GRLWEAP as the design tool, a 30% increase to foundation costs could be expected when utilizing LRFD design compared to ASD design. Pile capacity, whether established by static analyses, dynamic testing in the field at the time of driving, or load testing, was governed by the soil layer(s) shear strength around the pile perimeter and at the pile tip. Time and economic constraints dictated that only limited geotechnical sampling, testing, and logging of boreholes were performed. By assigning a higher  $\phi$  resistance factor, AASHTO declared that the pile driving analyzer (PDA) signal matching technique with CAPWAP technology was more reliable; however, use of this technology was cost prohibitive for many bridge piling contracts.

Use of the AASHTO and the FHWA approved GRLWEAP bearing graph for nominal capacity has two distinct advantages over signal matching with PDA and CAPWAP analysis. First, according to the AASHTO code, site statistical variability work does not have to be completed since *the inspector assesses each pile* at the time of driving. Second, the bearing graph check is a deliberate activity using observed field pile and hammer performance to determine that each pile meets the limit state axial nominal capacity. Geotechnical site variations are established by both site investigations and by the design team applying their own local experience, knowledge, and judgment. These variations can then be incorporated in region-specific input of soil parameters into GRLWEAP, including soil side and tip quake and viscous damping parameters, as well as soil layering across the site. This study was based only on default parameters to ensure recommended resistance factors can be applicable to a broad range of pile types and subsurface conditions.

### 1.2.1 GRLWEAP

GRLWEAP calculates the induced stress and displacement waves traveling along the pile after a single hammer blow and reports pile permanent set after elastic rebound, called quake (Q). It further assists in decisions about pile drivability and reports the change in static "equivalent" bearing capacity at the time of driving ( $R_{ult}$ ), from changes in field blow count by means of a bearing graph. For illustration purposes only, Figure 1.1 presents an example of the bearing graph with a range of possible capacities as a function of driving blow counts. When the field driving blow count is recorded, the graph can be used to read the static  $R_{ult}$  predicted by the program at the time of driving.

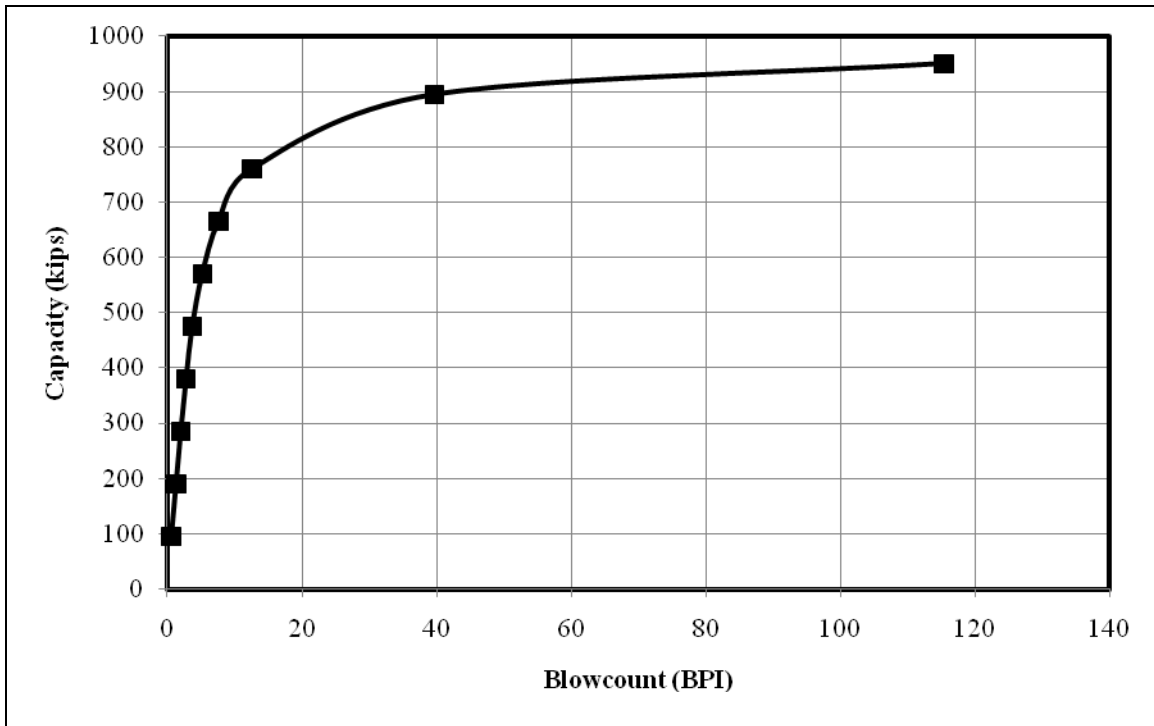


Figure 1.1: Example of a GRLWEAP bearing graph

Establishing bearing capacity from GRLWEAP becomes more difficult by the large number of site-specific variables, the modeling complexities, and the sensitivity of the output to all driving components, particularly the hammer efficiency. These site specific variables include the equivalent soil “springs” elastic quake movement ( $Q_i$ ) and the soil springs viscous damping values ( $J_i$ ) for each soil supported pile element. The typical application of GRLWEAP is often at two stages, both in design and construction: the first stage is during the pre-bid period to establish that the pile designed by static methods can be driven by available equipment, and the second stage is after the chosen contractor selects the final production hammer and driving accessories. At the second stage, the field bearing graph and hammer stroke to capacity plots, which control final penetration depths, are made available to the agency field inspector for confirmation of capacity and acceptance of the pile.

It is well known that pile long-term capacity will often show a capacity gain, called set-up, and occasionally show relaxation when the capacity drops. Under these conditions, the use of measured driving blow counts at EOID could yield either conservative or unconservative capacity results and the pile should be restruck after a waiting period (often a minimum of 24 hours) to give a more representative blow count. This is called the BOR blow count, and any associated use of a bearing graph must be established from the appropriate GRLWEAP model bearing graph. Even when static load tests have been conducted at the site, AASHTO recommends that GRLWEAP be used to extrapolate these load test results to the production piles. GRLWEAP features include improved set-up models, as well as the use of the static pile capacity DRIVEN software code (*Mathias and Cribbs 1998*) for input of soil resistance distribution data to GRLWEAP.

### 1.3 ODOT LRFD ISSUES IN PRACTICE

NCHRP 507 allowed some reliance on “local judgment” and “experience” in the application of any field verification procedures to establish factored nominal resistance. Two disturbing features in the report emerged that limited flexibility for implementation of dynamic testing to local conditions: first, the elimination of soil types as a variable when selecting  $\phi$  resistance factors for GRLWEAP and second, the previously reported absence of the GRLWEAP-BOR combination  $\phi$  resistance factor to be used after pile set-up has occurred. To capture the transportation agencies’ standard of practice, the AASHTO code acknowledges that regional implementation can proceed after local recalibration efforts are complete.

No agency implementation policy is discussed in the AASHTO code to assist in the transition from ASD to LRFD. Historically, the ODOT Bridge Section has generally followed the recommendations contained in all past and current FHWA manuals for driven pile design and the code requirements set by AASHTO. For most Oregon bridges, ODOT requires a minimum of one logged and sampled borehole per pier, with limited laboratory shear strength testing conducted. Foundation conditions throughout the Willamette Valley, coastal development regions, and the Portland metropolitan area are predominantly sand, silt, and clay. Bridge foundation piles, typically steel pipe and H section piles, are of sufficient length to be primarily friction piles and these soils are known to exhibit set-up after EOID.

The statistical studies reported in NCHRP 507 to establish  $\phi$  resistance factors for the AASHTO code used “default” soil and hammer parameters in GRLWEAP and had no restrrike condition included to capture any known soil set-up that may be large in Oregon soils. The AASHTO reported  $\phi$  values for static analysis are generally low, and static analyses are now relegated for use to establish preliminary pile sizes and lengths, for contract purposes only. However, static analysis do form the basis of pile side shear to pile tip capacity ratios used in the GRLWEAP program and are most often established from uncertain SPT blow counts that statistically have a large coefficient of variation (COV) between 15% to 40% (*Duncan 2000*).

The concern for predicting the ultimate capacity at restrrike is related to the pile gain set-up in resistance governed by uncertainty from geotechnical soil characteristics. About 70% of the Willamette Valley subsurface consists of flood deposits, clay and silt. In these soils, the capacity of a driven pile increases with time after driving, and the increased capacity is indicated by restrrike blow count. After the selected contractor proposes hammer and driving accessories and other specific details become known, the inspector’s graphs are prepared showing required blow count versus hammer stroke for a given static resistance. ODOT provides the soil input parameters for GRLWEAP in the contract specifications. ODOT has routinely used GRLWEAP for capacity at EOID and occasionally at BOR if significant set-up was expected and the EOID measured capacity was low. In ASD, both EOID and BOR capacity values were used with a recommended factor of safety of 2.5.

Within any DOT, the accumulated foundation engineering knowledge base helps establish the accepted standard of practice. Pile design is set by site investigation results for which the amount of data, data quality, and interpretation are locally and regionally specific. Much of the NCHRP 507 research findings removed the insensitive silt soil category, which is common in

Oregon, with no specific recommendations offered for this soil type. The AASHTO code cautions using the published  $\phi$  resistance factors when piles are over 24 in in diameter, most likely because a limited number of 24 in diameter piles are in the database used to establish the resistance factor. The most likely reason is that no piles over this diameter were used in the statistical calibration. However, these large sizes are not typical in present ODOT practice.

## 1.4 FIRST ORDER SECOND MOMENT AND MONTE CARLO METHODS

LRFD design separates uncertainties into two independent variables: load and resistance, expressed with separate load and resistance factors. Satisfactory design requires that the factored down resistance for a pile should be larger than the linear combination sum of the factored loads.

The sum of the factored loads may represent the possible largest statistical “acceptable” load combination. The nominal resistance (similar to ultimate capacity as defined in ASD) is established from the code-approved procedure. The resistance factor,  $\phi$ , is less than one, and applied to reduce the measured nominal resistance. The adoption of factors to increase the load and to reduce the resistance is based on probability theory to model uncertainty. Therefore, failure based on reliability methods is defined when the load exceeds the resistance, i.e. expressed by the area in which the two probability density functions (PDF) for load and resistance overlap. This overlap will be controlled by the resistance factor, because the PDF of source loads usually have much less variation than the resistance distribution. For this study, the resistance factor is calculated using reliability theory with both the FOSM, and more advanced probabilistic Monte Carlo random number based method (*Allen, et al. 2005*).

The FOSM method uses the first terms in a Taylor series expansion of the “performance function” to estimate the expected value and variance of the function. It is called a second moment method because the variance is a form of the second moment and is the highest order statistical result used in the analysis (*Baecher and Christian 2003*).

The limit state function is represented by the safety margin and can be defined as:

$$g(\mathbf{R}, \mathbf{Q}) = \phi R_n - \sum \gamma_i Q_i \geq 0 \quad (1-2)$$

where  $Q_i$  is the load,  $\gamma_i$  is the load factor  $g$  is the limit state function and, if  $g$  is less than zero, failure is predicted.

This function makes the two variable distributions (shown on the left of Figure 1.2) merge to one distribution (shown on the right of Figure 1.2) and illustrates the probability of failure as when the safety margin is less than zero.

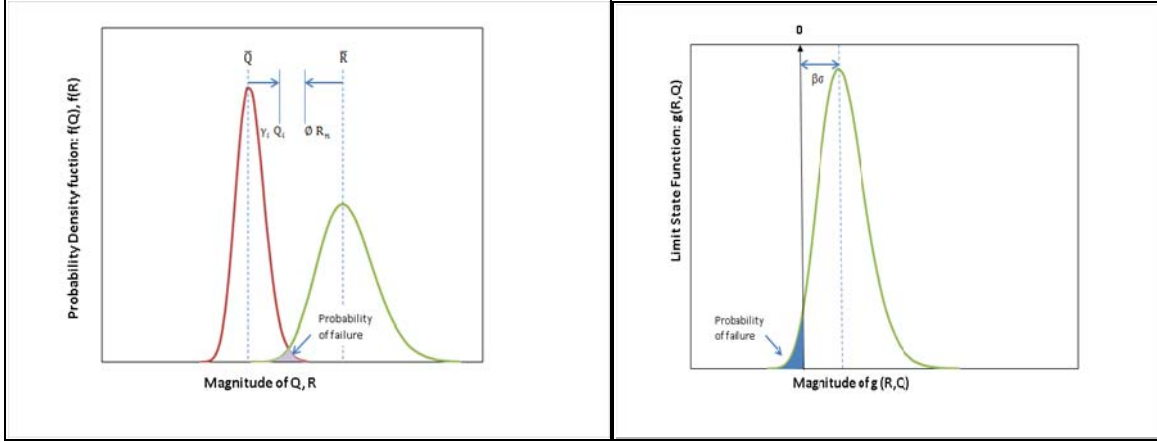


Figure 1.2: Probability of failure and reliability index (William, et al. 1998)

To establish the statistical parameter for the resistance, the ratio of the measured to the predicted capacity is established, called the bias factor,  $\lambda$ , from a population of case histories. In this study, the “measured” value is the Davisson’s pile failure capacity secured from the database. The predicted value from the GRLWEAP analysis is based on the bearing graph with the measured blow counts used both at the EOID condition and at the BOR condition, and is further discussed in Section 4.1.

The distance from the failure region,  $P_f$ , to the mean value of the limit state function,  $g$ , can be expressed, using mean bias,  $\lambda$ , and COV, as  $\beta\sigma$ , where  $\sigma$  is the standard deviation (s.d.) of the limit state function, and  $\beta$  is the reliability index.  $P_f$  is typically represented by the reliability index parameter,  $\beta$ , a function of both the load statistics and resistance statistics, i.e. the acceptable magnitude of  $\beta$  called the target reliability depends on the desired value of  $P_f$  for the pile. To permit final calculation of resistance values, some assumptions are needed. Dead load ( $Q_D$ ) to live load ( $Q_L$ ) ratios ranging from 2 to 5 have previously been investigated since this range is typical for bridges and similar structures (Allen 2005a) and the final  $\phi$  is typically found insensitive to this ratio. When only dead and live loads are considered, the resistance factor,  $\phi$ , can be found by FOSM method (See Section 7.1) the following equation:

$$\phi = \frac{\lambda_R \left( \frac{\lambda_D Q_D}{Q_L} + \gamma_L \right) \sqrt{\frac{(1 + \text{COV}_{Q_D}^2 + \text{COV}_{Q_L}^2)}{1 + \text{COV}_R^2}}}{\left( \frac{\lambda_{Q_D} Q_D}{Q_L} + \lambda_{Q_L} \right) \exp \left\{ \beta_T \sqrt{\ln(1 + \text{COV}_R^2)(1 + \text{COV}_{Q_D}^2 + \text{COV}_{Q_L}^2)} \right\}} \quad (1-3)$$

where:  $\lambda_R, \lambda_{Q_D}, \lambda_{Q_L}$  = resistance, dead and live load bias factor,  
 $\gamma_D, \gamma_L$  = dead and live load factor,  
 $Q_D/Q_L$  = dead to live load ratio,

$COV_R, COV_{QD}, COV_{QL} =$  coefficient of variation of the resistance,  
 dead and live load factors, and  
 $\beta_T =$  target reliability index.

In the above equation, all statistical values, except  $\lambda_R$  and  $COV_R$ , are generally taken at the given code values. In this study the statistical values for load follow NCHRP 507 (Appendix B) and the resistance  $\lambda_R$  and  $COV_R$  are taken from the result of the GRLWEAP database analysis performed for a variety of scenarios. However most of the resistance factors recommended for use from NCHRP 507 are the more advanced FORM method.

After careful review of source pile driving data, more sophisticated and accurate calibration using the AASHTO endorsed Monte Carlo probabilistic procedures can proceed. This procedure requires high quality PDF's, and has been discussed by Allen, et al. (2005). Variability in the total load from dead and live load sources, as well as the variability of resistance, are expressed in the form of the safety margin and are generated by random number Monte Carlo procedures according to the distribution mean and COVs. The safety margin defines risk of failure that arises from the fitting of the lower  $\lambda_R$  bias resistance distribution tail (where predictions are unconservative) and upper total load bias tail. Intermediate steps include constructing the PDF of the calculated  $\lambda_R$  resistance bias curves (from GRLWEAP measured capacities), conversion to cumulative distribution function (CDF), and finally via each case,  $\lambda_R$  creation of the standard normal variable (SNV) plots.

This research incorporated the recommendations and the example offered by WSDOT (Allen 2005b and Allen, et al. 2005) using lognormal “best fits” from the following three approaches: regressed fitting all the case history data points, regressed fitting by dropping data points from the upper (conservative) tail, and finally, fitting the lower tail by visual adjustment. Random number generation provided both the dead and live load distributions and the resistance distributions, and established the final safety margin distribution with the preset dead to live load ratio. By iteration the appropriate resistance factor,  $\phi$ , was found to produce the target reliability index  $\beta_T$  value. These probabilistic procedures used Excel<sup>®</sup> spreadsheet computation for convenience.





## 2.0 DRIVEN AND GRLWEAP SOFTWARE

FHWA (*Hannigan, et al. 2006*) endorses the dual use of DRIVEN 1.2 software (*Mathias and Cribbs 1998*) to calculate the likely pile static capacity resistance distribution and format the input file to GRLWEAP for bearing graph capacity calculation. This research employed all default parameters and options in both codes consistent with EOID and at BOR conditions. These procedures are discussed by FHWA and were diligently followed in derivation of the GRLWEAP capacities in this study. It is essential that any use of the wave equation to establish LFRD capacity with the recommendations contained in this report use only GRLWEAP as other programs contain differences that affect the bearing graph and capacity. Application discussion and, when required, rules for consistency in this research are discussed below.

### 2.1 DRIVEN APPLICATION RULES

DRIVEN performs static analysis computations utilizing Alpha method (*Tomlinson 1980*) for cohesive soil and Nordlund's method (*1963, 1979*) for cohesionless soil provided by FHWA (*Hannigan, et al. 2006*). Both the Alpha and Nordlund method are current methods and appear in the AASHTO code (*AASHTO 2009*) for static analysis capacity prediction. A consistent approach was taken by the research group in analyzing standard penetration test (SPT) blow count,  $N$ , data for input into DRIVEN for cohesionless soil layers.  $N$  values can be input directly into DRIVEN to calculate an effective friction angle for the layer using Meyerhof's method. DRIVEN accepts a maximum of five  $N$  values, creating a limitation in a layer which might include much more than five blow counts. Rather than picking five representative  $N$  values for input, the research group calculated effective friction angle values using the full set of reported  $N$  values for each layer as the DRIVEN program input. Analyzing the full set of values allowed for a more accurate representation of the layer, especially considering the inherent variability of SPT test results. In addition, obvious outliers could be removed prior to determining an effective friction angle from SPT results.

The applicability of the SPT to cohesive soils is largely agreed as minimal. The FHWA (*Hannigan, et al. 2006*) recommends the SPT solely for use with cohesionless soils. However, in many instances there was no other data other than the  $N$  values available for clay or silt layers. In the absence of other soil data,  $N$  values were used to estimate undrained shear strength using correlations published by Bowles (*Bowles 1996*). Bowles lists a range of uncorrected  $N$  values corresponding to a range of unconfined compressive strength values. Shear strength values based on SPT data were used only in absence of any other available soil data.

Default parameters were utilized for all inputs following the DRIVEN manual recommendations and those given by AASHTO and FHWA driven pile manuals. Some additional interpretation and judgment rules were required for DRIVEN analysis that went beyond the reference manual set. These included:

- The program could not export open ended pipe (OEP) piles to GRLWEAP. As the majority of OEP pile to penetration depth ratio fell within the FHWA plugged condition they were modeled closed end.
- H-Pile toe areas were taken to be the area of the metal while the side friction development utilized plugged box perimeter dimension.
- Only square concrete piles are supported in the DRIVEN program. The pile case histories recorded in this research's database were predominantly frictional piles; therefore, the outside perimeters of non-square shaped concrete piles were transformed into an equivalent sized square pile to retain proper area for side friction development during DRIVEN analysis.
- DRIVEN's prime purpose use was to calculate likely shaft and tip resistance distributions and the GRLWEAP input file. The program input prompts recommending capping cohesionless soil friction angles was disregarded and the gain/loss factors were not used.

Due to the methods accepted for static capacity analysis there were internal restrictions placed on the reported capacities. These were as follows:

- For cohesionless soil, Nordlund's method for side friction calculations' limits the acceptable range of friction angle to the 20° to 45° range. Values outside this range were not allowed.
- Pile end bearing capacities were limited following the recommendations of Meyerhof found in Table 7.2 in the DRIVEN manual. The program did not consider any capacities larger than those recommended by Meyerhof.

After creation of a soil profile distribution, the calculated side friction and end bearing was available and the tabulated output capacity screen was examined to determine each individual soil layer's contribution to side friction capacity, and the overall distribution of ultimate capacity. A general soil type category was assigned to the case for ease of case history organization. Each case was then placed into one of three subsurface categories: Clay, Sand, and Mixed. Cases that reported cohesive soils contributing to more than 80% of a pile's total capacity were considered Clay case histories. Cases that reported cohesionless soils contributing to more than 80% of a pile's total capacity were considered to be Sand case histories. Layered soil cases that fell in between these brackets were considered Mixed cases. Predominant bearing conditions along a pile's shaft and at the toe, together with the distribution of side friction between the layers and toe, were recorded for later use in the GRLWEAP analysis. All the recommendations offered by FHWA and the DRIVEN manual for a pile to plug in cohesive soils were followed for both EOID and BOR driving conditions.

## 2.2 GRLWEAP APPLICATION PROCEDURES

### 2.2.1 Overview

The basic principle of the Wave Equation Analysis for Pile driving is the expression, in finite difference form, of the governing partial differential equation modeling the transfer of kinetic energy into the pile to overcome the static and dynamic soil resistance. In the driving process, the hammer kinetic energy is delivered to the pile in the form of compressive force pulse (*Pile Dynamics, Inc. 2005*). At the bottom of the pile, the force pulse reflects and moves up to the top again. While the energy travels from the hammer to the bottom of pile and back to the top of pile, there are energy losses in pile, soil, and driving system including hammer, cushion, and helmet. This transmission of energy will produce a permanent set at the pile into the supporting soil. The principle of energy transfer is expressed from the GRLWEAP manual as follows:

$$\text{Kinetic Energy (E)} - \text{Energy losses (E}_{\text{loss}}) = \text{Resistance (R}_n) \times \text{permanent set (s)} \quad (2-1)$$

The penetration resistance,  $N$ , is the inverse of the permanent set,  $s$ , calculated by the pile and is expressed in either blows per foot (BPF) or blows per inch (BPI). This report uses the BPI expression of driving resistance exclusively. Wave equation modeling requires the following input to be available from every candidate pile case study:

- Input for pile stiffness and energy loss: pile size, elastic modulus, specific weight.
- Input for soil resistance and damping energy loss: percent friction contribution, quake and damping factors.
- Input for hammer energy and efficiency: hammer type (often in the hammer library).
- Input for driving system energy loss: helmet weight, cushion stiffness, coefficient of restitution, thickness, and elastic modulus.

GRLWEAP then provides an estimation of bearing capacity from a bearing graph and represents the relationship between “equivalent” static capacity at the time of driving and the pile penetration resistance, expressed as blow count,  $N$ . For this study, GRLWEAP 2005, with all updates and issued biannually up to July 2010, was supplied by Pile Dynamics, Inc. and used to predict the ultimate capacity with the field observed blow counts reported in the database at EOID, and at BOR following a time delay. Section 4.1 discusses specific details of using the assembled database to calculate these EOID and BOR capacities.

### 2.2.2 GRLWEAP application

Guiding the analysis process were the GRLWEAP 2005 Manual, the DRIVEN Manual, the two FHWA volumes on driven pile foundations (*Hannigan, et al. 2006*), and the original work performed by Goble, Rausche, and Likins (GRL) that formed the basis of the NCHRP 507 recommendations around the use of GRLWEAP (*Rausche, et al. 1997*). On occasions when the manuals were unclear, or omitted necessary steps, the standard interpretation for ODOT was determined through discussion with select research Technical Advisory Committee (TAC)

members. At key stages in program development, systematic steps, including careful review and sensitivity studies, were performed, as well as other activities to avoid gross modeling errors.

Importing the DRIVEN soil profile input into GRLWEAP requires the User select from the file menu “Open Pre 2002 input file (\*.GWI)” option. The file produces the DRIVEN soil profile and graphically represents the individual soil layer’s capacity contribution relative to one another. As the soil profile is constructed by DRIVEN, no alterations to soil properties are permitted in GRLWEAP. Therefore, any sensitivity analyses with variations of soil strength parameters, water table location, or profile geometry required a separate DRIVEN input file be produced. Hammer type is selected from the program pull down menus, and hammer model details and performance information are found in the GRLWEAP library. If the hammer library did not list the required hammer, a similar hammer type with matching energy/power and ram weight was selected. If no similar match to a hammer’s energy/power and ram weight was available, the hammer with the closest energy/power rating was selected. Default values for all hammer accessories and helmet weight were used unless specific values were provided in the field records. Hammer efficiencies, pressure, and stroke were never altered from their default values.

Figure 2.1 shows the GRLWEAP pile and hammer details and the distribution of pile resistance provided by DRIVEN for one of the piles analyzed.

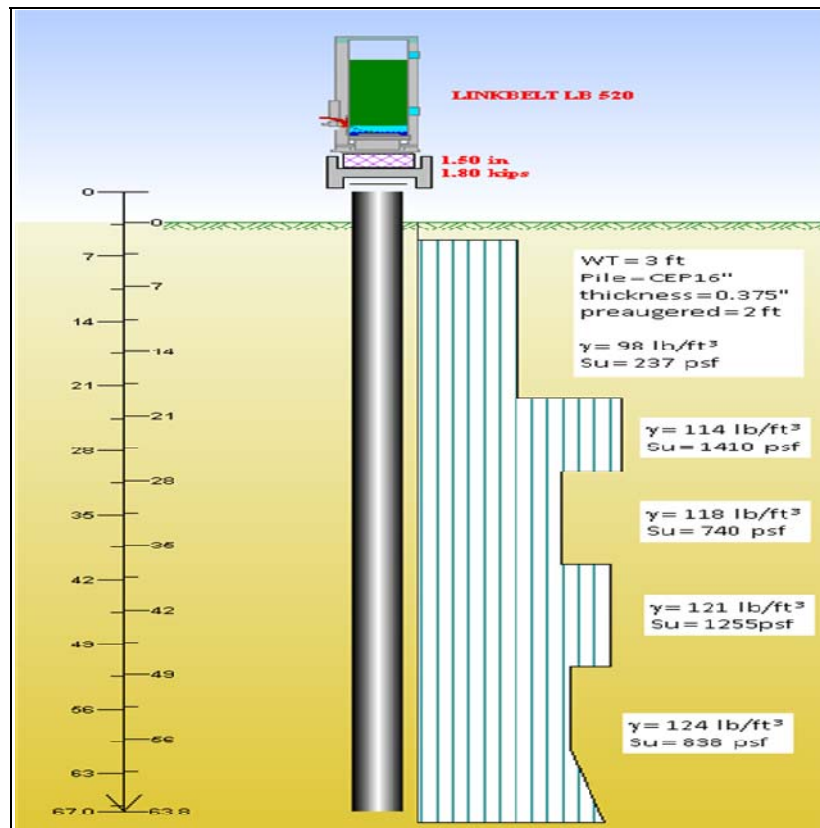


Figure 2.1: Example of DRIVEN provided soil resistance to GRLWEAP

Both the hammer and pile cushion provide protection to the hammer and pile and are key components in GRLWEAP modeling as they modify the delivered energy. Appropriate pile cushion input proved occasionally problematic for concrete piles and rarely was the hammer cushion or pile cushion properties reported in the source data. If multiple pile cushion options were available, then each option was selected successively and a sensitivity analysis was performed to assist in gauging the sensitivity of the prediction. Purpose designed rules beyond the GRLWEAP Manual that guide hammer cushion selections were discussed with the TAC member, Robert Miner. These discussions provided the following guidance:

- If multiple hammer cushion leads were available through the GRLWEAP library, a lead was selected that was 4-6 in larger than the diameter of the pile being driven. This countered the affect of a worn or damaged lead and insured proper contact.
- If no hammer cushion parameters were available in the GRLWEAP library, a cushion from the closest matching hammer with a matching ram weight was selected
- According to Robert Miner, Robert Miner Dynamic Testing Inc., likely pile cushion thickness should be no more than 12 in. An error was discovered for the Conmaco 300-C hammer aluminum cushion in the GRLWEAP library, which reported an unreasonable cushion thickness of 29 in.

GRLWEAP captures the dynamic effects of the soil/pile interaction through the use of its quake and damping factors. Quake is a measure of the elastic recoverable slip between the soil and pile after a single hammer strike. These quake and damping parameters are directly influenced by soil stiffness, and the FHWA (*Hannigan, et al. 2006*) suggests there may also be a difference between the EOID and BOR condition. These parameters and their role in GRLWEAP analysis are explained in detail in the GRLWEAP manual. Following the manual recommended procedures, and in consultation with the TAC, a research quake and damping selection methodology was developed. Shaft damping ( $j_s$ ) utilized a weighted average method to determine the appropriate single  $j_s$  value for modeling the soil conditions along the entire length of a pile's shaft. GRLWEAP recommends  $j_s=0.05\text{sec/ft}$  for cohesionless soils and  $j_s=0.20\text{ sec/ft}$  in cohesive soils and interpolation was employed for intermediate soil conditions. The Phase 1 effort (*Jackson 2008*), in consultation with ODOT and Robert Miner, developed the Table 2.1 recommendations of acceptable damping factors for variable soil layers. Each case history logged soil layer description along the length of a pile's shaft was assigned its appropriate  $j_s$  value from the table.

**Table 2.1: Acceptable damping factors for variable soil layers**

Soil Type	$j_s$ sec/ft	$j_s$ sec/m
Clay	0.20	0.65
Silty Clay	0.17	0.55
Clayey Silt	0.16	0.50
Clayey Sand	0.11	0.35
Silty Sand	0.10	0.30
Sand	0.05	0.15

A weighted single  $j_s$  value was calculated by multiplying a layer's appropriate  $j_s$  value by its percent contribution to the pile's total side friction capacity. The summation of the resulting partial  $j_s$  values yields the correct weighted average used for calculation. Toe damping,  $j_s$ , was always set at 0.1sec/ft, as recommended by the GRLWEAP manual.

Shaft quake ( $q_s$ ) was always set to 0.1in for all soil/pile types as recommended by the GRLWEAP manual. The toe quake,  $q_t$ , was calculated based on the predicted soil strength of the end bearing soil layer. GRLWEAP recommends non-displacement piles in all soil types utilize a toe quake value of 0.1 in. Displacement pile recommendations use a toe quake value equaling the pile diameter divided by 120 for "dense" soil and pile diameter divided by 60 for "soft" soil. No further information was available for assessing the break point between soft and dense soil strengths. The FHWA reference table (*Sabatini, et al. 2002*) was utilized in development of the subsurface profile to set the criteria for the different densities. The breakpoint for cohesionless soils was selected to be friction angles of  $34^\circ$ , while cohesive soils utilized undrained shear strength of 1500 psf to classify a soil as either dense (D/120) or loose (D/60). No linear interpolation was performed on the toe quake parameter based on the degree of soil density.

The last input requires the User to define the expected percent allocation of total capacity between a pile's side and toe. The DRIVEN calculated static capacity allocation was always used. DRIVEN's enforced end bearing capacity cap has the potential to alter this distribution. However, the majority of piles analyzed in the database were frictional piles; therefore, the data were not skewed by the limitation.

As stated in Section 2.1 in all cases the recommendations of both the DRIVEN software and GRLWEAP software default parameters were selected to conduct the analysis, unless field records provided in the database showed a different parameter, e.g. thickness and type of hammer cushion. In summary these GRLWEAP defaults were:

- The detailed soil resistance distribution option was used and imported from DRIVEN (see Figure 2.1) as well as the percent of capacity from side shear from the "Drive" option only.
- Unless indicated otherwise, all default hammer efficiencies and accessories were used. If multiple hammer cushion leads were indicated in GRLWEAP then a lead 4 in to 6 in larger than the pile diameter was used. If no hammer cushion parameter were available in the library a cushion was selected from the closest matching hammer ram weight was used.
- Following the Phase 1 recommendations of Mr. Robert Miner, a more detailed breakdown of side damping values was used for intermediate soil types between clays and sands as shown in Table 2.1. A single side damping value was determined based on each layer's percentage contribution to static friction capacity.
- The toe quake break point in moving from Dia/60 to Dia/120 was not defined by any manual. This was taken as  $34^\circ$  in cohesionless soils and 1500 psf in cohesive soils.

- Driving strength Loss Factors were left as 0.0 and no Set-Up Gain/Loss Factors were ever used. All recommendations contained in DRIVEN and the FHWA pile manuals for pile plugging of 'H' and pipe piles were followed.





## 3.0 PSU DATABASE DEVELOPMENT

The quantity and quality of information required for GRLWEAP pile analysis was considerable. The first key task for the research team was to search and build a complete and full case history detail database. ODOT offered two databases as the primary sources to begin gathering available pile case histories and build a master database: *PDLT2000* and Deep Foundation Load Test Database (*DFLTD*). An Excel<sup>®</sup> spreadsheet version of *PDLT2000* was created by WSDOT for LRFD calibration of the Modified Gates equation resistance factor and supplied to the research team. *DFLTD* compiled by FHWA was supplied by ODOT to the research team. (For clarity, any database names appear throughout this report in *italics*.) Two other large databases, called *FL database* and *FHWA database*, were secured and, together with *DFLTD* and *PDLT2000*, enabled researchers to build a quality, purpose designed, case history set of pile data. The additional databases helped ensure full confidence for this calibration effort by allowing cross checks for errors, including additional cases histories, and resolving anomalies. For consistency, names of the source database were not altered or renamed. The new database constructed for this research effort, called *Full PSU Master* database is described in Section 3.2.

### 3.1 SOURCES

#### 3.1.1 The PDLT2000

The *PDLT2000* database was compiled from approximately 77 different project sites by Paikowsky (1994) and was used for the LRFD performance evaluation of the dynamic methods contained in NCHRP 507. The database contained 389 driven pile cases, which appeared to be sorted from data provided mostly by Pile Dynamics, Inc. The database included some or all of the following pile case history data pertinent for this study:

- geographical location by state, province and country, and site reference numbers,
- pile type, size, length and penetration depth,
- soil type along the side or tip of the pile,
- hammer type, rated and delivered hammer energy,
- measured blow counts at EOID, BOR, or EOR,
- soil quake and damping parameters on pile tip and side,
- CAPWAP summary analysis data, and/or
- pile capacities, such as Davisson's Criteria or DeBeer, determined by the static load test results.

Of the 389 case histories, the database had a total 210 driven pile cases with separated driving times. Among these were 83 pile cases having data at the time of EOID and BOR, and 73 cases with BOR only, offering a total of 156 pile qualified cases known to be restruck. These are shown in summary form breakdown in Table 3.1 below. However, complete soil information for each layer, pile driving logs, the time delay from EOID to BOR, or the static load test complete result, did *not* exist in the database for all of the 156 piles. These were significant omissions when attempting DRIVEN and GRLWEAP for capacity and which required a considerable search effort to secure the missing data.

**Table 3.1: Pile case histories in PDLT2000 by pile type and driving time**

Number of Tested Piles			
Pile Type	#	Driving Time	#
Pipe Pile	71	EOID only	54
H-Pile	37		
Con'c Pile	98	BOR only	73
Timber	2		
Monotube	2	EOID & BOR	83
<b>Total</b>	<b>210</b>	<b>Total</b>	<b>210</b>

The *Full PSU Master* database (Section 3.2) included 156 qualified driven pile case histories from the *PDLT2000* database shown in Table 3.1. These 156 piles include a subset of 91 piles matched to the 99 piles reported in the NCHRP 507 study.

For DRIVEN and GRLWEAP software application, field subsurface profiles and shear strengths were required; however, the *PDLT2000* included only soil type information along the shaft and at the toe, with no indication of layering or soil properties. There were some parameters for which the *PDLT2000* was found to be consistently erroneous, or inexact, when compared to the values recorded for the same pile in other databases and from other reports and articles. These included the pile blow count, modulus of elasticity, pile length, and the penetration depth.

### 3.1.2 The FHWA DFLTD Database

The *DFLTD* developed by the FHWA (*Raghavendra, et al. 2001*) consisted of over 1000 load tests on driven and drilled deep foundations gathered and updated over a 15-year period with soil profiles and detailed foundation test data. Updates appeared to have stopped at, or about, the year 2000. The database did have a useful function for user-interface query applications, which made it easy for a User download of all of the pertinent information, e.g., location, pile and hammer details, driving logs, load-test, and soil-test data. Furthermore, the database included several analysis methods to predict the static bearing capacity with Alpha, Beta, Nordlund, Gates, and Coyle's static capacity methods, and the load test failure defined from Hansen, Davisson's criteria, DeBeer, and Max Curvature interpretation methods.

The information offered in this database supplemented very well the information provided in *PDLT2000*. However, after securing other materials, *DFLTD* was also shown to have anomalies, which were likely caused by simple input key-stroke mistakes during the compilation of the source data from the large number of project sites and state DOTs. One limitation of the database was that pile driving records showed the blow counts by depth, but had no calendar and/or clock time delay shown of the driving log for the restrrike or other driving interruptions. When generating the *Full PSU Master* database, the blow counts were checked, where possible, with other databases, e.g. *FL database*, *FHWA database*, and are introduced below. *DFLTD* also provided additional case histories *not* contained in *PDLT2000*.

### 3.1.3 Other Databases

With the assistance of Florida DOT, a load-test database established in 1994, in the LOTUS-123<sup>®</sup> format, was converted to Excel<sup>®</sup> spreadsheet format and was called the *FL database*. The database contained 72 driven pile load-tests gathered from 1985 to 1991 in Florida and 120 drilled shaft data from 1962 to 1989 at approximately 43 different project sites. It contained pile and hammer information, driving blows, load-settlement results, insitu test results, and the predicted capacity from the SPT91<sup>®</sup> program for the driven piles. Most information in the data seemed to have been used to build the Florida entries in *DFLTD* or to have the same background of data since all the information shown in both was similar.

The University of Florida provided an additional Florida database. The *Deep Foundations Database* was a product of the University of Florida and the Florida DOT. Prof. McVay of the University of Florida sent a copy of this database to the research group. This was a Microsoft Access<sup>®</sup> document that included: pile type and dimensions, boring log data, driving log, and pile load test results for a total 627 driven piles and drilled shafts. Not all of the driven pile case histories were included in the *PDLT2000* or the *DFLTD*, but most of the piles in the *Deep Foundations Database* with restrrike and load test information were included in these two databases. However, three new pile case histories were located in this database and entered in the *Full PSU Master*. Additionally, several case histories with anomalies and missing data were resolved by locating their records in the *Deep Foundations Database*.

From the cooperation of Prof. James Long at the University of Illinois, a database reporting almost 200 pile load test details, called the *FHWA Database*, was provided to the research group. Among the 200 pile cases, 99 pile case histories met requirements and were used for the wave equation calculations contained in the earlier FHWA effort at determining pile driveability and capacity (*Rausche 1997*). Included in these requirements in this earlier study were that blow counts at BOR should be less than 30 BPI and comparable time delay between EOID and BOR should be found between EOID and the static load test. The *FHWA database* showed a wide variety of information about the driven pile load tests, except the subsurface information for each soil layers. This *FHWA database* consisted of data in five areas: pile details, pile location, hammer, hammer ram and helmet weight, and penetration depth at the EOID and the BOR. Soil layer details from the *FHWA database* could be crosschecked with the *DFLTD* data by matching the static capacity and the dynamic capacity test results. A total of 25 pile cases could be identified that were not in the *PDLT2000* database, but they lacked water table information. Further, among the 200 data in the *FHWA database*, aside from the pile cases shown in

*PDLT2000* and *DFLTD*, 21 additional piles showed up as new cases. These pile cases had almost all the field test data, but no soil information of any kind. Unfortunately, this research effort was unable to locate the additional spreadsheets cited by the FHWA report (*Rausche 1997*) and therefore, these 21 additional piles could not be analysed.

Prof. Roy Olsen of the University of Texas at Austin supplied the research group the results of large numbers of California load tests conducted by Caltrans in a Microsoft Access<sup>®</sup> document. Each pile case history included project name and location data, site investigation and laboratory testing results, and static load test capacity. The database included 28 driven piles that were restruck and load-tested, but no blow counts at EOID or BOR were included in this document. A limited number of the piles were identified in the *Full PSU Master* database from previous sources; but the majority was inducted into the *Full PSU Master* as new pile case histories.

### 3.1.4 Other Sources

Additional pile case histories were found by an extensive review of recent geotechnical literature and requests to various DOTs for new pile case histories that were not present in any database previously reviewed by the research team. Considerable effort was spent in identifying new complete case histories, which required as a minimum for this research:

- A soil profile including a basis to determine shear strength from either in situ or laboratory testing,
- Pile type, size, and length,
- Full driving hammer and accessory details,
- Field blow counts at EOID and BOR, and
- Davisson's interpretation of pile capacity from the static load test.

Significant additional case histories, which qualified for analysis, were found in the states of Texas, South Carolina, Michigan, Utah, and Massachusetts. Other states providing incomplete case history documentation that subsequently could not be analyzed were North Carolina and Louisiana. In general, any private consultant and non-state transportation agency published case history rarely contained sufficient information for full analysis, but the data were included in the *Full PSU Master*.

## 3.2 FULL PSU MASTER DATABASE

The research group created two Microsoft Excel<sup>®</sup> spreadsheets containing separate tabs for the DRIVEN input, GRLWEAP input, Summary, Output, and Notes and References. Each of the fully qualified case histories was analyzed using DRIVEN and GRLWEAP and the results summarized for the purposes of statistical calibration of the resistance factor for EOID and BOR. The two created spreadsheets were the *PSU PDLT2000 Master* database and the *Full PSU Master* database. The *PSU PDLT2000 Master* database contained the 156 driven pile case histories extracted from the *PDLT2000* database supplemented by additional details from the *DFLTD*. The *Full PSU Master* reached a total sum of 322 driven piles from a number of

different sources identified above and included all the *PSU PDLT2000 Master* cases. *PDLT2000* and *DFLTD* cases contributed over 50% of the total number of case histories finally entered into the master. A breakdown of all sources included in the *Full PSU Master* database is shown in Table 3.2. There was considerable overlap between the numbers of pile case histories because data were tracked to more than one source, i.e. the total sum of the case histories in Table 3.2 is greater than the total number of case histories present in *Full PSU Master*.

**Table 3.2: Source of data for pile case histories for resolution of errors and anomalies**

Source of Pile Case History	Pile Case Histories in <i>Full PSU Master</i>
<i>PD/LT2000</i>	156
<i>DFLTD</i>	102
Prof. James Long	28
Data sent by state DOT	18
Data for state DOT project, but not sent by DOT	61
Scholarly articles	60
TOTAL – represents overlap between sources	425

### 3.2.1 Input Quality Tier

Allen et al. make clear (*Allen, et al. 2005*) that for any quality LRFD calibration, the statistical quantity and quality of case history data must be assessed and reported. In this study, the assumptions made to study effects of unresolved anomalies were expected to affect the quality and confidence of the case history capacity prediction. These may, if not tracked and assessed, erode the quality of the calibration resistance factor by increasing statistical coefficients of variation. For this reason, each pile case history included in *Full PSU Master* database was assigned an input tier number that described the level of reliance on assumptions in input to analyze the case history in both the DRIVEN and GRLWEAP software. Input tiers ranged in value from 1 to 3, where a pile case history with the most complete set of input parameters was assigned to Tier 1 and a pile case history with the most incomplete set of input parameters that could not be analyzed without further key information (e.g. pile blow count) was assigned to Tier 3. Each of the Tiers 1 and 2 had sub-categories with more specific requirements, as described in the following sections. The input tier classification of a pile was related implicitly to the quality and completeness of the data in the pile case history, which changed according to new information obtained during the course of the research.

A summary of the tier rubric developed is presented in Table 3.3. If anomalies were discovered during initial entry of a case history into the *Full PSU Master*, their severity would be reflected in the initial tier assigned. Once flagged, efforts were made to resolve the error.

Pile case histories placed in input Tier 1 could be analyzed in both DRIVEN and GRLWEAP with no assumptions and were broken down into three sub-categories: 1a, 1b, and 1c. Piles placed in Tier 1a had full soil data, including measured internal angles of friction and/or laboratory shear strengths of cohesive soils, the hammer type and driving accessory details were known, and the pile information was known including composition, size, and driving state

(plugged or unplugged). In addition to this, Tier 1a piles had Davisson’s capacity and PDA/CAPWAP capacity available with no anomalies reported in either the bore log or driving log that might significantly affect prediction. The number of BPI at EOID or BOR for Tier1a had to be less than 10.

**Table 3.3: Summary of the input tier rubric utilized for analysis**

Tier	Definition
1	a Full soil data is reported, including measured internal angles of friction and/or laboratory shear strengths of cohesive soils. Hammer type and driving accessory details are known. All pile information is known including composition, size, and driving state (plugged or unplugged). Davisson’s capacity and PDA/CAPWAP capacity is available (possibly reported in <i>DFLTD</i> ). No anomalies are reported in either the bore log or driving log that might significantly affect prediction.
	b All criteria is met for Tier 1a except no PDA/CAPWAP information is reported, or pile is driving harder and $10 \text{ BPI} < N < 15 \text{ BPI}$
	c Relaxation detected with blow count $\text{EOID} > \text{BOR}$ and should be confirmed, or Very hard driving with $N > 15 \text{ BPI}$ .
2	a Typically DRIVEN can be performed; however, GRLWEAP cannot be routinely performed but is attempted with assumptions. All pile and hammer information and details are known, but there may be some anomalies to resolve, data missing, or anomalies in EOID or BOR blow counts. Some soil strength properties with most other key properties known.
	b Typically neither DRIVEN nor GRLWEAP can be routinely performed. All criteria are met for Tier 2a, except assumptions on cohesive soil shear strength values are required, or there is a lack of water table information for granular soil.
3	No soil data or hammer information known. Non-typical soil types, e.g. sandstone. No field blow counts or load test results are available.

Dynamic testing to determine the ultimate static pile capacity requires that the driving system should mobilize most of the available soil resistance acting on the pile. However, when pile penetration resistances approach 10 BPI, the soil resistance may not be fully mobilized at, or near, the pile toe. Blow count effects are discussed in Section 6.2. In these circumstances, FHWA reports that dynamic test capacities tend to produce lower bound capacity estimates (*Hannigan, et al. 2006*). Pile displacement during dynamic testing must be large enough to fully mobilize the side shear and end bearing components to determine reasonable ultimate pile bearing capacity. However, matching to Davisson’s capacity may not increase bias to the conservative side necessarily as Davisson’s is a restricted settlement based criteria. Piles in Tier 1b met all of Tier 1a requirements but had either no PDA/CAPWAP information or the pile was driving harder so that the number of blow counts at EOID or BOR ranged from 10 to 15. Tier 1c piles were either very hard driving, with the number of blow counts greater than 15 at EOID or BOR, or relaxation was detected such that EOID blow counts were greater than those at the BOR condition.

Piles in Input Tier 2 could only be analyzed with certain assumptions and were broken down into subcategories, 2a and 2b. Piles in input Tier 2a could typically be used in DRIVEN without assumptions but needed to follow key assumptions to be used in GRLWEAP. Input Tier 2a piles were those cases for which all pile and hammer information and details were known, but they may have had some anomalies to resolve such as the BOR and/or EOID blow counts. Other small anomalies included moderate assumptions to analyze soil profile, e.g. extrapolation of soil

profile from the existing bore log data to a depth past the pile's tip, or poor correlation between the bore log's SPT count and driving log's installation record.

Tier 2b piles could not be performed in either DRIVEN or GRLWEAP without key assumptions, e.g. assumptions on cohesive soil shear strength values (values were based on CPT or SPT data, unless layer was not significant to bearing capacity), or for granular soil water table information.

Pile case histories in Input Tier 3 could not be analyzed by DRIVEN or GRLWEAP due to missing or fatally anomalous input parameters. For the most part, piles in Input Tier 3 were missing soil and hammer data. Some pile case histories were assigned to Input Tier 3 due to a lack of blow count data at either EOID or BOR despite a complete set of values in other parameters.

Missing data and data anomalies were continuously resolved for the *Full PSU Master* entries as new information became available. The assigned input tier for a specific pile could change over time often improving its ranking with the addition of data that allowed the pile to be analyzed with fewer assumptions. The quality improvement of the data set as a whole could be observed and shared by the research team by observing the number of piles in each tier. The change in the number of piles in each tier over the course of the research task can be seen in Figure 3.1 for the *Full PSU Master* piles throughout 2009 and early 2010 when a significant effort at data gathering took place.

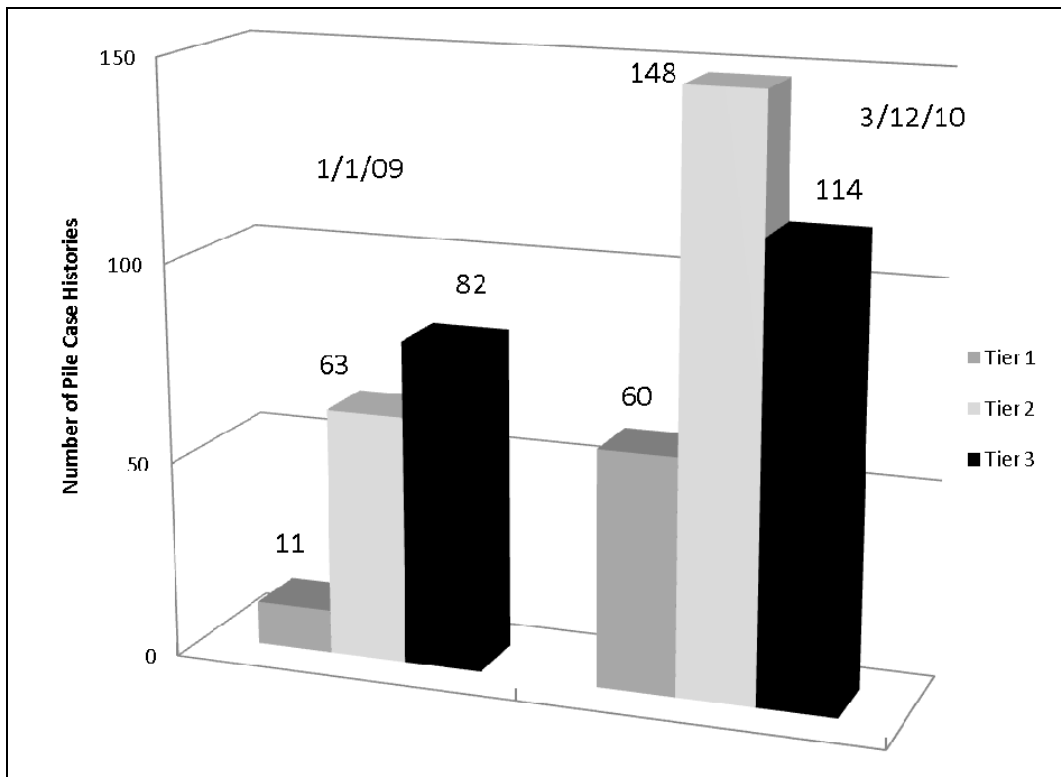


Figure 3.1: Growth of cases in the Full PSU Master by input tier



As the figure illustrates, in addition to the total number of pile case histories in the *Full PSU Master* database increasing, the number of piles in the upper two tiers steadily increased over the course of this 15 month period. This trend of increasing quality of input parameters was a product both of the deliberate search for new pile case histories with high-quality input data and the ongoing endeavor to resolve anomalies and locate missing data. Input tiers were a means of organizing data by level of reliance or degree of completion for input parameters. Following analysis, output results were also organized by level of confidence in prediction including reliance on the data. These output ranks are discussed in Section 4.3. Both input tiers and output ranks are recorded in the *Full PSU Master* spreadsheet.

### 3.2.2 Case Histories Overview

The construction of the *Full PSU Master* dataset was to ensure a reasonable match to piles by their pile/soil breakdown to those driven for ODOT bridges. The sources of the pile case histories included in the *Full PSU Master* spreadsheet were, however, unevenly distributed throughout the U.S. and other countries. The large majority of cases were within the U.S., but there were also a number of cases from Canada. A breakdown by percent is given in Table 3.4 and Figure 3.2 below.

**Table 3.4: Geographic distribution of Full PSU Master pile case histories**

Location	Number of Pile Case Histories	Percentage of Total
U.S.	267	83%
Canada	29	9%
Unknown	9	2.8%
All other countries	18	5.6%

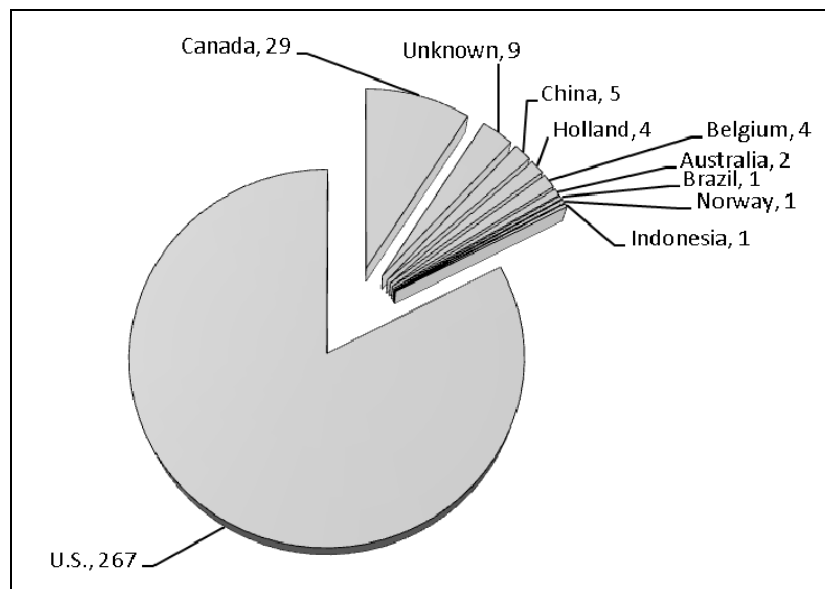


Figure 3.2: Distribution of Full PSU Master pile case histories worldwide

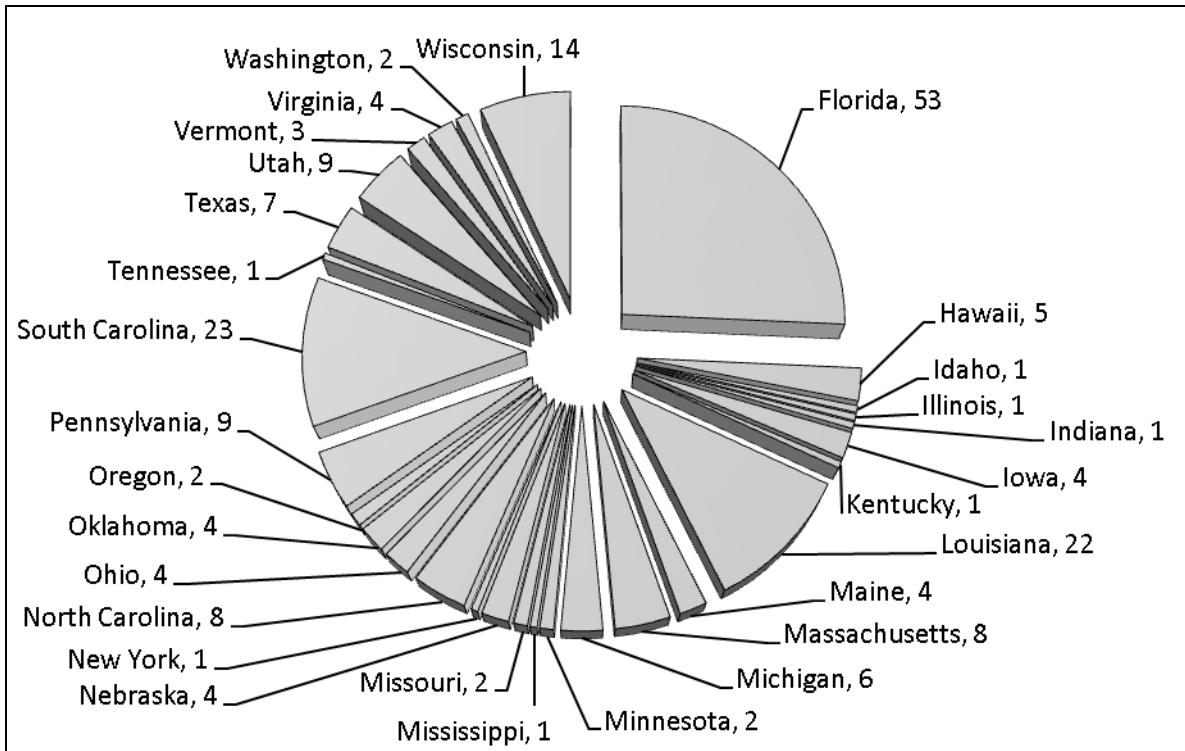


Figure 3.3: Number of pile case histories in *Full PSU Master* by state

Piles from the U.S. formed the vast majority of case histories. Figure 3.3 and Figure 3.4 break down the number of case histories per state and by the five FHWA regions. Clearly, the Northwest was under-represented. It should be noted that due to the FHWA regional division of the country, there were a considerable number of piles in California that were listed under the Southwest Region.

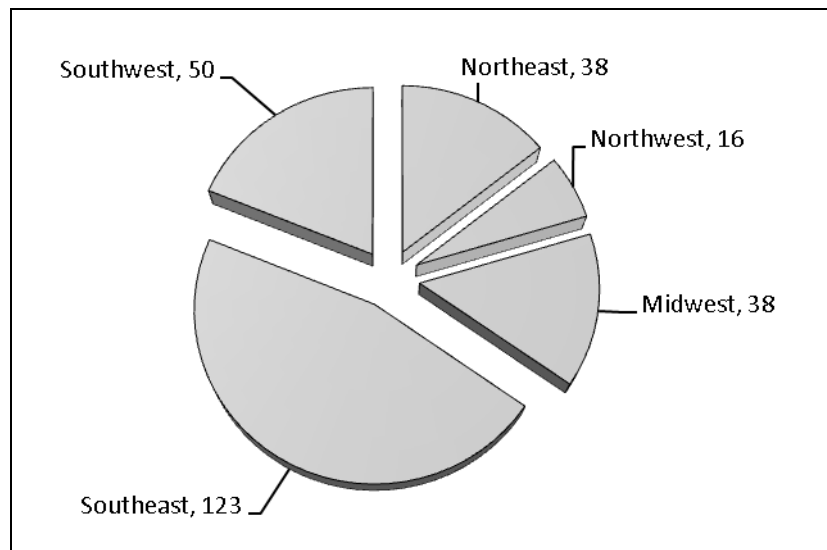


Figure 3.4: Source of *Full PSU Master* pile case histories by region

Approximately one-third of the original 156 piles identified in *PDLT2000* had insufficient data for satisfactory DRIVEN and GRLWEAP analysis and were in Tier 3. It should be noted that of the 322 piles in the *Full PSU Master* database, approximately one-third were also in Tier 3.

No useful soil profiles to obtain properties were contained in *PDLT2000*. Therefore, heavy reliance was placed on *DFLTD* and additional databases from the Universities of Illinois and Florida, Florida Department of Transportation (FDOT), and some published literature to secure SPT data and, occasionally, CPT data. As introduced in Section 2.1, three general subsurface soil types were used for categorization: Clay, Sand and Mixed. Soil types, broken down by both pile type and soil category, were assigned to the case history for ease of organization using an 80% threshold contribution from the DRIVEN calculated capacity and are shown in Table 3.5.

**Table 3.5: Breakdown of all 322 piles in the Full PSU Master by pile and soil type**

Major Contributing Soil Type	Pile Type					Total Cases for Soil Type
	Concrete Pile	H-Pile	Closed End Pipe Pile	Open Ended Pipe Pile	Other	
Sand	62	19	17	4	1	103
Clay	17	5	10	1	0	33
Mix	14	9	16	5	1	45
Unknown	54	24	38	20	5	141
Pile Totals	147	57	81	30	7	<b>Total Piles 322</b>

The *Full PSU Master* database contained 81 cases where the calendar and clock time were known at the time of EOID and at the BOR, as well as the time for static load test. This knowledge permitted an examination of cases where restrrike or load testing may have occurred either comparatively early or late for representative set-up to occur. A total of 84 piles reported multiple restrrike blows, but few qualified for DRIVEN and GRLWEAP analysis.

Cross examination of *DFLTD* and *PDLT2000* showed a total of 72 of the original 156 piles in *PDLT2000* had anomalies, and 29 piles in *PDLT2000* had no site I.D for any follow-up investigation. Of most concern was the misreporting on pile blow count, N, especially at BOR. A total of 28 piles had more than one anomaly. After resolution of errors and anomalies, 103 of the 156 *PDLT2000* entries were analyzed, and these are discussed in the following section. Based on thorough examination, the most reliable source, judged by multiple source data confirmation, was from *DFLTD*. Case history summary details for each case history contained in the *Full PSU Master* are given in Appendix A.

### 3.3 CASE HISTORY ANOMALIES AND ERRORS

It was essential that the most accurate data were used for reliable calibration, as well as the best possible case history population match. The majority of pile case histories in the *Full PSU Master* had some identification and some limited geographical location data, which allowed for

matching pile case history between the two principal sources of data: *PDLT2000* and *DFLTD*. The type and dimensions of the pile, blow counts at EOID and BOR, and other pile characteristics were available for most piles in both databases. Soil data in the *PDLT2000* were confined to an assigned value of soil type along the shaft and soil type at the toe with no values for strength, unit weight, or water table. Therefore, additional soil data from other sources was critical for use of DRIVEN. In cases where piles from the *PDLT2000* were matched with piles in the *DFLTD*, soil data were obtained from *DFLTD* by matching a pile to a specific soil profile. *DFLTD* often contained sets of site investigation data on multiple boreholes when determining the applicable soil profile to the pile’s identity. Matching soil data in the *Full PSU Master* to a pile case history in the *DFLTD* was achieved by comparing the driving log for the pile and the log of the SPT blow counts. The profile of SPT values in the boring log most applicable to the pile correlated quite well to the blow counts in the pile’s driving log. For example, areas of hard driving were seen to match with depth (or roughly with depth in the case of slightly different elevations) between the boring log and the driving log indicating that the soil properties were similar and could be modeled in DRIVEN. If possible, the missing data for each case history were found in other databases, such as *FHWA database*, or even from original site documents obtained by a thorough search of geotechnical literature, private companies, and state or local agencies. Unfortunately, not all pile case histories from the *PDLT2000* included in the *Full PSU Master* could be matched to piles in the *DFLTD*.

There were several piles in the *Full PSU Master* data set for which each database reported a different value for a specific parameter. For example, the *PDLT2000* reported a blow count of 7 BPI at BOR for a pile, while the *DFLTD* and source drive log reported 16 BPI on the same fully matched pile. For the most part, the majority of these “anomalies” were present in the *PDLT2000*-based cases of the *Full PSU Master* database as the pile case histories added to this original data set were less likely to have more than one source from which a disagreement in data values could result. It was often the case that a pile case history had more than one anomaly. The percentage of piles with anomalies and the breakdown by anomaly types for the *PSU PDLT2000 Master* database is shown below in Table 3.6 and Figure 3.5. The nature of an anomaly varied, though most of them resulted from a difference in blow count values from one or more sources.

**Table 3.6: Number of piles and anomalies found in the 156 from *PSU PDLT2000 Master***

Major Contributing Soil Type	Pile Type				Total Cases for Soil Type
	Concrete Pile	H-Pile	Closed End Pipe Pile	Open Ended Pipe Pile	
Sand	50	14	12	0	76
Clay	10	2	9	1	22
Mix	12	5	13	4	34
Pile Totals	72	21	34	5	132

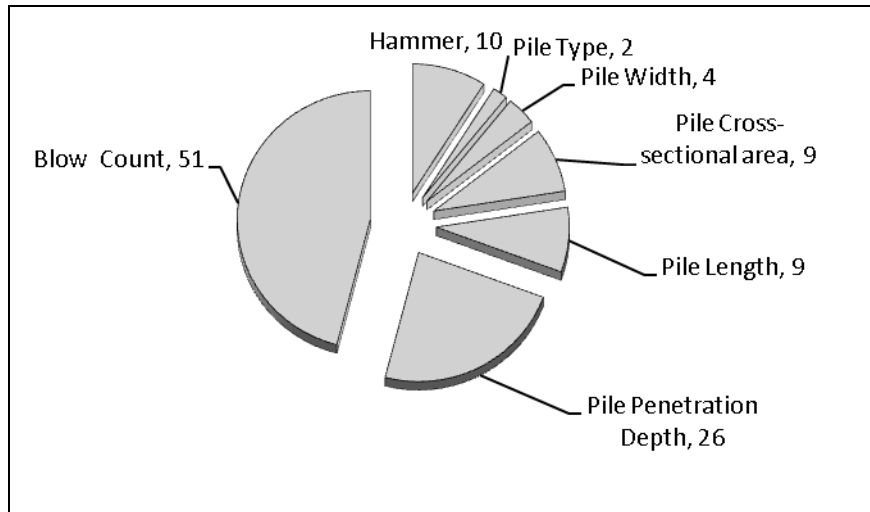


Figure 3.5: Source of anomalies between databases for *Full PSU Master*

Missing and anomalous data were first cross-checked with available databases. If the anomaly or missing data were still unresolved but sufficient site and location data were available to find the original project with the appropriate state or local agency, then direct inquiries were made. Some data could be obtained by using sources not associated with the pile itself. For instance, values such as the location of a water table or a range of typical cohesion values in local clays was obtained by searching the United States Geological Survey (USGS) data or directly from local geotechnical practitioners familiar with the pile's locale.

The structured approach for cross checking was the result of considerable planning and discussion, and all changes for anomaly resolution were carefully documented. For a pile case history with more than one source for a disputed value, if all sources were relatively equal in quality, then the value found in more than one source was determined to be more accurate. Two sources reporting the same data value were taken as more reliable than one other source reporting a different value. When more than two sources for a parameter were available, it was seldom that all of them disagreed on an anomalous value; usually two or more shared a value. There were instances in which all the available sources disagreed on the value of a parameter. In these cases, a thorough familiarity with encountering anomalies and cross-checking them with other sources led to a consistent approach to which source was most likely to be correct.

A reported value from the *DFLTD* was preferred over the *PDLT2000* value, all other circumstances being equal. This was due to the numerous times in which a value from the *PDLT2000* had disagreed with a value from the *DFLTD* or had been proven erroneous by the consistent approach of matching the pile record to another database or even original documents such as driving logs. The *PDLT2000* contained anomalous values such as pile length, penetration depth, and pile elasticity modulus. Matching values in order to resolve anomalies also revealed many cases in which blow counts were not accurately reported for EOID and BOR in the *PDLT2000*. In cases where the *DFLTD* value appeared to be erroneous or when another source disagreed with the *DFLTD* but agreed with the *PDLT2000* database, the *PDLT2000* value was used. Of the 74 *PDLT2000* matched piles in *DFLTD*, 18 had anomalies from the states of

AL, FL, LA, SC, and WI. Of these states, the highest percentage of any state contribution to *PDLT2000* with anomalies was in SC with 30%.

For parameters in which several had missing or anomalous data, a sensitivity analysis was performed in order to determine the criticality of the value. Sensitivity analyses were a critical portion of the research effort to establish that assumptions made would not have statistically significant effect on results. If the value in question was found to produce less than ten percent difference between the GRLWEAP reported capacity values, then the analysis was considered relatively insensitive to the parameter. It was determined that in the majority of cases, the calculated GRLWEAP capacity was largely insensitive to values for the water table. However, GRLWEAP was quite sensitive to values for hammer energy and driving accessories. Therefore, the resolution of missing hammer data was given more priority than that of missing water table data. The input tier value for a pile with missing hammer data was lower than for a pile with missing water table data (see Section 4.3).

In summary, of all AASHTO declared nominal capacity methods, the GRLWEAP bearing graph analysis was the most demanding for input data quality and quantity. Before calibration efforts began, any existing databases used were carefully reviewed and data were validated.

### **3.4 SUBSURFACE INFORMATION, QUALITY, AND INTERPRETATION**

The *Full PSU Master* database was created from several different source databases and other reports and articles; often data sets collected for research had a variety of different research foci and were not designed to perform GRLWEAP analysis. The quality and quantity of site investigation data varied across the pile case histories in the final database. This was expected given that these piles ranged in time over the past thirty or more years and across a vast geographical area. The original purpose of the *PDLT2000* was for the capacity prediction of driven piles as measured by PDA dynamic methods and did not include extensive analysis and discussion of the importance of soil types and specific characteristics. Therefore, soil data from the *PDLT2000* was extremely limited, and little attention was paid to obtaining additional soil data other than that provided by the sources of this database. Piles in the *PDLT2000* not identified in the *DFLTD* did not have sufficient soil data for DRIVEN analysis. This scenario was also true for piles from other databases, which included little or no soil data. As a result, the soil investigation quality of some cases in the *Full PSU Master* database was limited, so sensitivity analyses were conducted.

The DRIVEN program required a relatively modest amount of soil information, provided by most geotechnical explorations, including water table, soil unit weight, and strength parameters for either cohesive or cohesionless soils. In order to perform DRIVEN analysis, prior to final analysis in GRLWEAP, a certain minimum amount of soil information was required. For those pile case histories with soil profile data available, there were key parameters either absent or for which certain assumptions were still necessary.

For the majority of pile case histories, even when no other soil data were available, the soil type was available. Unfortunately, pile capacity could not be established by designating soil as “sand” or “clay” in DRIVEN. Additional soil documentation was necessary. When more specific data could not be secured, assumed values were used based on similar cases or from typical values. Typical values for soil unit weight from standard reference texts (*Coduto 2001*) were assumed applicable for certain soil layers in which a specific value was unavailable. However, as with other soil data, strength parameters for each pile case history were not always available. When present, they consisted predominantly of results from the SPT and, in some cases, the CPT. Laboratory data for soil strength parameters, such as Triaxial test results, were rarely present in the *DFLTD* or any of the other source databases and seldom reported in other sources of pile case histories. However, on some occasions, results from Atterberg limits testing were available from the *DFLTD*. In summary, soil strength parameters for the majority of the piles in the *Full PSU Master* were derived from in situ test results in the absence of laboratory testing results.

The applicability of specific in situ test results to a pile’s soil profile was hard to assess. The distance from a site investigation borehole to the pile was not included in any of the databases, and was rarely mentioned or included in other sources. For example, the *DFLTD* soil investigation data was matched to the pile’s driving log based on SPT data, but the actual distance of the referenced boring log to the pile was unknown. In addition to distance concerns, both the SPT and the CPT had shortcomings when used to calculate soil strength parameters, and neither test performed equally well for all soil types. For the majority of pile case histories, the only soil data available came from one or both of these two in situ tests. The majority of the in situ soil strength values were in the form of SPT blows per foot. These blow counts were uncorrected for energy or for overburden effects in the *DFLTD*. In other sources, the nature of the N value was often unspecified, in which case they were assumed uncorrected.

For some of the pile case histories, CPT data were provided and often reported in *DFLTD* in addition to SPT data. *DFLTD*-provided CPT data also included sufficient data to obtain undrained shear strength in cohesive layers. These data were included in the *Full PSU Master*, and were preferred to obtaining cohesive strength values using the SPT (not endorsed by FHWA). It should be noted that the *DFLTD*’s CPT analyses occasionally provided soil strength values that were high to the point of being erroneous in comparison with the soil’s density and consistency according to SPT results. In these cases, the cohesive soil strength was derived from SPT data using the method described previously. In some cases CPT data were provided in the absence of any other soil data, and a consistent approach was taken to deriving soil strength parameters.

## 4.0 BEARING CAPACITY METHODOLOGY

### 4.1 EOID AND BOR MODELING AND BLOW COUNTS

For the complete pile case history sets found in the *Full PSU Master* database input Tiers 1 and 2, GRLWEAP analyses provided a bearing graph as discussed in Section 1.2.1. Analyses required careful evaluation and separate analysis for a total of double the number of qualified cases, as each required both the EOID and BOR capacity predictions. As well as changes in blow count causing capacity changes viewed from the same bearing graph, different graphs for EOID and BOR can result from changes to hammer models and/or substitution of a well-used stiffer cushion on concrete piles, as endorsed by the FHWA. Default GRLWEAP parameters called for a plywood pile cushion of 6" thickness with an elastic modulus of 30 ksi at EOID on concrete piles. Due to driving effects, BOR analysis on concrete piles always followed the rule-of-thumb discussed in FHWA (*Hannigan, et al. 2006*) that a used pile cushion was inserted of usually half the thickness and twice the stiffness relative to its EOID properties. The BOR pile cushions were assumed to be 3" thick plywood cushion with an elastic modulus of 60 ksi. Stiffer cushions will allow a larger amount of driving energy to be delivered to the pile and will lower the blow count required to overcome the same static capacity. It is more likely on BOR that a stiffer cushion will show a similar or higher blow count compared to EOID indicating pile set-up. Further, a reduction in observed blow count at BOR, for the same hammer, may not necessarily indicate relaxation. This difference in bearing graphs and the relationship between blow count and blows for EOID and BOR is illustrated in Figure 4.1 for one of the prestressed concrete PSC piles in the *Full PSU Master*: a 16.5" octagonal prestressed concrete pile.

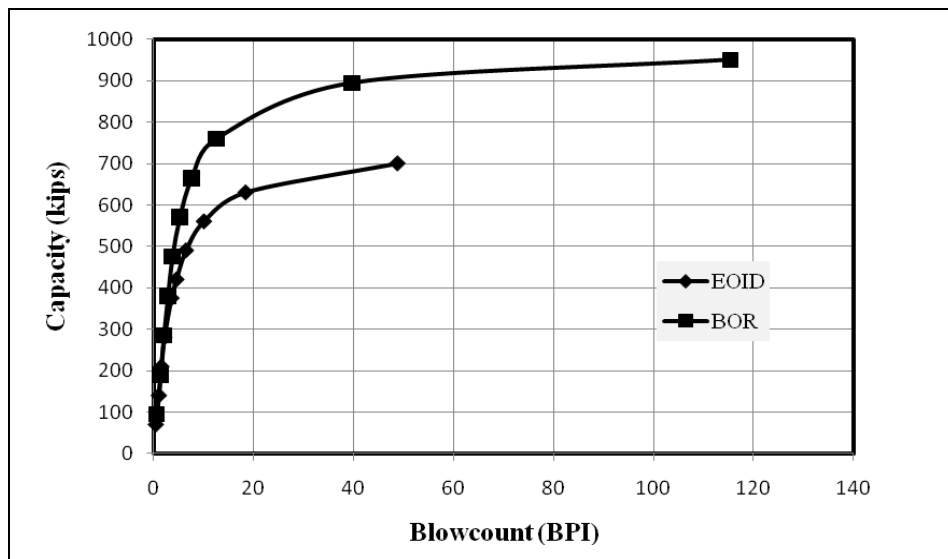


Figure 4.1: PSU Case History #293 - effects to the bearing graph of stiffer restrrike cushion



Comprehensive discussion on the User input requirements to GRLWEAP were discussed in Section 2.2 covering pile, hammer, driving accessories and the soil model. In summary, all EOID and BOR modeling used only default parameters for the hammer, accessories, and the soil distribution given by DRIVEN.

The recalibration effort utilized the ratio between Davisson’s criteria measured load test capacity and the corresponding GRLWEAP capacity prediction at both EOID and BOR condition with:

$$\lambda = \frac{\text{Davisson's Capacity}}{\text{GRLWEAP Bearing Graph Capacity}} \quad (4-1)$$

So,  $\lambda$  expresses the GRLWEAP capacity of each case history as either a safe or unsafe prediction. Clearly, a case history  $\lambda$  value at EOID or BOR that is less than 1 is unconservative, while a value greater than 1 is a conservative prediction compared to the Davisson measurement. The average  $\lambda$  from a sample of case histories is called the bias and has previously been designated  $\lambda_R$  for resistance factor calculation, but hereafter will be termed mean  $\lambda$  for the full sample statistical mean ratio of bias.

## 4.2 OUTPUT RANKING

In accordance with the quality metric guidelines suggested by AASHTO (*Allen, et al. 2005*), the GRLWEAP output was assigned a qualitative output rank ranging from 1 to 4 designed by the research group to record confidence levels in results. Ranking of the outputs allowed researchers to accomplish the following: summarize the analysis process, tag critical assumptions, and flag problematic cases for further examination including discussion with selected members of the TAC and conduct possible re-analysis. Table 4.1 summarizes the output ranking designed for this study.

**Table 4.1: Summary of output ranking requirements**

Rank	Definition
1 Good	No key assumptions were required for analysis and no anomalies present in output. Typically in soft soils GRLWEAP capacity approximately equals DRIVEN capacity, and for harder soils GRLWEAP capacity is less than DRIVEN.
2 Acceptable	Possible minor anomalies present, or non critical assumptions made, e.g. hammer type not clear but matched from library, assumed water table in sand, GRLWEAP capacity greater than CAPWAP. Davisson’s capacity is significantly greater than the DRIVEN capacity. (Disagreement to Davisson’s is possible in end bearing piles or hard driving which may not be mobilizing significant side friction.)
3 Poor	No hammer cushion match. Significant anomalies. Pile showed relaxation on BOR. Bearing graph overly sensitive to damping and/or side friction to total capacity percent distribution.
4 Ineligible	Lacking information to become a statistical $\lambda$ , e.g. lacking Davisson’s capacity or field blow count.

Placing pile cases into both input tiers (Section 3.2.1) and output ranks enabled researchers to target and troubleshoot problematic cases and address any trends that showed during statistical analysis.

### 4.3 GENERAL SENSITIVITY COMMENTS

As discussed previously, GRLWEAP is a finite difference based pile driving modeling program that reports permanent pile “set” in units of length, and calculates from the “set” inverse the pile advancement rate in BPI. Any pile placed in Tier 1 or Tier 2 had EOID and BOR blow count values known, and the GRLWEAP bearing graph established predicted equivalent static capacity. The stepping up of static capacity by GRLWEAP, with the bearing graph option, produced the graph and caused the output to be relatively insensitive to minor alterations in soil properties and variations of pile length. Holding the same soil type constant would require significant differences to the center of soil resistance depth and/or the percent allocated to side shear to modify the predicted capacity. However, sensitivity analyses were always performed when assumptions were required. A threshold of 10% difference in predicted capacity values was used to separate those cases overly sensitive to assumptions from those that were not overly sensitive. Site investigations should always comply with the minimums recommended by FHWA (*Hannigan, et al. 2006*) to produce satisfactory GRLWEAP capacities. The statistics reported in Section 5 show a correlation between input quality of the source data and output quality confidence of the predictions. Sensitivity analyses were always used to determine what the affect of a missing piece of input information had on a case’s calculated GRLWEAP capacity.

Values for the location of the water table were also assumed for both cohesive and cohesionless soils based on the relative insensitivity of pile capacities calculated using GRLWEAP to the state of the soil as saturated or unsaturated. The resulting sensitivity was determined for each pile, when necessary, on a case-by-case basis. Though DRIVEN can be insensitive to the water table location and soil unit weight, the calculation of pile capacity in the program was strongly dependent on the input soil strength parameters. The general trends found were the following:

- Water table location only mildly affected results in cohesionless soils.
- Shear strength variations showed little effect on capacity as the percent allocated to side shear and the shape of the distribution may not change.
- GRLWEAP capacity proved to be relatively insensitive to slight variations in pile tip depth.

The trends discovered during the analytical process were consistent with those reported in Phase 1 research effort (*Jackson 2007*). The ability to study by sensitivity analysis the effect of assumptions on a case-by-case basis enabled researchers to promote more cases to a higher output rank than to demote cases to a lower rank.

## 4.4 PILE BLOW COUNTS

Of all case history variables, the GRLWEAP nominal bearing capacity was most sensitive to pile blow count, which was the easiest to reliably document. However, there was no consistent definition of the restrike blow count in any pile national standard or design manual. The source databases confirmed this lack of clarity. A large variation in installation condition requirements, calendar times, and field practice norms existed in the database due to the large span in years and geographic locations from which the cases originated. Fortunately, for the purposes of resistance factor calibration, the inherent variability of national standards was captured in the *Full PSU Master* by keeping a broad database. For the best possible resistance factor accuracy, any known errors in the restrike blow count were detected and corrected. *DFLTD* had no separation between EOID and BOR blow count, but it did present the complete driving record.

Among the 156 piles based on *PDLT2000* listed in the *Full PSU Master* sheet, 74 piles were matched in the *DFLTD* database. These offered high quality data confidence when the data matched exactly in each database. There were some blow count assumptions made to use the 74 piles in Tier 1 and Tier 2 for this calibration analysis. Driving records in *DFLTD* represented the blows that increased depth by one-foot intervals up to a maximum integer value with subsequent values in decimal format. It was assumed the integer values were for initial driving and the decimal values were for restrike. A particular problem existed with the 82 piles not found in *DFLTD*. Some had listed BOR blow count but did not list the EOID blow count in *PDLT2000*. The research team worked to independently secure the missing EOID blow count.

*DFLTD* had a group of field entries for hammer and PDA delivered energy as well as entries for EOID, BOR, and EOR driving blow counts. In all cases the database value showed “0”. Without confirmation for these EOID and BOR field entries, the research group was required to use the decimal depth assumption discussed above in interpretation of the full driving log. The blows given by the decimal feet format indicated restrike had begun and represented an equivalent number of the blows per foot (this was also supported by additional data from Florida), not the actual blows between the two decimal depths. This is illustrated below in Figure 4.2.

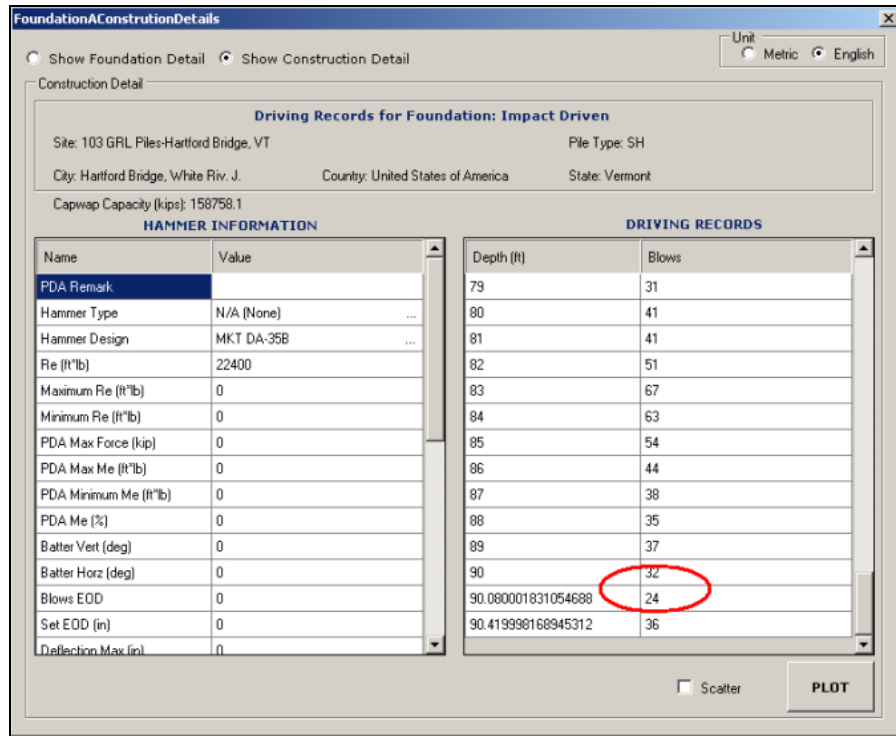


Figure 4.2: Illustration of *DFLTD* presentation in digital feet for restrrike

The penetration resistance at EOID and BOR in BPI was then simply calculated from the BPF. Following this assumption, the blow count of 32 in the figure was the penetration resistance at EOID when moving from 89 to 90 ft, and the blow count of 24 was the BOR count in the unit of BPF (but it travelled only 1 in as shown in Figure 4.2) in the *DFLTD* database. Those corresponded respectively to blow counts of 2.67\* and 2 BPI in the *PDLT2000* where the database author's asterisk denoted the blow count based on blows per real foot of penetration. After making the separation between EOID and BOR using the assumption above, only 16 of the 74 matched piles, without other anomalies, showed the blows at EOID and BOR reported in both databases were exactly the same. Of the remaining matched 58 piles between the two databases:

- 10 piles had the EOID blow count missing in *PDLT2000*, but the blow count at BOR was the same in both databases,
- 8 piles had the BOR blows missing in *DFLTD*,
- 17 piles had one of the blow counts at EOID and BOR different between both databases, and
- 23 piles had neither of the blow counts for EOID and BOR the same in both databases.

This illustrated the difficulty encountered in relying solely on blow counts in a single database and suggested that other recalibration efforts using this data may contain flaws. For each pile case matched by any source in *DFLTD*, blow count was determined by employing the decimal feet entry assumption described above.

In the *Full PSU Master* dataset only 19 case histories had multiple restrikes and load test clock times in Tier 1 and Tier 2. These blow count series carried the designation BOR1, BOR2, BOR3, etc., corresponding to their sequential order and were recorded on the *Full PSU Master* Spreadsheet “Summary” tab. Therefore, without knowing both restrike calendar day and load test calendar day, no decision could be made on choosing the multiple restrike blow number matching the load test for the large majority of piles.

In theory, it is always appropriate to leave the longest possible time before restrike to capture sufficient regain in capacity, but with production scheduling constraints in the field, contractors will often be reluctant to remobilize a crane and will likely seek restrike close to the minimum established in the specifications. Currently ODOT allows a minimum of one day. So, the best population sample fit to practice might be after a first restrike, typically of one to two days only. It is likely, with the associated repeat rise in excess pore water pressure for cohesive soils, and large soil fabric changes that piles undergoing multiple restrikes do not belong to the same GRLWEAP capacity statistical population as those at BOR1. It can also be argued that a pile at BOR2 time would not have the same driving blow count BPI as if a BOR1 had been conducted with the same time delay from EOID.

Following TAC discussions and the wide variation in case history locations and dates that load tests were conducted, the following rules were applied:

- For the 19 cases with multiple restrike values: the first beginning of restrike blow count series was selected for use in analysis.
- For cases that required driving log interpretations, the guidelines (*Hannigan, et al. 2006*) from the FHWA were followed, with a restrike recorded within the first 6 in or a maximum blow count of 50 BPI, whichever came first.
- Restrike was taken from *DFLTD* when depth began recording in decimal feet format.

For consistency, when encountering anomalies or confusing data, the GRLWEAP capacity was established using the above rules for restrike to establish BOR.

## 5.0 STATISTICAL PROFILING OF RESULTS

### 5.1 REANALYSES OF NCHRP 507 CASE HISTORY SET

To confirm the validity of the research group’s GRLWEAP predictions and to reveal any serious modeling violations, a comparison was made with the 99 pile case histories reported in NCHRP 507 using the *PDLT2000 Master*. The NCHRP 507 authors reported that the 99 case histories for GRLWEAP calibration were inherited from the earlier FHWA study conducted by the authors of GRLWEAP (*Rausche, et al. 1997*). These were assumed to contain only well defined case histories, which all included PDA/CAPWAP work, and would have placed them all in Tier 1 and Tier 2 in this study. The BOR analysis of these 99 piles was contained in the NCHRP 507 report appendix and not discussed in the main text. No description was offered in NCHRP 507 of any input and output case history quality ranking structure or the specific definition of BOR used. The research reported here compared the mean  $\lambda$  standard deviation (s.d.) and coefficient of variation (COV) utilized in NCHRP 507’s calibration of GRLWEAP to those produced in this study.

Due to the lack of full and complete source data for identification purposes, a small portion of the original NCHRP 507 cases could not be identified. Therefore, the current research comparison included a limited number of case history data from outside the original 99 case history set, but still within the NCHRP 507’s *PDLT2000* database. The inclusion of these data allowed for a comparable size population of 91 cases for statistical profile comparison. The *Full PSU Master* database for this research grew to 322 cases with 179 cases in Tier 1 and Tier 2 qualified to produce  $\lambda$  values. A summary of the results from the 99 piles reported in NCHRP 507 and the 91 NCHRP 507 matched cases, along with the full 179 cases, are shown in Table 5.1.

**Table 5.1: Comparison between NCHRP 507, PSU matched piles, and all analyzed 179 piles in the Full PSU Master**

Source	Soil Type	Pile Type	# cases	EOID			BOR		
				$\lambda$	S.D.	COV	$\lambda$	S.D.	COV
Original GRL-99 Series as Reported in NCHRP 507	All	All	99	1.656	1.199	0.724	0.939	0.399	0.425
PSU Recalculation of Original NCHRP 507 Source Data			91	1.661	1.264	0.761	1.009	0.599	0.594
PSU Tier 1 and 2 Source Data			179	1.633	1.27	0.78	0.995	0.47	0.47

The re-analysis of 91 cases from the original NCHRP 507 source data and the full analysis of the complete Tier 1 and Tier 2 source data cases at EOID matched closely to the reported EOID values in NCHRP 507. The similarities in the EOID reported results placed credence on the

present research modeling. The mean  $\lambda$  at both EOID and BOR showed improvements for the *Full PSU Master* 179 piles due to the considerable effort expended on identifying and correcting anomalies in the *PDLT2000* and *DFLTD* databases. The *Full PSU Master* s.d. results at BOR did not correspond as closely to the reported NCHRP 507 appendix values, as shown in italics in Table 5.1. But the current research improved significantly the mean  $\lambda$  at BOR, which was no longer unconservative. It can be seen that all BOR statistics displayed a much more accurate mean  $\lambda$  value with a significantly tighter statistical variation from that mean expressed by the COV. Considering the analytical methodology and no use of outlier definitions, the discrepancy between the two results was not of concern

It was inferred from the NCHRP 507 report that the data reported at EOID and BOR were not produced entirely by NCHRP 507 researchers, but made available to the NCHRP 507 study group by GRL, Inc. (*Paikowsky 2004*). Despite the fact that not all the source data were made available to this current research team, the close match was excellent verification of the present study’s analytical equivalency. It also confirmed that any assumptions made for individual case histories were defensible. It should be noted the statistics offered in NCHRP 507 may also have had outliers removed beyond +/- 2 s.d. prior to calibration which improved the statistics characteristics. In this study, statistics calculations using the 91 cases from the *PSU PDLT2000 database* and the 179 cases from the *Full PSU Master* had no outliers removed.

## 5.2 FULL POPULATION SAMPLE ANALYSIS

The *Full PSU Master* database contained 194 cases categorized in Input Tier 1 and Tier 2. After GRLWEAP analysis, 179 cases produced valid case  $\lambda$  values placed in output Ranks 1, 2, or 3 and shown above in Table 5.1. These cases made up the full statistical population sample available to provide LRFD resistance factors for GRLWEAP. The missing 15 cases were placed in output Rank 4 because they lacked either a documented Davisson’s capacity or a reported blow count. The comparison between the EOID and BOR capacities predicted by GRLWEAP for the 179 pile case histories is illustrated in Fig. 5.1.

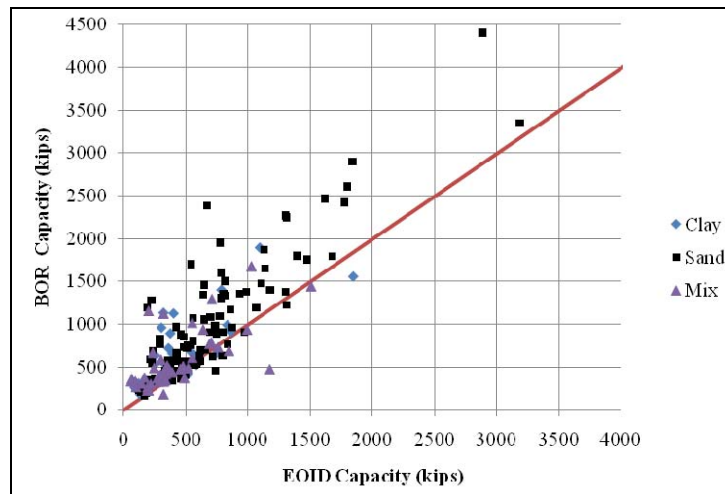


Figure 5.1: Predicted BOR capacity to predicted EOID capacity from GRLWEAP

GRLWEAP indicated a drop in capacity for 25 of these 179 cases. The percentage drop from EOID to BOR capacity varied from 1.2% to 43%. If a GRLWEAP predicted capacity difference of 5 % is considered significant less than 5% difference may indicate little, to no, confirmed capacity change. By this measure seven piles of the 25 piles were shown likely to be capacity neutral between EOID and BOR. It suggested that of the 179 cases, 18 piles exhibited possible relaxation based on GRLWEAP predicted capacities.

To provide a  $\phi$  calibration best representing typical Oregon soils, considerable effort was made to attain quality cohesive soil case histories. When completed, this offered a total of 38 clay sites and 43 mixed soil sites available in Input Tier 1 and Tier 2 that should exhibit significant pile “set-up” on restrrike. A series of statistical steps were taken to produce samples of the population for analysis and that were representative of the ODOT standard of practice. In constructing samples, consideration was given to the following:

1. Examine trends observed in the full population sample data set,
2. Study population statistical outliers and any “mismatched” cases requiring a filter criteria, and
3. Select a subset group of scenarios extracted from the full population that best represents ODOT site investigation, design analysis, and field installation standard of practice.

Some concern existed on the possibility that gross data entry errors compiling the source databases (*PDLT2000*, *DFLTD*) were responsible for the large number of anomalies discussed in Section 3. Unfortunately, significant discrepancies in a GRLWEAP capacity prediction can arise from erroneous reporting of field blow count, which was the largest single source of anomalies reported above between source databases. Errors on the blow count low side reduce predicted capacity, raise mean  $\lambda$ , and increase the COV, especially for the EOID. To help identify these possible errors, a simple blow count-based BOR/EOID set-up ratio (SR) breakdown was performed that used the same hammer on restrrike. This allowed a closer study on a case-by-case basis and ensured no rogue case histories distorted the statistics. This is shown below in Figure 5.2 that indicates of the total 322 case histories, a large majority had consistently low SR (SR < 5) and were highly unlikely to contain any errors.



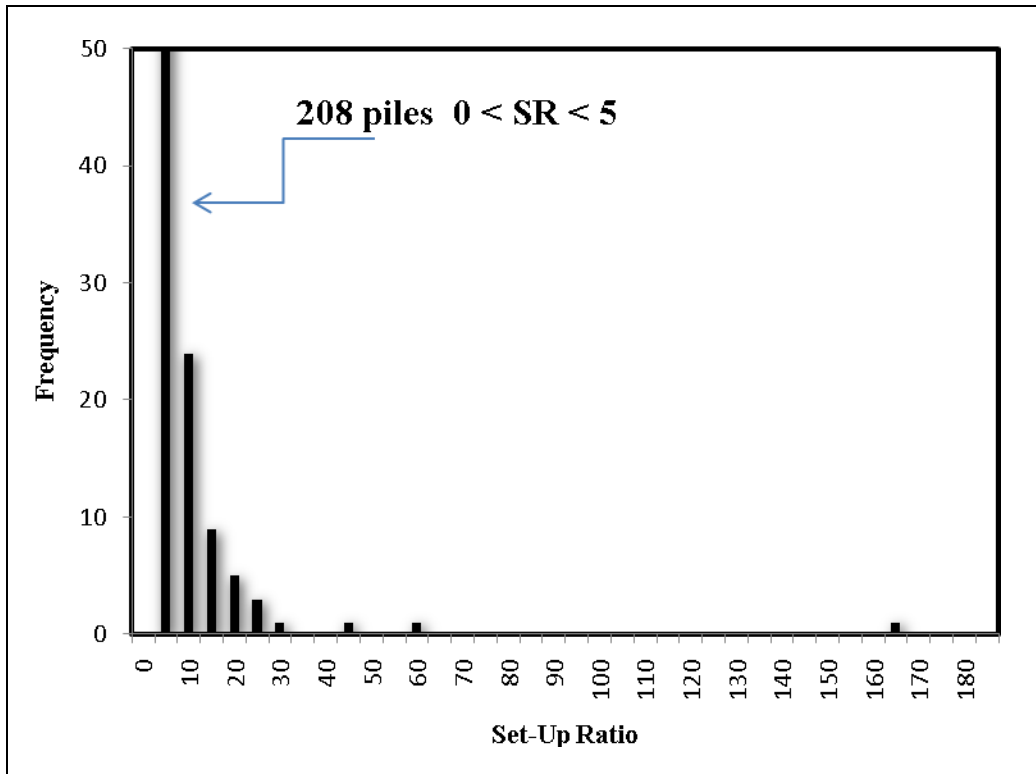


Figure 5.2: Frequency of set-up ratio in the Full PSU Master

The four single cases with  $SR > 30$  had ratios of 32, 48, 63, and 166. Of these, two were from Utah in highly sensitive clays, and this soil type did appear to be a mismatch to the stable soil types in the remainder of the dataset. The remaining two were in Texas and South Carolina. In the case of the Texas pile, the boring log stopped 18 feet short of the pile tip, was ranked in the low input Tier 2b, and ranked poorly on output in Rank 3. The South Carolina pile showed the SR of 166 and delivered the predicted GRLWEAP capacity 7 times higher moving to BOR from the EOID condition; however, CAPWAP suggested only 8% capacity increase moving to the BOR restrike capacity. With South Carolina having the largest percent of anomalies of any state DOT in the source data (Section 3), this was treated as an EOID or BOR data entry keyboard blow count error and/or a hammer efficiency issue at the BOR condition. All four piles were flagged and did not feature in any scenario for statistical study. This established the total number of valid cases for the resistance factor calibration effort to be 175, which was 75% more than reported in NCHRP 507. The final statistical parameters, broken down by pile type and soil type, for the 175 qualified case histories are shown in Table 5.2 below.

**Table 5.2: Statistical characteristics for GRLWEAP based capacity of the 175 qualified cases by soil and pile type\***

Soil Type	Pile Type	# of Cases	EOID			BOR**		
			$\lambda$	S.D.	COV	$\lambda$	S.D.	COV
Clay	All	34	1.94	1.42	0.73	1.1	0.61	0.55
	Concrete	15	1.21	0.53	0.44	0.71	0.24	0.33
	CEP	15	2.52	1.83	0.73	1.31	0.59	0.45
	OEP	0	-	-	-	-	-	-
	H-pile	4	2.45	1.19	0.49	1.8	0.96	0.53
Sand	All	98	1.27	0.66	0.52	0.9	0.46	0.51
	Concrete	60	1.21	0.61	0.5	0.76	0.36	0.48
	CEP	18	1.44	0.79	0.55	1.11	0.43	0.39
	OEP	2	1.96	0.13	0.07	1.24	0.08	0.07
	H-pile	18	1.23	0.61	0.5	1.12	0.59	0.52
Mixed	All	43	1.9	1.47	0.77	1.12	0.41	0.36
	Concrete	14	1.22	0.34	0.28	0.92	0.32	0.35
	CEP	15	2.89	2.09	0.72	1.24	0.38	0.31
	OEP	5	1.37	0.39	0.29	1.1	0.36	0.33
	H-pile	9	1.62	0.76	0.47	1.25	0.51	0.41
All Soils	All	175	1.555	1.1	0.71	0.993	0.47	0.47

\*All GRLWEAP capacities used the 2005 version, with updates, normalized by Davisson reported capacities in the databases accessed.

\*\* The time between EOID and BOR is known for 64 of the 175 cases and varied between 16 hours and 93 days (see also Section 6.3)

Overall, without any filtering of the data, EOID analysis displayed a much larger statistical spread than at the BOR condition. The conservative nature of EOID capacity, the considerable variations in the cohesive soils, and frequent large capacity well above Davisson’s in sands were determined to be the driving influence of this scatter. The Sand cases comprised over 50% of the total sample and the COV, expressing the spread, was slightly lower than the Clay and Mixed sites, and overall the COV did not improve between EOID and BOR. Sands also showed a less conservative  $\lambda$  bias compared to Clays and the Mixed cases. Frequency of occurrence histograms were plotted to visually display both EOID and BOR population trends in Table 5.2 broken down into soil type, and these are shown in Figures 5.3 and 5.4 respectively. Attention should focus on the overall “fit” and also the tail shapes fit, particularly high and low predictions, as these dictate the COV and the difference between FOSM and Monte Carlo based resistance values predicted in Section 7. Monte Carlo based calibration results were driven by the lower portion of the  $\lambda$  distribution, where capacity predictions were unconservative and risk of failure was higher.

The predominance of the Sand site cases in the lower bias tail (high capacity predictions compared to Davisson capacity) are seen in both Figures 5.3 and 5.4. Normal and lognormal curve fits and associated statistics were shown to visually determine the likely statistical distribution types for both populations and to compare to NCHRP 507. Visual examination clearly showed both EOID and BOR populations were represented better by lognormal distributions than by normal distributions, in agreement with previous calibration efforts. The tightening of the BOR histogram, with a lower COV, displayed the more reliable prediction at restrike of the Davisson capacity with all soils, especially capturing the influence of pile set-up.

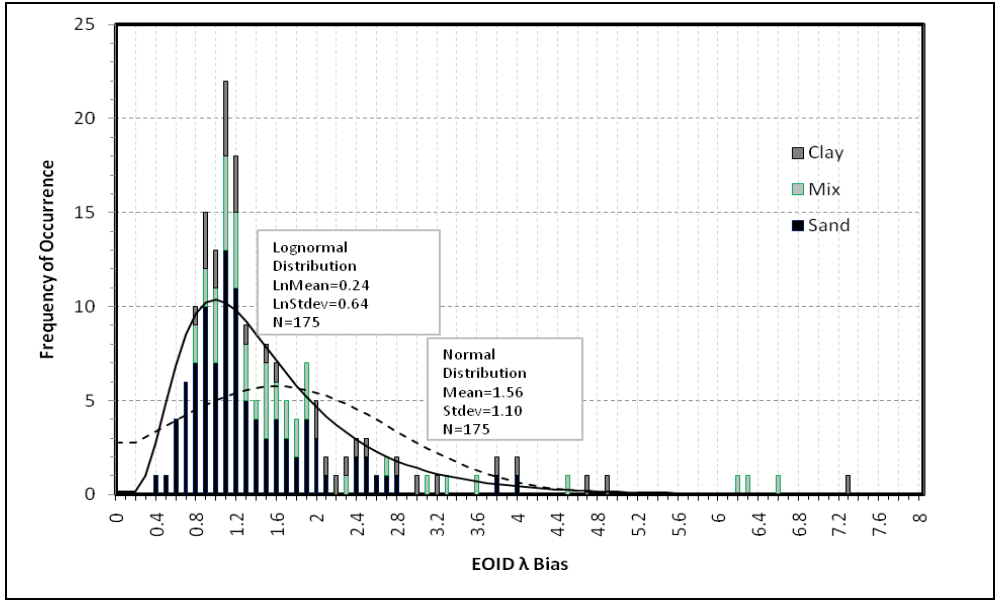


Figure 5.3: EOID  $\lambda$  histogram

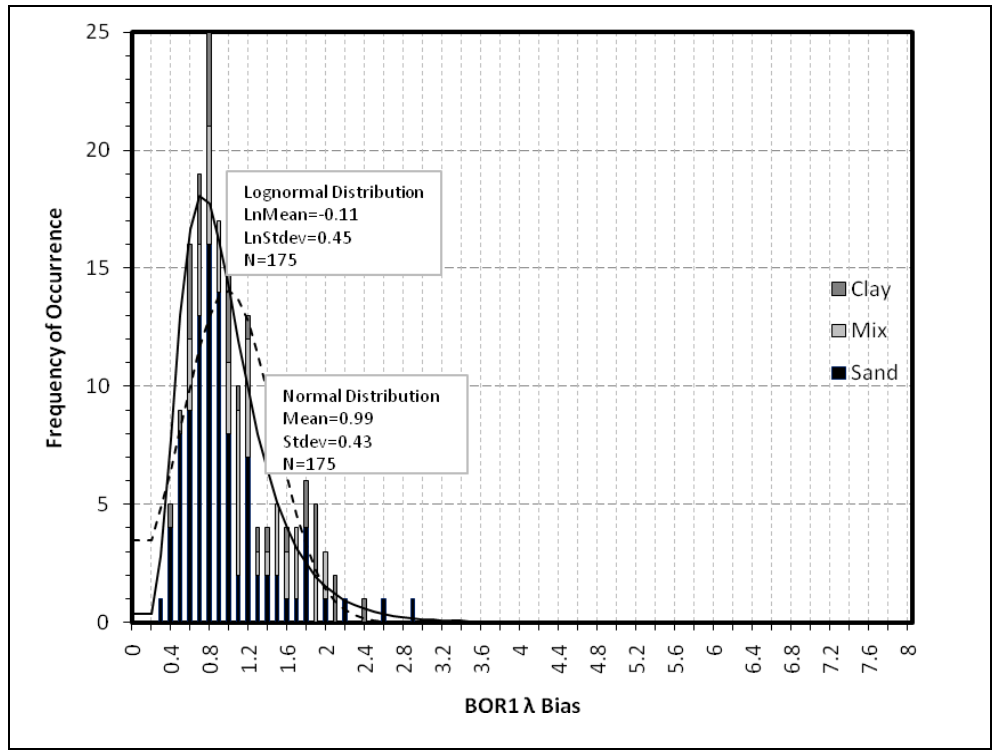


Figure 5.4: BOR1  $\lambda$  histogram

### 5.3 SCENARIO DEVELOPMENT

A series of different scenarios were designed to study existing pile capacity LRFD statistical filters, input tier differences, outlier definitions, and ODOT practice. Statistical filters and presentation formats appearing in NCHRP 507 for CAPWAP based nominal capacity were selected and used primarily for comparison. Both GRLWEAP and CAPWAP use the finite difference based wave theory, and it was of interest to determine whether both methods exhibited similar statistical trends. The NCHRP 507 visual presentation of the  $\lambda$  changes with blow count suggested a dramatic increase in data scatter for pile capacity predicted by CAPWAP in easy driving conditions at and below 2 BPI. This was adopted to detect its effect and is discussed in detail in Section 6.2.

Scenario A contained the full 175 case history population after removal of the four high SR cases and was the best match to NCHRP 507's reported work, but now with over 70% more case histories. It did not employ any kind of filtering of data. This set of case histories was selected to be the control scenario, and the histograms for the cases were shown in Figure 5.2 and Figure 5.3 for EOID and BOR respectively.

Scenario B contained only those cases in top Tier 1 and Tier 2a that had the best possible site investigation source data and required no key assumptions in the driving analysis.

Scenario C used the same NCHRP 507 arbitrary  $\pm 2$  s.d. range tail outliers filter and removed cases beyond this range out of Scenario A. This disqualified only nine cases as the tails on Scenario A were evidently already well conditioned with few extreme values.

Scenario D used the 2 BPI cut off from NCHRP 507 to modify Scenario A.

Scenario E employed the  $\leq 2$  BPI cutoff indicated in NCHRP 507 and the  $\pm 2$  s.d. outlier definition to modify the higher input tier quality cases extracted from Scenario B.

Scenarios A to E were designed to examine these different NCHRP 507 filter effects and draw conclusions on the changes in base  $\lambda$  and COV statistics. However, the following two additional scenarios moved closer to ODOT practice.

Scenario F modified Scenario B and was designed to reflect current ODOT practice by using the easy driving cutoff at 2 BPI and, recall, used the higher input quality Tier 1 and Tier 2a without any outlier definitions.

Scenario G modified Scenario F by also including the Tier 2b cases when output ranked in the very satisfactory highest Rank 1 and were, therefore, shown to be insensitive to assumptions.

Scenario H was an attempt to study the present combined AASHTO and FHWA guidelines on restrike (TR) and time to static load test (TST) by enforcing wait times extracted from the total of 69 piles in Scenario F that reported calendar TR and TST times (see also section 6.3).

The base statistics, including the number of qualifying cases, mean,  $\lambda$ , s.d., and COVs for these different scenarios, A through H, are presented in Table 5.3. The table illustrates well the statistical effect on mean and COV to  $\lambda$  that each filter had on each scenario. The baseline NCHRP 507 reported statistics for EOID and BOR from CAPWAP and GRLWEAP are given at the top of the table again for reference.

**Table 5.3: Base statistics for Scenarios A-H compared to NCHRP 507\***

Pile Resistance Prediction Method		Case	# of Piles	Mean $\lambda$	S.D.	COV
NCHRP-507	CAPWAP	EOID	125	1.626	0.797	0.490
		BOR**	162	1.158	0.393	0.339
	GRLWEAP	EOID	99	1.656	1.199	0.724
		BOR	99	0.939	0.399	0.425
PSU Scenario A	Tier 1-2	EOID	175	1.555	1.102	0.708
		BOR	175	0.993	0.468	0.472
PSU Scenario B	Tier 1-2a	EOID	82	1.685	1.100	0.653
		BOR	82	1.030	0.447	0.434
PSU Scenario C	Tier 1-2 +/-2 S.D.	EOID	163	1.372	0.669	0.488
		BOR	165	0.938	0.399	0.425
PSU Scenario D	Tier 1-2 BPI>2	EOID	138	1.269	0.614	0.484
		BOR	162	0.967	0.459	0.475
PSU Scenario E	Tier 1-2a BPI>2 +/-2 S.D.	EOID	65	1.394	0.603	0.433
		BOR	73	0.970	0.397	0.409
PSU Scenario F	Tier 1-2a BPI>2	EOID	69	1.406	0.596	0.423
		BOR	79	1.012	0.429	0.424
PSU Scenario G	Tier 1-2a, 2b Rank 1 BPI>2	EOID	94	1.328	0.564	0.425
		BOR	114	0.985	0.430	0.437
PSU Scenario H	Tier 1-2a, 2b Rank 1, BPI>2 TR and TST Filters	EOID	58	1.330	0.570	0.429
		BOR	69	0.974	0.408	0.419

\*All GRLWEAP capacities used the 2005 version, with updates, normalized by Davisson reported capacities in the databases accessed.

\*\* The time between EOID and BOR was known for 64 of the 175 cases and varied between 16 hours and 93 days (see also Section 6.3)

The two highlighted rows in the table represent the closest fit to NCHRP 507's main reported work, which was the basis for AASHTO LRFD Manuals (2006, 2009) at EOID. The Scenario A's expanded total pile count of 175, without any filters or outliers, had a slightly less conservative  $\lambda$  at EOID than the 99 piles reported in NCHRP 507. However, the BOR  $\lambda$  of 0.993 did reveal less unconservatism with almost an exact match to the Davisson's capacity when compared to BOR statistics in the appendix of NCHRP 507. Recall Scenario G was created by loosening input quality restrictions on likely ODOT match Scenario F by including the lower input Tier 2b cases (which required more assumptions) that were in Rank 1. This demonstrated

the value of output quality ranks by gaining a considerable number of cases. Loosening the tier restriction added close to 50% more cases and showed no degradation of statistical quality compared to Scenario F at either EOID or the BOR condition. Case history count in Scenario G was comparable to those used for GRLWEAP in NCHRP 507. Scenario H followed the much stricter guidance on TR and TST delays set by AASHTO and FHWA and showed improvement of EOID and BOR conditions. However, this was not a fair assessment when applied to cases whose installation and load test took place before the code requirements. It did not apply to ODOT practice and was not used in the more advanced Monte Carlo Reliability Method calibration presented in Section 7.2

## 5.4 DISTRIBUTION TESTING

Pile resistances are statistically random variables and calibration of the LRFD resistance factor requires assumptions on the shape of their PDF distribution. Scenarios A to F were examined to determine how their populations fitted to both a normal and lognormal distributions. The statistical analysis software Minitab16 (*Minitab 2009*) was used to create each scenario's PDF, CDF, and SNV, described for calibration purposes by Allen (*Allen 2005b; Allen, et al. 2005*). A scenario's population distribution can be visually scanned utilizing the PDF and CDF plots. Normal distributions show linear on the SNV plot and both normal and lognormal distribution fits were tested by Minitab.

The rigorous Anderson Darling (AD) test and the P-tests use the SNV plots to determine statistical distributions fits employing a null hypothesis theory. The null hypothesis being the distribution does fit in either the normal or the lognormal distribution. The P-value is a measure of the risk associated with false rejection of the null hypothesis and offers indications that the data fits a specified distribution. If the P-value is less than 0.05, then there is a greater than 95% chance that the specified distribution is incorrect and the null hypothesis can be rejected without risk. The AD test was employed to determine the "goodness of fit" accuracy of the distribution to model each scenarios sample and was used in conjunction with the P-value. The AD and P-values for all scenarios at EOID and BOR for both normal and lognormal distributions were examined. This is shown for Scenarios A at the EOID on Figure 5.5 for the lognormal fit. A true lognormal would appear as a straight line on the SNV to  $\log \lambda$  bias plot. The lognormal EOID and BOR set for each of the final implementation scenarios of interest to ODOT (Section 7.2) can be seen in Appendix B.

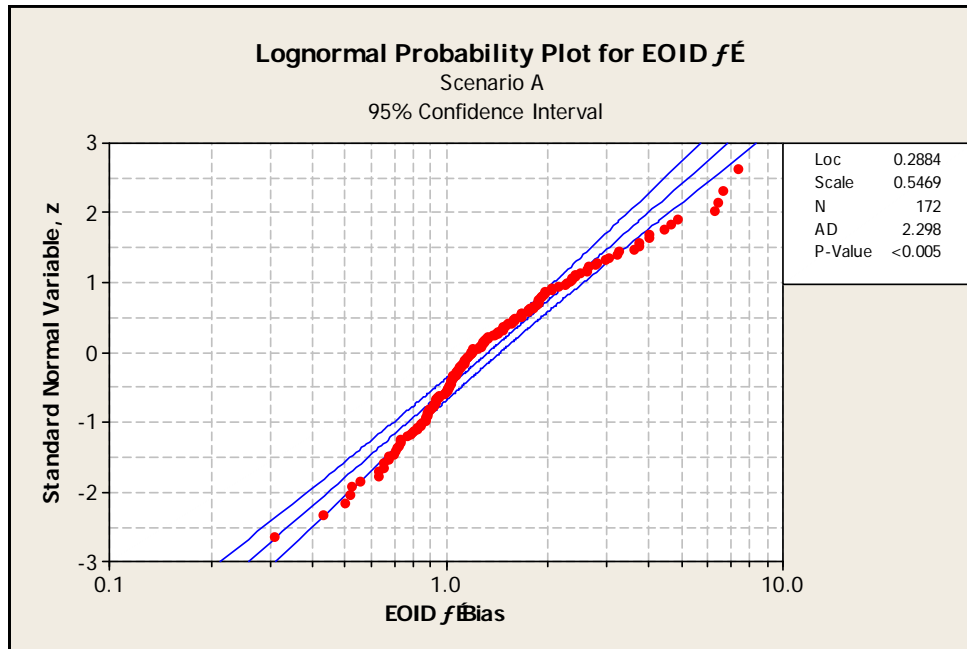


Figure 5.5: Lognormal distribution fit to Scenario A at EOID

To aid interpretation of the standard normal plots, the +/-5% variant from the mean was plotted represented by the two lines beyond the mean. In general, all scenarios' populations fit the lognormal distribution with one exception: Scenario A at EOID produced a P-value < 0.005. Graphically, the visual degree of scatter in the data at both upper and lower EOID tails was the cause of the rejection. Consistent with all other published LRFD calibration work and for the purpose of this research, all scenarios, including Scenario A at EOID, were modeled as a lognormal distribution fit.

## 6.0 OUTLIER EXAMINATION

As with any population sample, a careful examination for those data that do not belong in the sample, improves validity. A variety of driven pile characteristics were investigated to determine their influence on the overall sample and to help detect mismatched case histories. When any trend was discovered, it was considered as a possible filter before final  $\phi$  calibration analysis proceeded. The +/- 2 s.d. outlier imposed on all NCHRP 507 sets (*Paikowsky 2004*) was examined, but not considered a valid outlier definition, as it produced artificial tail modifications. This outlier approach was not employed in any final implementation scenario selection (see Section 7). After selecting the fit to a log normal distribution the tail controlled accurate recalibration efforts. The removal of extreme data points without any other justification was not easily defensible. All the efforts to identify mismatched case histories are reported below and include input tiers to output ranks, blow count ranges, the time to restrike (TR), and time to static load test (TST).

### 6.1 INPUT TIER AND OUTPUT RANK

A statistical breakdown was performed on both the population’s input tiers and the output ranks to assess if clear trends existed and to help determine the usefulness of both criteria. Table 6.1 presents a breakdown of data at EOID and BOR performed on three input tier subset variations for Scenario A: Tier 1 only, Tier 1 and 2a only, and all Tier 1 and Tier 2 cases.

**Table 6.1: Statistical breakdown of Tier 1, Tiers 1 & 2a, and Tiers 1 & 2 for EOID and BOR**

Input Tier	Soil Type	Pile Type	# of Cases	EOID			BOR		
				$\lambda$	S.D.	COV	$\lambda$	S.D.	COV
<b>1</b>	All	All	55	1.63	1.01	0.62	1.01	0.46	0.46
<b>1 and 2a</b>	All	All	86	1.64	1.02	0.62	1.04	0.44	0.42
<b>1 and 2</b>	All	All	175	1.56	1.10	0.71	0.99	0.47	0.47

As previously discussed, the input tiers were used to evaluate the quality and completeness of a case’s source input data. As expected, the comparison from Table 6.1 showed that the inclusion of less complete source data produced degradation of the statistical parameters, but only at EOID. Little difference was evident when including Tier 2a with Tier 1 at EOID, while the BOR parameters remained relatively constant. Tailoring the recalibration effort to ODOT standard field practice required the inclusion of case histories that were well defined. The use of any questionable source data would induce an undesirable skew in the calculated resistance factor. Trends displayed on the EOID analysis in Table 6.1 suggested that adding Tier 2a to Tier 1 was acceptable, and that the combined use of Tier 1 and Tier 2a could form an appropriate basis to study ODOT practice.



Table 6.2 displays the statistical  $\lambda$  and COV breakdown for EOID and BOR by soil and pile type for the top input Tier 1 and Tier 2a. Table 6.3 displays the same breakdown statistics but for the higher output Ranks 1 and 2. Only 50% of these cases were in the top Tier 1 and Tier 2a, but almost 80% of the total cases were in the excellent and good output rank. It is apparent no serious degradation of statistics arose from increasing the number of reasonable assumptions made throughout the analysis. No clear trends were determined between the different qualitative output ranks between each input tier and sub tier in Table 6.2. This was expected as the issues relating to assigning a case to an output rank were varied.

**Table 6.2: Top input Tier 1 & 2a statistical breakdown by soil and pile type\***

Soil Type	Pile Type	# of Cases	EOID			BOR**		
			$\lambda$	S.D.	COV	$\lambda$	S.D.	COV
Clay	All	15	1.87	0.68	0.36	1.20	0.62	0.52
	Concrete	4	1.59	0.93	0.59	0.73	0.35	0.48
	CEP	8	1.73	0.41	0.24	1.10	0.35	0.32
	OEP	0	-	-	-	-	-	-
	H-pile	3	2.62	0.50	0.19	2.09	0.21	0.10
Sand	All	42	1.31	0.56	0.42	0.88	0.36	0.41
	Concrete	29	1.19	0.51	0.43	0.74	0.22	0.30
	CEP	6	1.31	0.44	0.33	1.12	0.44	0.39
	OEP	2	1.96	0.13	0.07	1.24	0.08	0.07
	H-pile	5	1.79	0.69	0.39	1.28	0.50	0.39
Mixed	All	29	1.99	1.47	0.74	1.18	0.38	0.33
	Concrete	9	1.29	0.39	0.30	1.03	0.33	0.32
	CEP	12	2.63	2.06	0.78	1.13	0.36	0.31
	OEP	1	1.88	-	-	1.43	-	-
	H-pile	7	1.82	0.75	0.41	1.41	0.45	0.32
ALL	All	86	1.64	1.02	0.62	1.04	0.44	0.42

\*All GRLWEAP capacities used the 2005 version, with updates, normalized by Davisson reported capacities from the databases accessed.

\*\* The time between EOID and BOR was known for 64 of the 175 cases and varied between 16 hours and 93 days (see also Section 6.3)

**Table 6.3: Top output ranks 1 & 2 statistical breakdown by soil and pile type\***

Soil Type	Pile Type	# of Cases	EOID			BOR**		
			$\lambda$	S.D.	COV	$\lambda$	S.D.	COV
Clay	All	25	2.31	1.59	0.69	1.12	0.61	0.55
	Concrete	11	1.28	0.61	0.48	0.64	0.19	0.29
	CEP	9	3.21	1.96	0.61	1.44	0.51	0.35
	OEP	0	-	-	-	-	-	-
	H-pile	5	2.93	1.16	0.40	1.59	0.71	0.45
Sand	All	76	1.37	0.69	0.50	0.87	0.43	0.50
	Concrete	52	1.26	0.63	0.50	0.75	0.36	0.48
	CEP	12	1.71	0.84	0.49	1.18	0.51	0.43
	OEP	2	1.96	0.13	0.07	1.24	0.08	0.07
	H-pile	10	1.41	0.66	0.47	1.06	0.42	0.40
Mixed	All	34	2.13	1.58	0.74	1.11	0.39	0.35
	Concrete	9	1.32	0.34	0.26	0.90	0.37	0.41
	CEP	13	3.16	2.12	0.67	1.21	0.36	0.30
	OEP	5	1.37	0.39	0.29	1.10	0.36	0.33
	H-pile	7	1.81	0.75	0.41	1.21	0.48	0.40
ALL	All	135	1.74	1.27	0.73	0.98	0.53	0.55

\*All GRLWEAP capacities used the 2005 version, with updates, normalized by Davisson reported capacities from the databases accessed.

\*\* The time between EOID and BOR was known for 64 of the 175 cases and varied between 16 hours and 93 days (see also Section 6.3)

## 6.2 BLOW COUNT INVESTIGATION

The pile driving process is an energy balance of two phenomena: an input of relatively known energy at the top of a pile and the surrounding soil’s ability to absorb this energy. The soil absorbs this delivered energy when the tip is advanced through the displaced soil. A basic assumption of this model is that the pile, hammer, and soil be considered a lumped mass-spring system. GRLWEAP employs the Smith’s lumped mass model to approximate the external pile supporting soil resistance. If a pile is driving too easily, the large energy loss developed by the displaced soil and the complex large dynamic strain pattern over time and distance introduces possible plug and other violations to the assumptions in the model. NCHRP 507 reported that at easy driving, the complex interaction and energy loss due to the high velocity and acceleration displacement of the soil at the pile tip is unable to be captured accurately. Further, the GRLWEAP manual stated that during easy driving of less than 2 BPI, inaccurate results may be produced so reduced energy should be employed. The GRLWEAP manual also warned against sustained hard driving conditions, as did the FHWA manual, inducing a hammer “serviceability” issue rather than affecting the accuracy of a capacity prediction. Damage to the pile and/or hammer can occur under these conditions, which typically causes an upper range of 15 to 20 BPI to be recommended by the hammer manufacturer.

NCHRP 507 did not analyze blow count spread versus GRLWEAP predicted capacity, but did report this spread for CAPWAP. The report text stated that, measured by mean  $\lambda$  and COV, a statistical change at 4.5 BPI occurred, which visually was better expressed from 2 BPI. As both

GRLWEAP and CAPWAP are dynamic methods using the lumped mass model, a similar relationship between  $\lambda$  and blow count may exist for GRLWEAP. Figure 6.1 shows the blow counts for the 175 cases, at both EOID and BOR, plotted against their respective  $\lambda$  values to help determine if statistical accuracy trends existed between BPI and the case-by-case calculated  $\lambda$ .

Figure 6.1 does clearly show in a similar trend to CAPWAP, GRLWEAP's inability to accurately and reliably predict capacity at the lower blow counts. The data displayed supports the idea that as blow counts increased, there was less permanent set between each successive blow count and the soil-pile-hammer model behaved more predictably when modeled by GRLWEAP. To determine a reasonable quantitative break point in the data, the blow counts shown in Figure 6.1 were placed into 2 BPI incremental ranges, following the format used in NCHRP 507, and each range average  $\lambda$  and s.d. calculated.

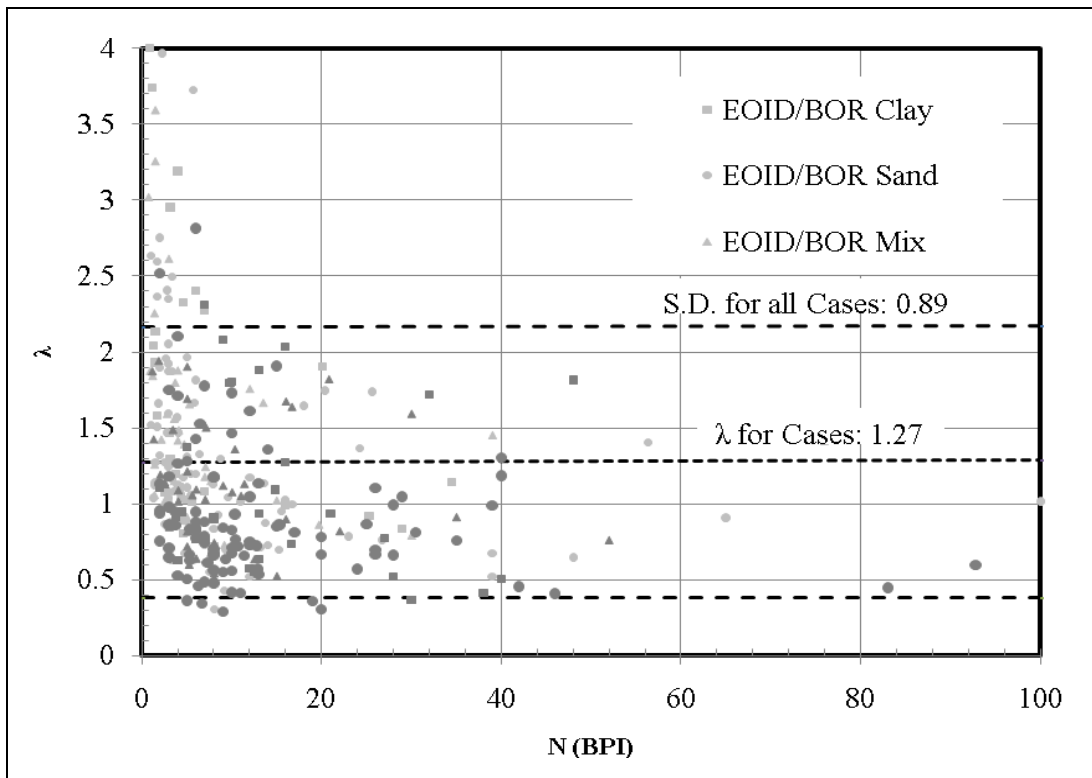


Figure 6.1: All EOID and BOR qualified 175  $\lambda$  values plotted to blow count by soil type

The number of cases in each range, mean  $\lambda$ , and the vertical bar in the range expressing  $\pm 1$  s.d. are shown in Figure 6.2, together with the overall sample mean  $\lambda$  and s.d. range with a dashed line for all 175 piles. Each pile case history generated two data points: one for EOID and one for BOR.

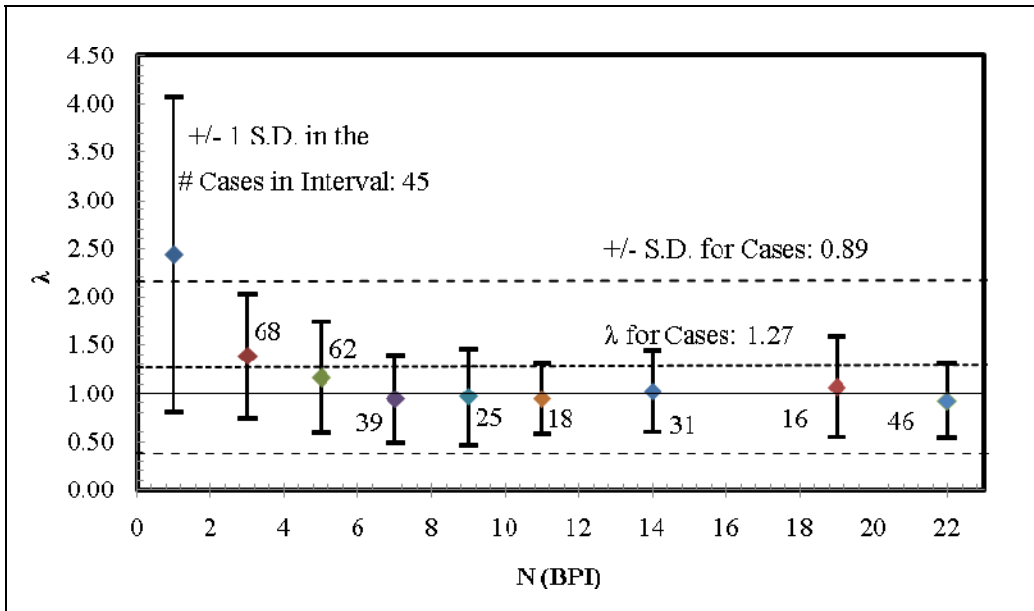


Figure 6.2: All EOID and BOR qualified 175  $\lambda$  values plotted to blow count in 2 BPI intervals

There were insufficient data points to make reasonable comparisons for every 2 BPI increments after 12 BPI. Therefore, Figure 6.2 shows the BPI categories greater than 12 to less than or equal to 16 combined, and greater than 16 to less than or equal to 22 combined to correct this lack of data. The 46 instances where pile blow counts were greater than 22 BPI for presentation clarity. All blow count ranges above 2 BPI showed relatively consistent statistical variation up to the last recorded data point of 100 BPI. This fell into line with both the GRLWEAP manual recommendations and NCHRP 507’s interpretation for CAPWAP.

**Table 6.4: Blow count ranges for EOID and BOR in Full PSU Master**

BPI	EOID		BOR		Total	
	# Cases	Total %	# Cases	Total %	# Cases	Total %
>0 to 10	207	78%	162	59%	369	68%
>10 to 15	19	7%	36	13%	55	10%
>15 to 20	12	5%	25	9%	37	7%
>20 to 30	13	5%	24	9%	37	7%
>30 to 40	7	3%	10	4%	17	3%
>40	6	2%	18	7%	24	4%
Sum	264	100%	275	100%	539	100%

Table 6.4 offers a breakdown of the blow count ranges between EOID and BOR from *the Full PSU Master* database for all input tiers and output ranks. (Recall that 179 of the 322 cases received complete DRIVEN and GRLWEAP analyses.) The difference in case numbers between

the EOID and BOR count was due to cases having no reported blow counts at either EOID or BOR.

Prior to 2009, ODOT set their acceptable range for driving blow counts at  $3 \leq \text{BPI} \leq 15$  to avoid easy driving at the lower limit and possible hammer damage at the upper limit. Field practice reported by TAC members confirmed high blow counts were tolerated for the strictly limited time duration of the restrike. These statistics do not support implementing any upper cutoff for capacity by GRLWEAP; in fact, 29% of the case history piles have pushed hammer blow counts greater than the 15 BPI limit on restrike for the BOR blow count series. As reported in the GRLWEAP manual, an upper cutoff represents a hammer serviceability concern rather than accurate capacity determination concern. As the blow counts greater than 15 BPI were field recorded values in the database, no use of an upper BPI cut off for the purpose of the resistance factor recalibration was used.

### 6.3 TIME TO RESTRIKE AND TIME TO LOAD TEST INVESTIGATIONS

The contribution of soil set-up has been shown to statistically improve the GRLWEAP prediction of a pile’s ultimate capacity when using BOR. The research group investigated the database pile case histories level of adherence to current AASHTO and ODOT required minimum wait time to restrike (TR) and time to static load test (TST) times. Among the 175 piles accepted for  $\phi$  resistance calibration, 64 in Tier 1 and Tier 2 had TR and TST recorded in the *Full PSU Master* database. This pile count is shown in Table 6.5, broken down by pile and soil type.

**Table 6.5: Pile counts complying with current AASHTO and ODOT TR and TST times**

	Con	CEP	HP	OEP	Total
Clay	8	6	3	0	17
Sand	18	9	2	2	31
Mix	6	4	4	2	16
Total	32	19	9	4	64

The distribution of soil and pile type as well as the statistical averages at EOID and BOR for the 64 cases was similar to that reported in the full population sample of the 175 cases in Table 5.2. This allowed observations made from the smaller 64-pile subset to be considered appropriate for the full population sample with relative confidence. AASHTO recommends the required wait time before restrike based on one of the following: clean sands at 1 day, silty sands at 2 days, sandy silts at 3-5 days, and clays at 7 days (*AASHTO 2009*). ODOT bridge foundation construction specifications typically require a one-day minimum set-up period before a restrike can be performed. AASHTO mandates a minimum of five days after initial driving has passed before a static load test can be conducted.

The times stated by both ODOT and AASHTO were compared to those recorded in the database for the 64 piles, and the majority of cases did not meet both the TR and TST requirements. At restrike, six piles failed ODOT's wait time requirement, while 16 piles failed AASHTO's wait time recommendation. Further, 48 out of 64 piles failed to wait the AASHTO's recommended required time after initial driving before the static load test was conducted. The 64 cases were examined to determine if any trends could be detected to assist identifying mismatched cases that were restruck too early and, therefore, captured little set-up or were load tested much later. Figures 6.3 and 6.4 presents the ratio of TR to TST times compared to their corresponding BOR case-by-case  $\lambda$  values broken down by soil type and by pile type respectively. Load testing would have occurred after restrike for  $TR/TST < 1$  and restrike would have occurred after the load test for  $TST/TR < 1$ .

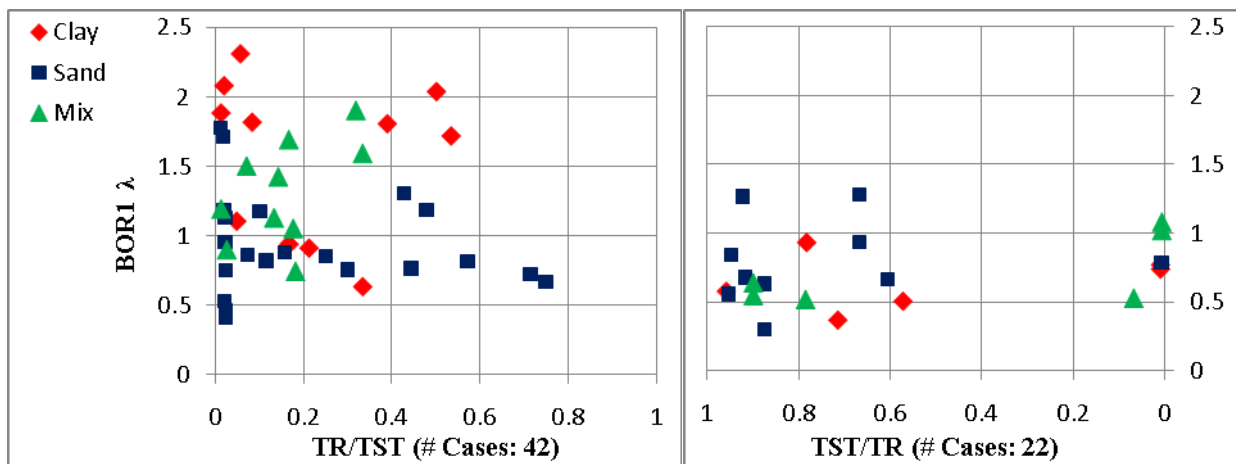


Figure 6.3: Restrike and load test time ratios by soil type

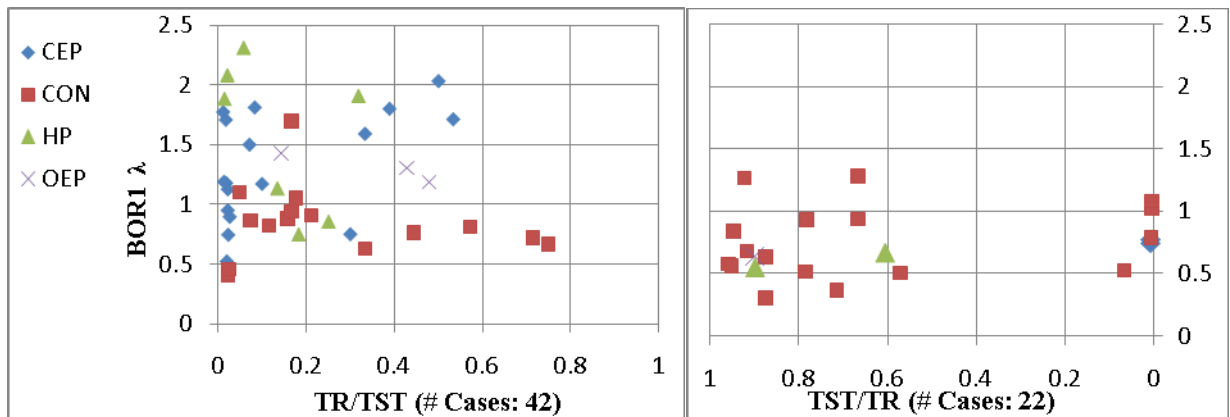


Figure 6.4: Restrike and load test time ratios by pile type

The majority of the piles that did not meet the standard TR and TST time requirements were in cohesive soils. A 'cloud' of conservative, high  $\lambda$ , cohesive soil pile cases that had been restruck

early and load tested late ( $TR/TST \ll 1$ ), was prominent in Figure 6.3. The majority of this cloud was made up of CEP and HP pile sections. Also five sites showed very late restrike performed well after the static load test ( $TST/TR \ll 1$ ).

Calibration for the resistance factor by the FOSM method uses lognormal  $\lambda$  distributions, which are sensitive to both upper and lower tails. The more advanced, and appropriate, Monte Carlo based recalibration method, employed using data from the lower tail, was not as concerned with the conservative ( $\lambda > 1$ ) side of the  $\lambda$  distribution; therefore, these cases did not affect the calculated  $\phi$  value and did not have the same degree of concern for this study. The presence of unconservative sand cases with low  $\lambda$ , and shown in Figure 6.3, was similar in ratio to the statistics seen in the full 175 case distributions; however, this group of sand cases did not violate the TR and TST requirements.

Without any compelling, consistent, and clear trends, all the cases that violated the TST and TR requirement set forth through ODOT and AASHTO were included. The rationale to include these cases was the following:

- Cases that violated their TR and TST were conservative because they failed to capture adequate set-up and, therefore, did not negatively influence the calibration effort.
- A large majority of the cases that violated TR and TST were cohesive. By eliminating them from the calibration effort, the soil type balance of case history data would no longer have represented the broad distribution of soils found in Oregon.
- Only 64 of the 172 cases available for analysis had TR and TST values. This would unduly have eliminated a quality subset of data from analysis.

A large variation in installation condition requirements and field practice norms existed in the database due to the differences in TR and TST time and geographic location of the case histories. The inherent variability of national piling standards was captured by keeping a broad database that should produce more representative and generally applicable conservative resistance  $\phi$  factor results.

In summary, no cases were removed from the dataset before calibration began for reasons of falling outside any arbitrary s.d. range, input tier position, or restrike and load test delay timing. When grouped by blow counts, cases were shown to dramatically increase their COV and  $\lambda$  for the lower blow counts; therefore, a minimum cut-off of 2 BPI was adopted.

## 7.0 RESISTANCE FACTOR DEVELOPMENT

Section 5.3 of this report discussed the composition of eight scenarios, A through H, which were used to produce the bias  $\lambda$  statistics to examine differences in input tiers, the use of NCHRP 507 outlier definitions, and likely matches to ODOT practice. The resistance factor calibration employing these statistics was performed with the procedures outlined by AASHTO (Allen, *et al.* 2005). Both the FOSM equation and the Monte Carlo probabilistic procedures outlined in Section 1.4 were used. The statistical breakdown and the outlier studies, discussed in Section 5 and 6, did reveal some differences between sites, mainly those deriving resistance in granular materials to those sites predominately deriving resistance in cohesive soils. Pile set-up, and the associated increased capacities, are likely to arise in cohesive soils, but are also detected in granular soils. If restrrike decisions are made based on poor EOID capacity, then different resistance factors should be available at BOR derived from the restrrike population statistics. These differences, expressed in the field by blow count changes, are the key to appropriate project-by-project decisions around capturing set-up and optimizing pile acceptance under LRFD. With the amount of set-up possible in piles founded in mainly cohesive soils being higher, two additional practice scenarios were created to assist in implementation of this research's findings. The breakout of cohesive and cohesionless soils from Scenario A could not be done with equal confidence as some doubt was statistically detected (see section 5.4) on the appropriateness of the lognormal assumption. Scenario A also contained a large number of poorly defined Tier 2b case histories. Therefore, both new scenarios were derived from Scenario G and are listed below.

Scenario I was extracted from Scenario G but contained only those sites that derived at least 20% DRIVEN predicted capacity from cohesive soils.

Scenario J, for comparison purposes, was also extracted from Scenario G but contained only sites with at least 80% of resistance from granular soils.

Recall Scenario G (Section 5.3) had over 100 case histories, matched well to ODOT practice, which follows standard AASHTO and FHWA recommendations, and used blow counts  $> 2BPI$  to remove easy driving mismatches. A total of ten scenarios, A through J, were examined with simple closed form FOSM, with Scenarios A, F, G, I, and J also undergoing the considerably more complex Monte Carlo reliability method.

### 7.1 FIRST ORDER SECOND MOMENT (FOSM) $\Phi$

When the  $\lambda$  bias ratio is taken as lognormal distributed, the closed FOSM calibrated resistance  $\phi$  can be quickly calculated by the closed form Equation 1-3 from Section 1.4, which is repeated here.



$$\phi = \frac{\lambda_R \left( \gamma_D \left( \frac{Q_D}{Q_L} \right) + \gamma_L \right) \sqrt{\frac{1 + \text{COV}_D^2 + \text{COV}_L^2}{1 + \text{COV}_R^2}}}{\left( \lambda_D \left( \frac{Q_D}{Q_L} \right) + \lambda_L \right) \exp \left[ \beta_\tau \sqrt{\ln \left[ (1 + \text{COV}_R^2) (1 + \text{COV}_D^2 + \text{COV}_L^2) \right]} \right]}$$

Contributions to total load from  $Q_D$  and  $Q_L$  sources are included, expressed by their bias and COV. These were set at the values required by ODOT, were used in Phase 1 (*Smith and Dusicka 2009*), and for consistency were the values most often selected by LRFD researchers for driven pile studies (*Long 2009; Paikowsky 2004*). For redundant pile groups of five or more, the target reliability index was 2.33, and for fewer than five piles, the target reliability was 3.0. The full set of statistical parameters used in this study is shown in Table 7.1.

**Table 7.1: Statistical load parameters used for calibration**

Load Type	DL	LL
Distribution	Lognormal	Lognormal
Monte Carlo Value	800 kips	400 kips
$\lambda$ Bias	1.05	1.15
COV	0.10	0.20
$\gamma_{DL}$	1.25	
$\gamma_{LL}$	1.75	

More superior capacity methods should predict capacity more accurately and precisely, and they may be quickly compared by their COV's or by the efficiency ratio,  $\phi / \lambda$ , which normalizes the LRFD capacity reduction factor by the detected method bias. A high COV corresponds to a low efficiency value, and the  $\phi / \lambda$  and COV efficiencies can be used to rank the optimum method: either EOID capacity or BOR capacity to show the method with the least over-capacity in the field. To aid implementation, this optimization is further explored in Section 7.3. Table 7.2 reports all the FOSM calculated resistance values and  $\phi / \lambda$  efficiencies for both reliability  $\beta$  values of 2.33 and 3.0, and also for comparison, the reported NCHRP 507 values by GRLWEAP and CAPWAP at the EOID and BOR condition. In Table 7.2, the NCHRP 507 BOR statistics are shown in italics to denote they did not appear in the text of that report.

The FOSM resistance values shown for the baseline Scenario A, and from NCHRP 507 at EOID (forming AASHTO recommendations), are highlighted and are very similar, but they do, in fact, illustrate some differences. The parameters under which NCHRP 507 generated the FOSM resistance factors most likely had used the strict +/- 2 s.d. outlier cutoff to improve COVs. Further, the original GRL based work (*Rausche, et al. 1997*) appears to have applied a 10 BPI blow count cap to select acceptable case histories. If these different constraints are recognized, the Scenario A statistics with 175 piles were slightly superior to the 99 piles of the original NCHRP 507 work and reflected the considerable effort the current study expended for the resolution of anomalies and the inclusion of only carefully selected, and well documented, case histories in the *Full PSU Master* database.

**Table 7.2: FOSM resistance values and efficiencies for  $\beta=2.33$  and  $\beta=3.0$** 

Pile Resistance Prediction Method		Case	# of Piles	Mean $\lambda$	S.D.	COV	FOSM			
							$\phi$ Factor		$\phi/\lambda$ Efficiency	
							$\beta=2.33$	$\beta=3.0$	$\beta=2.33$	$\beta=3.0$
NCHRP 507	CAPWAP	EOID	125	1.626	0.797	0.490	0.59	0.42	0.36	0.26
		BOR	162	1.158	0.393	0.339	0.58	0.45	0.50	0.39
	GRLWEAP	EOID	99	1.656	1.199	0.724	0.36	0.23	0.22	0.14
		BOR	99	0.939	0.399	0.425	0.39	0.29	0.42	0.31
Scenario A	Tier 1 and 2	EOID	175	1.555	1.102	0.708	0.35	0.22	0.23	0.14
		BOR	175	0.993	0.468	0.472	0.38	0.27	0.38	0.27
Scenario B	Tier 1 and 2a	EOID	82	1.685	1.100	0.653	0.43	0.28	0.26	0.17
		BOR	82	1.030	0.447	0.434	0.42	0.31	0.41	0.30
Scenario C	Tier 1 and 2 +/-2 S.D.	EOID	163	1.372	0.669	0.488	0.50	0.36	0.37	0.26
		BOR	165	0.938	0.399	0.425	0.39	0.29	0.42	0.31
Scenario D	Tier 1 and 2 BPI>2	EOID	138	1.269	0.614	0.484	0.47	0.33	0.37	0.26
		BOR	162	0.967	0.459	0.475	0.36	0.26	0.38	0.27
Scenario E	Tier 1 and 2a BPI>2 +/-2 S.D.	EOID	65	1.394	0.603	0.433	0.57	0.42	0.41	0.30
		BOR	73	0.970	0.397	0.409	0.42	0.31	0.43	0.32
Scenario F	Tier 1 and 2a BPI>2	EOID	69	1.406	0.596	0.423	0.59	0.43	0.42	0.31
		BOR	79	1.012	0.429	0.424	0.42	0.31	0.42	0.31
Scenario G	Tier 1 and 2a+ Tier 2b Rank1 BPI>2	EOID	94	1.328	0.564	0.425	0.56	0.41	0.42	0.31
		BOR	114	0.985	0.430	0.437	0.40	0.29	0.41	0.30
Scenario H	Tier 1 and 2a BPI>2 & TR, TST	EOID	58	1.330	0.570	0.429	0.55	0.40	0.42	0.30
		BOR	69	0.974	0.408	0.419	0.41	0.30	0.42	0.31
Scenario I Clay & Mixed	Tier 1 and 2a+Tier 2b Rank1 BPI>2	EOID	43	1.464	0.595	0.406	0.64	0.47	0.44	0.32
		BOR	56	1.123	0.457	0.407	0.49	0.36	0.44	0.32
Scenario J Sands	Tier 1 and 2a+Tier 2b Rank1 BPI>2	EOID	51	1.214	0.515	0.424	0.51	0.37	0.42	0.31
		BOR	58	0.852	0.358	0.421	0.36	0.26	0.42	0.31

Measured by  $\phi/\lambda$  efficiencies alone, both Scenario A and NCHRP 507 indicated using restrrike capacity to optimize the number and/or pile depth, but was much less clear under all other scenarios. Similarity was seen in the  $\phi/\lambda$  efficiencies at BOR of all scenarios, and was in close agreement with NCHRP 507. The BOR  $\phi$  values were generally lower than the EOID  $\phi$  values. As expected, the EOID on Scenario A offered the lowest  $\phi$  and  $\phi/\lambda$  efficiency of any in the table due to the previously reported poorly defined upper  $\lambda$  tail inflating the COV. Efficiencies on all other scenarios for both EOID and BOR were generally twice that reported by NCHRP 507 at EOID. Of significance was the effect shown in Scenario C of employing the +/- 2 s.d. NCHRP 507 outlier definition. From the direct comparison to Scenario A, which used the data in all qualified tiers, the  $\phi$  factor was inflated by 42%, up to 0.501, for EOID at the  $\beta$  of 2.33, by the artificial removal of extreme tail data at both ends.

Not illustrated in the table were the individual soil type specific effects when constructing Scenario G from Scenario F. The statistical effects of adding the lower Tier 2b Clay sites to Scenario F was identical to adding Tier 2b Mixed sites to Scenario F; the COV at EOID increased slightly and BOR was unchanged. But the opposite was found when adding the Tier 2b Sand sites to Scenario F. This supported treating Clay and Mixed sites as a single sample, as in Scenario I, and treating Sand-only sites to form Scenario J. A clear difference in statistical sample characteristics existed between piles supported in predominately cohesive soils to those in cohesionless soils since they were showing as different populations.

## 7.2 ODOT SCENARIOS AND MONTE CARLO RELIABILITY $\Phi$

To recap, Scenario A represented all 175 acceptable Tier 1 and Tier 2 cases that generated separate  $\lambda$  values and did not employ any kind of data filtering. With a good match to NCHRP 507, this scenario was selected as the baseline for comparison. Scenarios F and G were determined likely to be the best fit to the ODOT standard of practice requiring a single  $\phi$  at EOID and a single  $\phi$  at BOR, with high quality site investigation data and field supervision and documentation during pile driving. These scenarios eliminated the statistical scatter associated with easy driving (eliminating less than and equal to 2 BPI) and accepted only high tier source data. In the interest of developing a larger population for calibration analysis, Scenario G included Tier 2b cases that received an output Rank 1 classification. Output Rank 1 signified that a sensitivity analysis was conducted on the missing piece of source information and resulted in less than a 10% difference in the GRLWEAP predicted ultimate capacity. As stated earlier, Scenarios B through E were for studying the effects of a variety of published filters and outliers and not designed to represent ODOT practice. Scenario H was a derivative of Scenario G with those cases removed violating AASHTO current guidelines on TR times and TST times in all soil groups, irrespective of input tier or output rank. This was overly strict as current AASHTO code requirements would not have been in force at the time the load tests were conducted.

Scenario I at BOR was selected for further investigation as it allowed GRLWEAP analysis in Oregon's cohesive soils for the benefit of soil set-up. Scenario J for cohesionless sands was kept as this could be used to compare to the calibrated resistance factor effects for cohesive soils used in Scenario I. Examination of trends in soil types throughout the previous figures all showed cohesive soils displaying set-up at BOR, while the mean  $\lambda$  illustrated the cases behave conservatively in Scenario I. (Recall, this scenario included all the Clay sites as well as the Mixed sites.) After review, ODOT selected four scenarios: A, F, G at both EOID and BOR for full Monte Carlo Reliability based calibration of  $\phi$ , and Scenario I. The cohesionless Scenario J was also of interest.

In past studies (*Paikowsky 2004; Allen 2005b; Long, et al. 2009*), generally, there was a 5% to 10% increase found in a calculated  $\phi$  from FOSM to those found from reliability based methods; however, this may not always be the case as the change depends on the distribution of the data. The same dead and live load statistical parameters, reported previously in Table 7.1 for FOSM, and a constant live load to dead load ratio of two were selected for use during Monte Carlo analysis. Previous studies had shown that altering the load ratio resulted in little variation to resistance calculation results (*Allen 2005b; Long, et al. 2009*). The Monte Carlo  $\phi$  calibration

effort on the approved scenarios was driven by the data located in the lower tail  $\lambda$  sections and was used to construct the most accurate safety margin distribution, where  $g \leq 0$ . The high unconservative predicted resistance (low  $\lambda$ ) case histories were therefore of most interest, but as pointed out by Allen (*Allen, et al. 2005*), due to the nature of geotechnical data, there can often be insufficient data to confidently model this portion for any calibration effort. The Monte Carlo technique extrapolates the trends displayed in the lower  $\lambda$  tail of each scenario and fills the gaps in data smoothly to establish the distribution of the safety margin. As previously described, the standard minimum  $\beta$  for redundant pile groups of 2.33 was selected for analysis and corresponded to a probability of failure of 1/100 representative of the level of acceptable risk for an individual pile within a pile group large enough to have sufficient redundancy. A modified  $\phi$  value was repeatedly selected until the calculated  $\beta \geq 2.33$  was reached, at which point the acceptable  $\phi$  had been determined and the calibration process was complete. The Monte Carlo technique utilized multiple sets of 10,000 randomly generated variables for loads and resistance sufficient for calculation to this  $\beta$  of 2.33. Calculations were conveniently conducted on Excel<sup>®</sup> spreadsheets. Any alterations in the random variable statistics affected the  $\beta$  calculations and even a re-execution could change  $\beta$  as different random number sets were used. This variation was accounted for by running at least three iterations for a single input  $\phi$  value. If the calculated  $\beta$  consistently produced  $\beta < 2.33$ , which was unconservative because of unacceptable probability of failure, then  $\phi$  would be reduced by 0.01 and the iteration process repeated until the target  $\beta \geq 2.33$  was met.

The Monte Carlo reliability method was performed on each of the four final ODOT selected scenarios: A, F, G, and I. For each of these scenarios, the probability density function (PDF), cumulative distribution function (CDF), and standard normal variable (SNV), for both EOID and BOR driving conditions are shown in Appendices C through F. Three curves are shown on each of the standard normal to log bias plots and represent the lognormal regressed fit to all data, the best lognormal regressed fit to the unconservative lower tail, and the best visual adjusted fit to the lower tail. Following Allen (*Allen, et al. 2005*) this last visual adjustment was achieved by manipulation of the mean resistance  $\lambda$  and COV from the scenario under consideration to better match the lower tail and was considered the most superior of all the three fits. Shown in Figure 7.1 is the EOID plot on Scenario A illustrating this technique. Here the improved fit to the tail reduced the COV and consequently increased the  $\phi$  significantly for the  $\beta \geq 2.33$ . Lowering the COV had the visual effect of rotating the line counterclockwise up from the regressed fit to “all data” line and produced a higher resistance factor. For each scenario at EOID and BOR, the statistical parameters were modified and the Monte Carlo procedure repeated each time until the minimum target  $\beta$  of 2.33 was confirmed for the three fits.

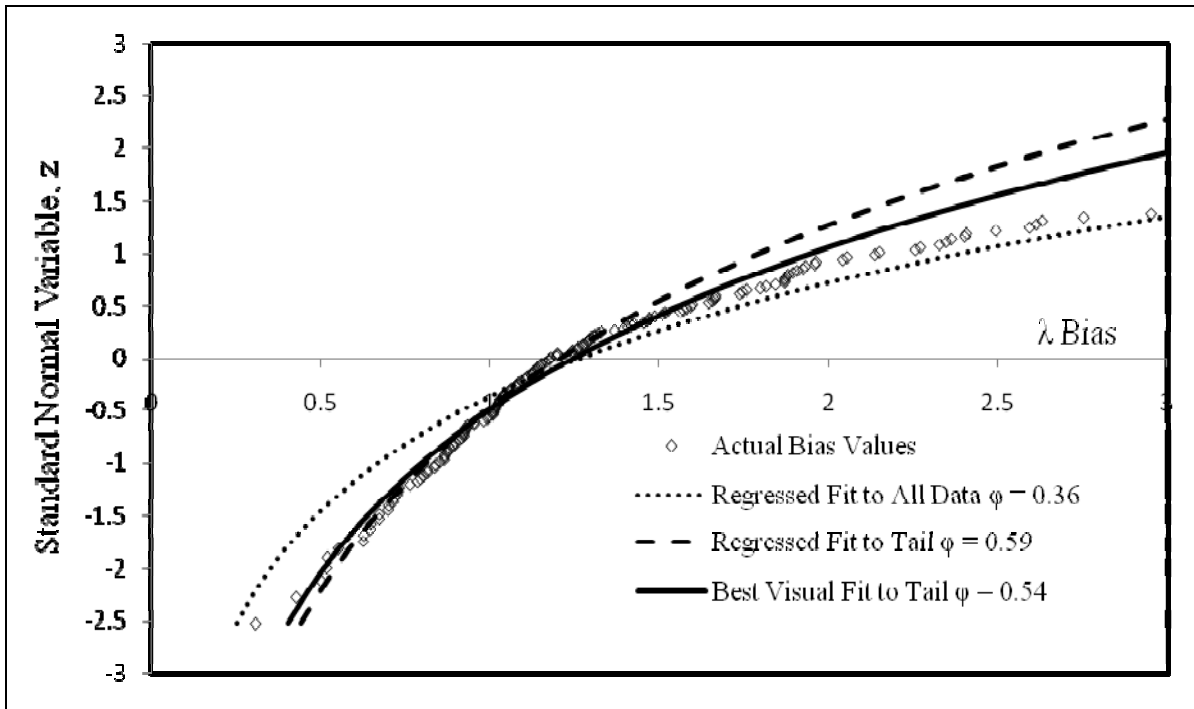


Figure 7.1: Scenario A Monte Carlo reliability method CDF fits at EOID

The study of Scenarios F and G were of more significance for ODOT implementation, as they represented the likely match to practice (single  $\phi$  without considering soil type) especially at EOID. The three lowest data point case-by-case  $\lambda$  values on Scenario F, in both EOID and BOR conditions (shown in Appendix D) all came from sands in Florida where Davisson's criteria had underreported capacities compared to the GRLWEAP capacities. Scenario G's lower tail in Appendix E was better populated and conditioned to the lognormal distribution by the additional 25 case histories found from Tier 2b having output Rank 1.

For each scenario at both EOID and BOR conditions, a summary of the FOSM and Monte Carlo  $\phi$  and  $\phi/\lambda$  results for the three curve fits described above, including the cohesionless sites forming Scenario J for comparisons, is shown in Table 7.3.

**Table 7.3: All scenarios FOSM and Monte Carlo fit based  $\phi$  and  $\phi/\lambda$  efficiencies for  $\beta = 2.33$**

							FOSM		Monte Carlo	
Model and Curve Fit		# Cases	Mean $\lambda$	S.D.	COV	$\phi$	$\phi/\lambda$	$\phi$	$\phi/\lambda^*$	
Scenario A	Fit to All Data	EOID	175	1.555	1.102	0.708	0.35	0.23	0.36	0.23
		BOR	175	0.993	0.468	0.472	0.38	0.38	0.39	0.39
	Fit To Tail	EOID	-	1.309	0.541	0.413	-	-	0.59	0.38
		BOR	-	0.993	0.468	0.472	-	-	0.39	0.39
	Best Visual Fit	EOID	-	1.380	0.650	0.471	-	-	0.54	0.35
		BOR	-	0.910	0.410	0.451	-	-	0.39	0.39
Scenario F	Fit to All Data	EOID	69	1.406	0.596	0.423	0.59	0.42	0.62	0.44
		BOR	79	1.008	0.427	0.424	0.42	0.42	0.45	0.45
	Fit To Tail	EOID	-	1.380	0.558	0.405	-	-	0.64	0.46
		BOR	-	0.978	0.386	0.395	-	-	0.46	0.46
	Best Visual Fit to Tail	EOID	-	1.380	0.610	0.442	-	-	0.59	0.42
		BOR	-	0.960	0.410	0.427	-	-	0.42	0.42
Scenario G	Fit to All Data	EOID	94	1.328	0.564	0.425	0.56	0.42	0.59	0.44
		BOR	114	0.985	0.430	0.437	0.40	0.41	0.43	0.44
	Fit To Tail	EOID	-	1.308	0.532	0.407	-	-	0.6	0.45
		BOR	-	0.985	0.430	0.437	-	-	0.43	0.44
	Best Visual Fit	EOID	-	1.280	0.550	0.430	-	-	0.57	0.43
		BOR	-	0.960	0.430	0.448	-	-	0.41	0.42
Scenario I Clay & Mixed	Fit to All Data	EOID	43	1.464	0.595	0.406	0.64	0.44	0.68	0.46
		BOR	56	1.123	0.457	0.407	0.49	0.44	0.51	0.45
	Fit To Tail	EOID	-	1.251	0.335	0.268	-	-	0.80	0.55
		BOR	-	1.049	0.382	0.364	-	-	0.52	0.46
	Best Visual Fit	EOID	-	1.230	0.300	0.244	-	-	0.83	0.57
		BOR	-	1.080	0.450	0.417	-	-	0.49	0.44
Scenario J Sands	Fit to All Data	EOID	51	1.21	0.515	0.424	0.51	0.42	0.55	0.45
		BOR	58	0.85	0.358	0.421	0.36	0.42	0.39	0.46
	Fit To Tail	EOID	-	1.19	0.486	0.409	-	-	0.51	0.42
		BOR	-	0.84	0.339	0.406	-	-	0.39	0.46
	Best Visual Fit	EOID	-	1.17	0.510	0.436	-	-	0.55	0.45
		BOR	-	0.82	0.360	0.439	-	-	0.36	0.42

\* All Monte Carlo efficiencies are calculated using the mean  $\lambda$  bias fit to all the data in that scenario

The superior visual fit to the tail data are highlighted in each scenario and represents the highest degree of confidence in the modeling process between the three cases. (Since the two tail fits did not use all the available individual cases history  $\lambda$  values, the number of case histories was not displayed.)

Data points to the left of the CDF log normal fit line were viewed as unconservative relative to the curve. The best visual fit to the tail allowed for a more accurate model the lower tail section

without allowing an anomalous data point to skew the overall trend. It can be seen from Figure 7.1 that at EOID for Scenario A, a single low, rogue,  $\lambda$  data point dominated the lognormal regression with all the data. This pile case had been placed in a low input Tier 2b, ranked very low in an output Rank 3, and with noted suspicions of incorrect EOID blow count, possibly not properly recorded in the original database. The much better visual tail fit raised the calculated resistance factor compared to all other scenarios significantly, as shown in Table 7.3, up to 0.54. The Scenario A FOSM  $\phi$  at EOID had been depressed severely by this single data point. The BOR on Scenario A data, shown in Appendix C, was already well fitted to the lower tail with little change to mean  $\lambda$  and COV being required. The creation of cohesive sites in Scenario I permit a better targeted EOID and BOR calibration applicable to ODOT for high set-up sites. This better targeting was also true for Scenario I in the EOID plot where a large reduction in COV was possible to fit the lower tail at EOID, with corresponding improvements in the resistance factor. However, few case history data points were present in the lower tail to count this at the same degree of confidence compared to other EOID scenarios. Other observations were:

- Studying  $\phi/\lambda$  efficiencies of the “Fit to All Data” with the exception of the large improvement in moving to BOR in Scenario A, almost no change was found indicating no clear improvement, or decay, in statistical efficiency by moving to a restrike.
- Scenario F and G were comparable and illustrated no decay in statistics by including those soils in Tiers 2b from all sites where assumptions were required to complete DRIVEN and GRLWEAP. Comparing Monte Carlo to FOSM calibrations for “Fit to All Data” in these scenarios showed improvements in  $\phi$  between approximately 6% to 7% at EOID and 5% to 6% at BOR.
- In all scenarios for the “Fit to All Data”, the presence of a few individual high  $\lambda$  values at EOID from high set-up soil sites raised the COV and degraded the FOSM  $\phi$  and the Monte Carlo  $\phi$ . The advantages in Scenario A of the Monte Carlo fit to the lower tail was illustrated by removing these few data points, which showed a corresponding  $\phi$  increase of 50% from 0.35 by FOSM to 0.54 with the Monte Carlo “Best Visual Fit” to the tail method.
- The “Best Visual Fit” to the tail showed little change in Scenario G and F compared to “Fit to All Data” and confirmed a well-conditioned lognormal fit, but did have a 22% improvement in  $\phi$  at EOID for the cohesive sites in Scenario I.
- Both Scenario G and F had very similar EOID and BOR efficiencies and appeared GRLWEAP capacity neutral. However, both the cohesive Scenario I and Sand Scenario J revealed higher EOID efficiencies.
- Increases in  $\phi$  factors were found for both EOID and BOR when the higher input quality tiers were applied in Scenario F and G compared to Scenario A.

Design efficiency is most often reported by the  $\phi/\lambda$  ratio when comparing methods to establish the highest usable capacity under LRFD design principles. This quickly permits a comparison between scenarios and EOID and/or BOR choices for design. However, this efficiency measure can be skewed by extreme data points and should be viewed as an average for the data set.

### 7.3 LRFD FACTORED CAPACITY OPTIMIZATION

Implementation decisions are made on a project-by-project basis by ODOT and make use of design office issued bearing graphs keyed to the field hammer/pile performance match observed by the inspector. A choice must be made on underperforming piles during initial driving: either to continue driving deeper for increased capacity or to delay and monitor restrike blow count after approved delay in those soils expected to set-up.

It was reported previously that for all scenarios,  $\phi$  at BOR was less than  $\phi$  at EOID. The GRLWEAP capacity most often increases on restrike, simply because of the blow count increase. However using the resistance factor at the BOR conditions, that is lower than the EOID condition, it is possible that the calculated factored BOR resistance is lower than the factored EOID condition. The LRFD inequality was given in Equation 1-1 and is repeated here:

$$\sum \gamma_i Q_i \leq \phi R_{kn}$$

If the load factors are held constant on the left hand side of the equation for the purpose of comparing different nominal capacity methods then the foundation engineer, to minimize cost, seeks the maximum on the right hand side of the equation. This has been addressed in previous work by simply comparing efficiency measurements,  $\phi / \lambda$ , or just seeking the lowest COV. However, both run a risk of being skewed by a limited number of extreme  $\lambda$  case histories in the sample, especially when no outliers have been removed, such as the +/- 2 s.d. used in NCHRP 507.

Table 7.3 shows the final statistical parameters and number of cases for ODOT final Scenarios F and G, and Scenarios I and J in cohesive and cohesionless soils, respectively, compared to baseline Scenario A, at both EOID and BOR. For ODOT Scenario F and G, for all soil and pile types, these efficiency results were not conclusive between EOID or BOR as each  $\phi / \lambda$  value was similar and each factored capacity, on average, was neutral between EOID and BOR.

To offer a clearer representation and assist interpretation of the  $\phi/\lambda$  efficiencies, each case history was viewed as a data point around the factored equivalency relationship,  $\phi R_{kn} \text{ (BOR)} = \phi R_{kn} \text{ (EOID)}$ . This presentation is found in Figures 7.2, 7.3, and 7.4, using the most appropriate Monte Carlo best visual fit to tail  $\phi$ , broken out into Clay, Sand, and the Mixed soil sites respectively for the Scenarios A, F, and G.



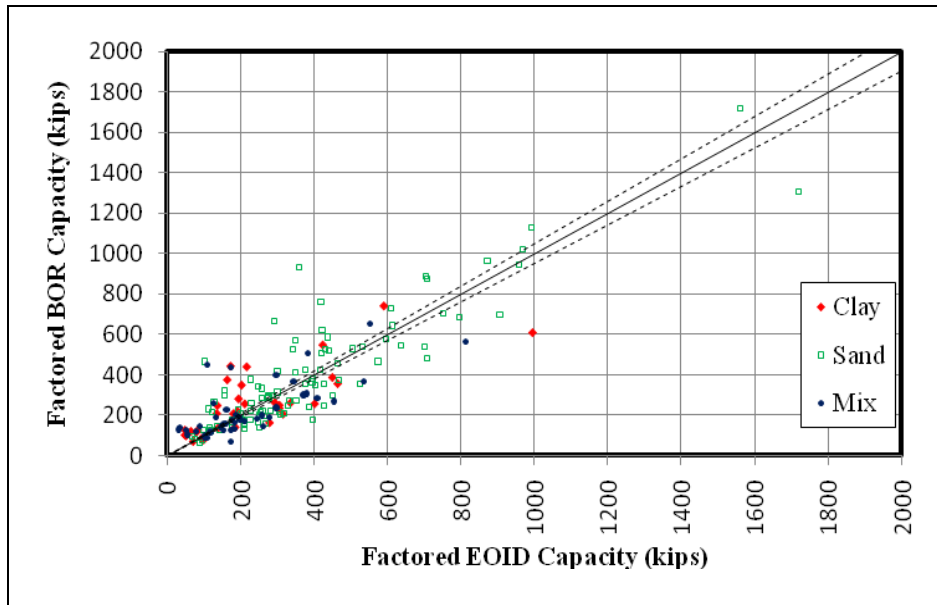


Figure 7.2: Factored BOR plotted to factored EOID for Scenario A

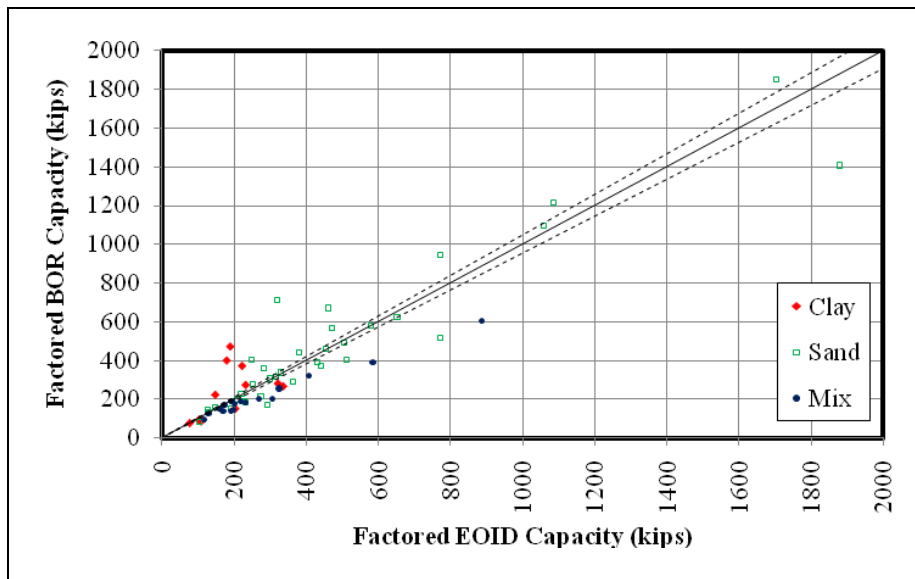


Figure 7.3: Factored BOR plotted to factored EOID for Scenario F

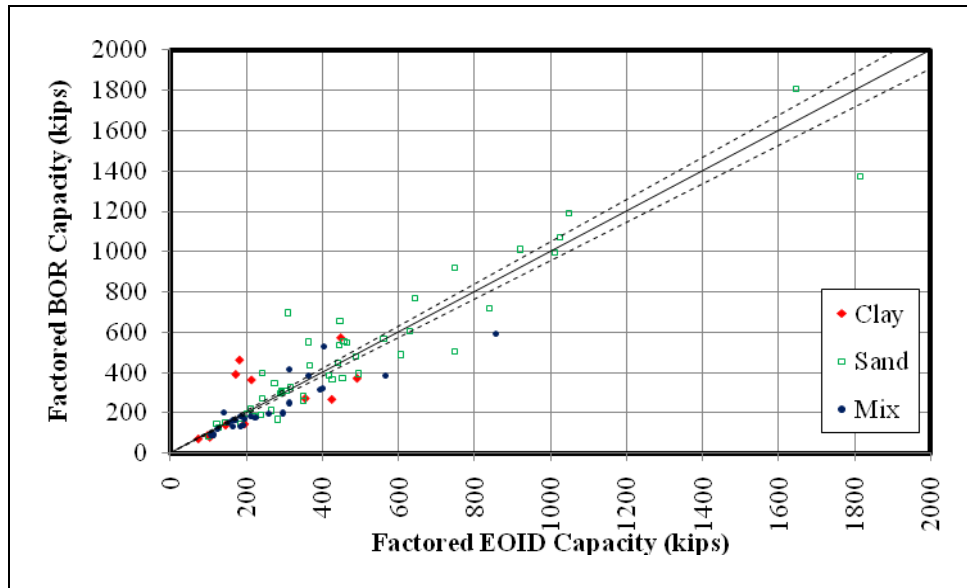


Figure 7.4: Factored BOR plotted to factored EOID for Scenario G

These figures can be compared to Figure 5.1 and nicely illustrated that the range of factored capacity was not equally distributed but was at the lower end for each scenario, with few piles of GRLWEAP factored capacity beyond 1000 kips. The role played by the likely higher set-up cohesive soils was the rationale for the creation of Scenario I and can be presented in a way to assist in making field decisions. For example, at the time of initial driving the pile was a sample member of Scenario G and, when checked for LRFD factored capacity,  $\phi R_{kn}$  (EOID), might be found deficient. By choosing to restrike, the pile now was a member of Scenario I and the  $\phi$  calibration at BOR was now valid (Table 7.3). Figure 7.5 plots Scenarios G and I's factored resistances,  $\phi R_{kn}$ , from their respective EOID and BOR  $\phi$  and predicted GRLWEAP EOID and BOR capacities,  $R_{nk}$ , on each of the 56 case histories contained in Scenario I at restrike. In a similar approach, Figure 7.6 plots the corresponding Scenario G factored EOID resistance to Scenario J factored BOR resistance set for cohesionless soils.

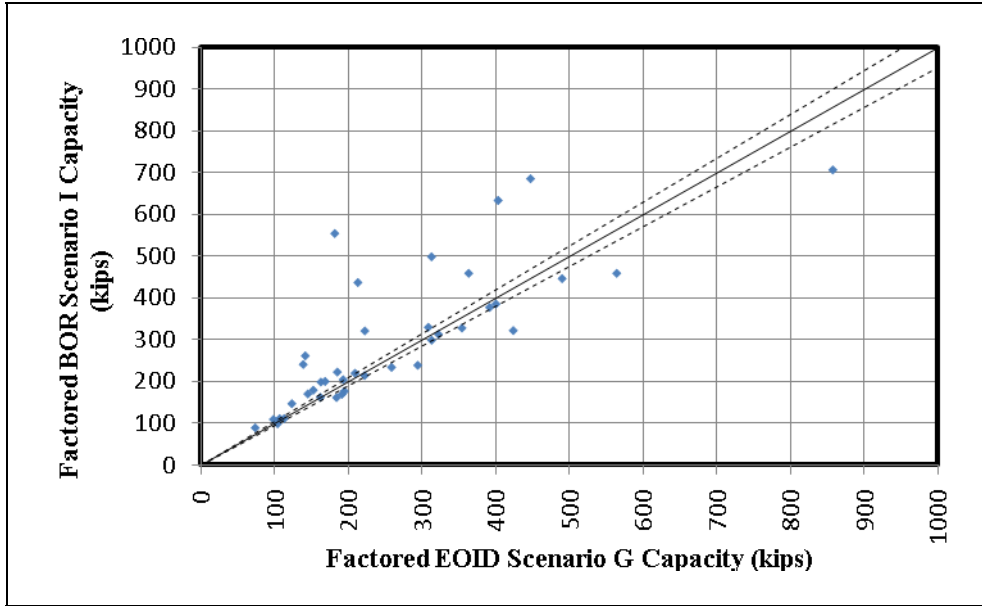


Figure 7.5: Set-up implementation on cohesive soils factored BOR Scenario I to factored EOID for Scenario G

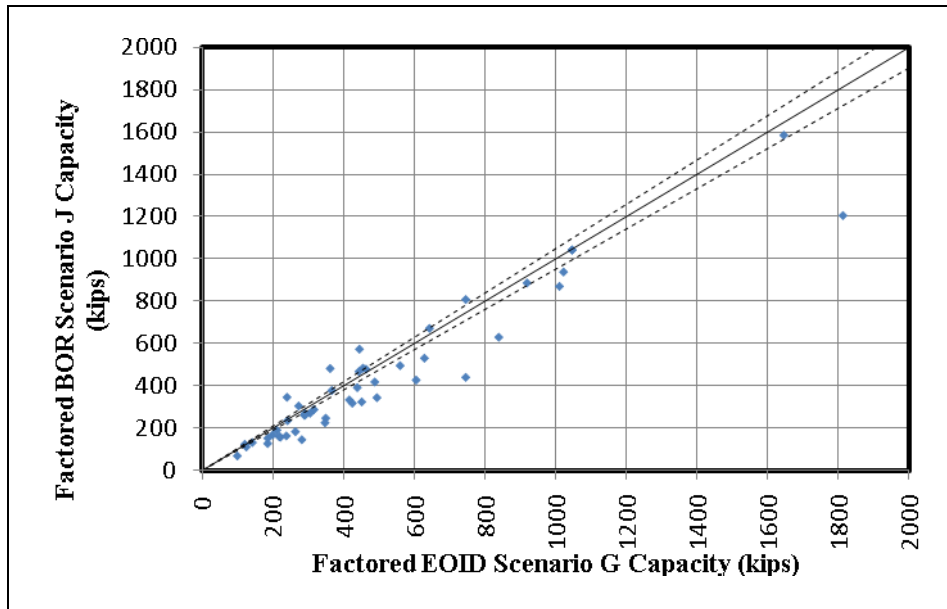


Figure 7.6: Set-up implementation on cohesionless soil factored BOR Scenario J to factored EOID for Scenario G

Judging by the larger number of piles in the database above the  $\phi R_{kn}(\text{EOID}) = \phi R_{kn}(\text{BOR})$  equivalency line in Figure 7.5, on average for these two scenarios in the database, the factored capacity for Clay and Mixed soil sites was more likely to increase on restrike. However, it should be made clear any decision on whether or not to restrike should be made on a case-by-case basis depending upon the expectation that set-up will occur. These decisions are to be furthered explored for ODOT specific practice in a separate implementation Phase 3.

## 8.0 CONCLUSIONS AND RECOMMENDATIONS

For this research, a diverse but complimentary group of existing databases were accessed and merged and then cross-checked for anomalies. Over 150 new cases were added to the ODOT supplied *PDLT2000* and *DFLTD* databases to establish a new *Full PSU Master* database with 322 piles. Each case history was placed into one of three input tiers for statistical profiling to assist in preserving quality and repeatability. The final *Full PSU Master* database supplied 179 cases. All cases were fully analyzed by DRIVEN and GRLWEAP, version 2005 with all updates, to generate bias mean  $\lambda$  and COV statistics for a range of scenarios and for resistance factor calibration. These scenarios were constructed to study the effects from NCHRP 507 removal of arbitrary outliers in the tails, the easy driving mismatched cases, restrike and load test calendar times, and the difference between cohesive and cohesionless soils. The 322 piles ranged up to 40 inches in diameter and up to approximately 200 ft in embedment length. The 179 analyzed piles ranged up to 36 inches in diameter and approximately 166 ft in embedment length with driving blow counts up to 100 BPI.

### 8.1 CONCLUSIONS

It was previously stated that a large variation in installation condition requirements and field practice norms existed in the database due to the differences in time to restrike (TR) time to static test (TST) and the geographic location of the case histories. The inherent variability of national piling standards was captured by keeping a broad database to produce more representative, generally applicable, and conservative resistance  $\phi$  factor results.

From database construction and statistical profiling, it was concluded:

- The qualified 179 cases in the expanded *Full PSU Master* represented a broad spread of soil and pile types typical of ODOT practice. The sand sites represented approximately 54% of the cases, and 46% of the sites were considered to have significant cohesive soil contributions.
- Locating a considerable new set of case histories to expand the database allowed researchers to capture and record the calendar and clock times for restrike and the load test on 69 cases. This proved valuable for study purposes and is recommended for all future database building efforts.
- Subsurface information was generally poor across the source databases and caused over 75% of the 179 cases analyzed to be placed in lower input Tier 2, which required some assumptions for analyses. Sensitivity analysis proved GRLWEAP capacities for these piles were relatively insensitive to the missing detailed input, including water table and shear strength, provided that at least SPT data and the soil log were available.

- Input tiers and Output ranks proved an invaluable aid to sorting data quality and assisting case-by-case interpretation and should always be employed in LRFD calibration.
- The single largest source of anomalies and missing data was the field-reported blow count, especially for the BOR condition. The restrike blow count had no clear definition across the source databases. For the few cases when BOR was absent but the driving log was available, a definition consistent with FHWA of averaging the blows for the first 6 in was used. This provided sufficient movement to capture considerable set-up capacity and mobilize shaft friction.
- Neither of the two largest source national databases, *PDLT2000* or *DFLTD*, was always correct on every piece of the large amount of source input required for DRIVEN and GRLWEAP. For any database calibration work, independent verification from original sources was recommended. From extensive cross checking in this research of the two national databases, *DFLTD* was considered to be the more accurate and more useful as it contains detailed soil logs.

The 175 qualified cases included 91 cases extracted from *DFLTD* and *PDLT2000* matching the original 99 reported in NCHRP 507's appendix. Key general guidance notes from the DRIVEN and GRLWEAP analysis used in this research were:

- All default parameters were used in both EOID and BOR models to establish the GRLWEAP bearing graph. The GRLWEAP restrike options and the set-up and gain/loss factors were never used.
- FHWA endorses the use of a used cushion in BOR modeling with concrete piles. They recommend a used pile cushion of half the thickness and twice the stiffness (*Hannigan, et al. 2006*). This recommendation was always followed.
- A weighted average by percent contribution to resistance from DRIVEN for the side damping,  $j_s$ , in layered soils was always used. Damping, quake, and percent side friction was held constant between EOID and BOR models.
- A uniform first restrike blow count was selected for those piles containing multiple restrikes.

NCHRP 507 gave considerable attention to the needs of dynamic capacity evaluated by the CAPWAP-based signal matching technique to establish implementation recommendations using the efficiency ratio  $\phi/\lambda$ . These new studies here showed similar trends for GRLWEAP capacity on the statistical effects from variables such as blow count ranges and the time to restrike when determining nominal capacity. However, the objective of this research was not to compare to other calibration efforts, only to NCHRP 507 as a reference work of interest. ODOT does use the PDA/CAPWAP technology for piles under certain conditions at select locations. PDA and CAPWAP results are used to develop pile acceptance criteria and work hand in hand with GRLWEAP to reduce uncertainty from variability in site conditions. It should be understood CAPWAP capacity bias and COV statistics are different from GRLWEAP, and  $\phi$  alone should not be the basis of selecting the most efficient method. Unlike limited piles selected for CAPWAP, every driven pile has a recorded field blow count and a predicted bearing capacity is available from the bearing graph generated by GRLWEAP analysis.

Statistically a driven pile may belong to one, or both, of two categories for the purposes of capacity determination by any dynamic method: at the EOID condition and at the BOR condition from restrike. Both these categories are shown by all dynamic methods to possess different mean  $\lambda$  bias and COVs that change the resistance factor that can, from this research, be used in either situation for LRFD design. For this research the database qualifications by soil type, pile type, driving blow count and the load test and restrike times were kept as broad as possible without eroding the statistical quality of the data for GRLWEAP capacity. The expected higher set-up capacity gain would be those piles founded in cohesive soils contributing large capacity from side friction; however, piles in cohesionless soils also show significant set-up.

In this study, Scenario A for EOID was established as a broad match to NCHRP 507 and formed the baseline to measure to other scenarios of interest and likely ODOT practice scenarios. Using an input tier structure, key statistical subgroup scenarios were examined. These scenarios applied filters which included: re-applying the  $\pm 2$  s.d. outlier definition from NCHRP 507, using the AASHTO time to restrike and time to load test recommendations, and exploring the low blow count mismatched cases. From the results of these scenarios, it was concluded:

- Across the full database sites defined by Scenario A choosing a restrike to partially capture the set-up gain in strength reduced the positive bias  $\lambda$  from EOID and lowered the COV; both were desirable in providing a more accurate and reliable prediction. For all scenarios shown in Table 7.2 the restrike lowered the  $\lambda$  bias and illustrated set-up occurred in all cases, including the Sand, Scenario J, sites.
- Sub-grouping by blow count revealed a clear decay in easy driving mean  $\lambda$  bias and COV parameters with blow counts  $\leq 2$  BPI. Above 2 BPI, little difference was found in these parameters and no upper limit was identified. This was in agreement with the NCHRP 507 report presentation for CAPWAP (but was reported in the report text to be 4.5 BPI).
- In the database, the time to restrike (TR) and time to static load test (TST) were known on 64 of the 179 piles analyzed. Of these, only 19 had multiple pile restrikes; therefore, few candidates were available to choose the option of the BOR closest to TST. A uniform first BOR designation was adopted for consistency and also to avoid changes in soil properties and repeat consolidation effects on the 19 piles, which would have tainted the restrike data.
- A study of TR/TST and TST/TR ratios offered valuable insight to assist interpretation and identify possible mismatched case histories. Premature BOR restrike times captured insufficient set-up gain, had low capacity and high  $\lambda$ , and were ignored by the Monte Carlo Reliability method option focused on the lower tail. However, they did feature in FOSM calibration by distorting the calibration statistics, especially in EOID for Scenario A.
- Both GRLWEAP and DRIVEN manuals must be very well understood by foundation practitioners and, in addition, all the parameters for which the LRFD calibration was conducted. Recall that recalibration efforts in all scenarios used default parameters.
- The diverse Scenario A “Best Visual Fit” yielded the EOID  $\phi$  factor of 0.54 from 175 cases, including 18 exhibiting relaxation.

ODOT practice is quite diverse and often project-specific with dependency on private-sector consultants and subcontractors for site investigation, pile design, and field monitoring. This diversity required keeping case history scenario definitions as broad as possible in order to be inclusive, rather than narrowing the parameters for the sole purpose of improving COV to raise the  $\phi$  value. Narrowing the scenario data range of qualifications has the penalty of generating a larger number of pile/soil/driving combinations with each requiring  $\phi$  factor, which complicates implementation and reduces the number of cases available for the statistics. The principal division in this study between EOID and BOR conditions for ODOT implementation came from separating cohesive sites from the cohesionless sites. Three likely practice scenarios are of interest to ODOT:

1. Scenario F used the higher Tier 1 and Tier 2a input quality only.
2. Scenario G used Tier 1 and Tier 2a from Scenario F plus those in Tier 2b with output Rank 1 showing insensitivity to assumptions.
3. For restrike, Scenario I used those sites where cohesive soils generated greater than 20% of predicted capacity based on DRIVEN and were likely to display considerable set-up.

These final three scenarios, and the Scenario J created for sand sites, were statistically explored by FOSM and rigorous Monte Carlo reliability methods in addition to the control Scenario A. Conclusions from the FOSM and Monte Carlo reliability method calibrations for these scenarios were:

- Generally, gains from the FOSM resistance factor to the more accurate Monte Carlo method factor were 4% to 6%.
- Expressed by s.d. changes a tighter statistical distribution and a lower  $\lambda$  bias value was found for the BOR condition compared to EOID for all scenarios.
- Extreme outlier data points inflated the FOSM statistical COV's which can be better modeled by the lower  $\lambda$  tail Monte Carlo fits.
- The choice of conducting a restrike on a pile was shown in all cases to reduce the  $\phi$  compared to EOID, except for FOSM  $\phi$  in Scenario A.
- Often the gain in restrike resistance,  $R_{rk}$ , was somewhat negated for LRFD compliance by the reduction in the resistance factor, since the same Davisson capacity is used as the target in calculating the bias.
- Application of the superior best visual fit to the tail in the Monte Carlo method focused on the higher risk unconservative predictions of capacity. This showed a 51% improvement in the baseline Scenario A  $\phi$  at EOID up to 0.54 over the poor FOSM  $\phi$  of 0.35 on all 175 cases.
- At the EOID condition, ODOT Scenarios F and G were very comparable, irrespective of which method was used for  $\phi$ , but with the advantage that Scenario G had approximately

40% more cases compared to Scenario F, and both were superior to  $\phi$  in Scenario A. At the BOR condition, all scenarios were similar using Monte Carlo methods.

- Scenario G represented the broadest and best inclusive ODOT category for all piles in all soils with 94 case histories used at EOID and 114 used at BOR (20 were removed at EOID by the field blow count > 2 BPI requirement).
- The range of Monte Carlo  $\phi$  values from the three fits for Scenario G at EOID was 0.57 to 0.6, and the most conservative value arose from the visual tail fit. It is possible other state DOT's standards of practice using in-house databases may fit the upper end of this  $\phi$  range, or may be even higher.
- Cohesive soil sites in Scenario I yielded Monte Carlo best visual fit EOID and BOR  $\phi$  resistance factors of 0.83 and 0.49 respectively. This Monte Carlo best visual tail fit raised  $\phi$  by 30% at the EOID compared to the FOSM resistance value of 0.64. However, these EOID safety margin high capacity tail fits, illustrated in Appendix F, did produce unusually low COVs with few data points but well conditioned lognormal tails. They are shown to be lowest COVs of any fit in all scenarios and would benefit from more data populating the tail. The cohesionless sites in Scenario J yielded Monte Carlo based EOID and BOR  $\phi$  resistance factors of 0.55 and 0.36 at EOID and BOR respectively.
- Scenarios I and J represent the only breakout by soil type. Comparing the  $\lambda$  bias drop from EOID to BOR shows equally significant time dependant capacity gain in the sand sites compared to the cohesive sites. This is in agreement with the CAPWAP based soil specific changes in  $\lambda$  bias in both NCHRP 507 and the work for Wisconsin DOT (*Long, et al. 2009*)

## 8.2 RECOMMENDATIONS AND FUTURE WORK

This study showed GRLWEAP, under well defined conditions, was a reliable measure of nominal capacity for a broader array of soil and pile types than had previously been recognized for EOID and BOR conditions. To provide a more focused ODOT practice group of parameters, Scenarios G, I, and J, are offered around which to establish implementation recommendations in a Phase 3. The Scenario I created from Scenario G captured the set-up in cohesive soils by merging clays and mixed soils to establish the EOID and BOR  $\phi$  factors.

Based on the results of Scenarios G the EOID Monte Carlo resistance factor  $\phi$  for all soils and pile types was calibrated to be 0.57, and restrike BOR resistance factor was 0.41. For implementation most past investigators follow AASHTO stated  $\phi$  step increments of 0.05. From this present research study that leads to recommendations of 0.55 at EOID and 0.4 at BOR. To recap, Scenario G possessed these features:

- Had no outlier definition, abandoned the +/- 2 s.d. NCHRP 507 outlier approach, and had a number of cases comparable to NCHRP 507.



- One case history was removed from the full dataset after examination of the ratio of restrike to load test times (TR/TST) in Figure 6.3. This case was in clay, re-struck less than 24 hours (in violation of ODOT standard), and left 51 days before load test.
- Removed piles driving at and under 2 BPI as mismatched and offered 94 piles at EOID for calibration and 110 for the BOR calibration. The difference in case histories arose from cases being removed at EOID with the easy driving mismatch.
- Contained piles in Sands, Clays and Mixed sites, of diameter up to 36 in and 142 ft embedment length and comprised of closed end pipe (CEP), open end pipe (OEP), H section steel and prestressed concrete (PSC) sections.
- Counted the best site investigation and case history reporting practices specified by input Tier 1 and Tier 2a definition.
- Included input Tier 2b cases placed in output Rank 1 since they were shown to be insensitive on the bearing graph to typical assumptions made concerning the water table and/or shear strength ranges.
- Kept the source sample as representative as possible to the broad pile and soil types found across Oregon including CEP, OEP, concrete piles, clays, sands, and mixed soils, with 8 piles exhibiting relaxation coming from the highest Tier 1 and 2a input quality.

Considerable time elapses between pile installation and the full design axial loading. Those sites exhibiting set-up will reach close to their maximum capacity after dissipation of excess pore water pressure in cohesive soils, and by reconstitution of the soil fabric. If restrike is delayed and sufficient time for the AASHTO recommendation of 75% set-up is allowed to occur, then the use of effective stress analysis methods for BOR may be appropriate. However, drained analysis in clays is not supported in DRIVEN but are supported by AASHTO. Fortunately, it has been reported that dynamic methods do capture the set-up more quickly than static load tests would. The bias  $\lambda$  presented in Table 7.3 reveals differences between cohesionless soil sites and the cohesive soil sites for both EOID and BOR. As expected higher bias is revealed for the cohesive Scenario I compared to cohesionless Scenario J. Measured by GRLWEAP  $\lambda$  bias reductions from EOID to BOR the amount of average strength gain for the sites in each of these scenarios is comparable.

This research has provided baseline statistics and built a comprehensive database that will permit more scenario sub-sets to be examined for  $\phi$  calibration, including the effects of pile type, use of field hammer observed and PDA monitored performance, and the derivation of CAPWAP resistance  $\phi$  factors for comparison to those presented here from the *Full PSU Master*.

This research showed cohesive and cohesionless pile GRLWEAP based capacities belong in different populations. The mixing of both in a single scenario raises the combined COV and lowers  $\phi$  resistance factors. Any future work should consider separation by soil type. The following recommendations for future study and final implementation work in a Phase 3 are offered:

- The differences between steel and concrete piles are worthy of additional studies. Additional scenarios should be created and  $\phi$  calibrated to include the effects of

hammers, cushion differences on steel and concrete piles, and field documented hammer performance. Special attention should be given to the common ODOT field condition of pipe piles driven into sands.

- Implementation would benefit from a study of the effects to GRLWEAP capacities from the simpler soil side friction distribution models and the effects of a single side damping,  $J_s$ , values specific to either cohesive (Scenario I) soil only and cohesionless (Scenario J) soil.
- Additional efforts should be made to update the master annually with new data when available, to locate missing information, and to raise the number of case histories to better populate the tails and permit their  $\phi$  values to be considered. Calibration in new scenarios should treat cohesive and cohesionless soils as belonging to two different statistical population sets.
- Those cases that report CAPWAP “measured” damping and quake values should be reanalyzed in GRLWEAP with these values, and  $\phi$  recalibrated.
- A database of drained soil properties should be compiled. Consultants and agency testing laboratories should be allocated sufficient resources to measure drained properties on all soils as well as undrained shear strength for cohesive soils. No reliance should be placed on the SPT as source data for cohesive strengths.
- The use of CAPWAP and wave trace PDA monitoring technology will likely continue for ODOT projects. Those cases from the *Full PSU Master* database with CAPWAP capacities should undergo calibration for comparison to NCHRP 507. Implementation decisions around GRLWEAP and associated CAPWAP reported capacities can then be better understood.
- It is likely that larger pile sizes will become more common. New scenarios should be created to investigate larger pile diameters effects, pile type, and calibration.
- Custom designed input tiers and output ranks are encouraged for all future calibration efforts. This study showed the inclusion of less complete source data case histories produced a degradation of statistical parameters more pronounced at the EOID condition.
- A carefully planned Phase 3 for implementation of this work should be undertaken for both agency and private sector consultants to understand and adhere to the calibration controlling parameters and modeling techniques. Decisions around those conditions that merit a restrike should be identified. Changes to more recent AASHTO code releases can be examined and incorporated into implementation activities. The PI and research group should be prominent in preparation and delivery across ODOT regions of this implementation package, including preparation of a PowerPoint presentation.



## 9.0 REFERENCES

- AASHTO. *AASHTO Bridge Design Specification, 3<sup>rd</sup> Edition*, American Association of State Highway Transportation Officials, Washington, DC. 2004.
- AASHTO. *AASHTO Bridge Design Specification, 2006 Interim Revision*, American Association of State Highway Transportation Officials, Washington, DC. 2006.
- AASHTO. *AASHTO Bridge Design Specification, 4<sup>th</sup> Edition*, American Association of State Highway Transportation Officials, Washington, DC. 2007
- AASHTO. *AASHTO Bridge Design Specification, 2009 Interim Revision*, American Association of State Highway Transportation Officials, Washington, DC. 2009.
- Allen, T.M. *Development of Geotechnical Resistance Factors and Downdrag Load Factors for LRFD Foundation Strength Limit State Design*. National Highway Institute, Federal Highway Administration, Report No. FHWA-NHI-05-052. 2005a.
- Allen, T.M. *Development of the WSDOT Pile Driving Formula and Its Calibration for Load and Resistance Factor Design LRFD*. Report No. WA-RD 610.1. Washington State Department of Transportation and Federal Highway Administration, US Department of Transportation. Washington, D.C. 2005b.
- Allen, T.M., A.S.Nowak, and R.J.Bathurst. *Calibration to Determine Load and Resistance Factors for Geotechnical and Structural Design*. Transportation Research Circular, E-C079, September 2005, Transportation Research Board, Washington, DC. 2005.
- Baecher, G. B. and J. T. Christian. *Reliability and Statistics in Geotechnical Engineering*, John Wiley & Sons. 2003.
- Bowles, J.E. *Foundation Analysis and Design*. 5th edition, McGraw-Hill. 1996.
- Coduto, D. *Foundation Design: Principles and Practices*. Prentice-Hall, New Jersey, US. 2001.
- Duncan, M. J. Factors of Safety and Reliability in Geotechnical Engineering. ASCE. *Journal of Geotechnical and Geoenvironmental Engineering*. Vol. 126, No.4. April, 2000.
- Hannigan, P., G. Goble, G. Likins, and F. Rausche. *Design and Construction of Driven Pile Foundations, Volumes 1 and 2*, National Highway Institute, Federal Highway Administration, US Department of Transportation, Washington, DC. 2006.
- Jackson, B. N. LRFD: Case Studies for ODOT Bridge Pile Foundations. Thesis in partial fulfillment of the Master of Science degree. Portland State University. 2008.

Long, J. H., J. Hendrix, and D. Jaromin. *Comparison of Five Different Methods for Determining Pile Bearing Capacities*. Report #0092-07-04, Wisconsin Highway Research Program. Wisconsin Department of Transportation. 2009.

Long, J.H., J. Hendrix, and A. Baratta. *Evaluation/Modification of IDOT Foundation Piling Design and Construction Policy*. Research Report ICT-09-037. Illinois Center of Transportation. 2009.

Mathias, D. and M. Cribbs. *DRIVEN 1.0: A Microsoft Windows™ Based Program for Determining Ultimate Vertical Static Pile Capacity*. Report No. FHWA-SA-98-074, Federal Highway Administration, Washington, DC. 1998.

Minitab. Minitab16 Statistical Software, ©Minitab, State College, Pennsylvania. 2009.

Nordlund, R.L. Bearing Capacity of Pile in Cohesionless Soils. ASCE. *Journal of Soil Mechanics and Foundation Engineering*, Vol. 89, SM3. 1963.

Nordlund, R.L. Point Bearing and Shaft Friction in Sand. 5<sup>th</sup> Annual Fundamentals of Deep Foundation Design. University of Missouri - Rolla. 1979.

Paikowsky, S.G. *A Simplified Field Method for Capacity Evaluation of Driven Piles*. Report No. FHWA-RD-94-042, Federal Highway Administration, Washington, DC. 1994.

Paikowsky, S. G. *Load and Resistance Factor Design (LRFD) for Deep Foundations*. NCHRP Report 507. National Cooperative Highway Research Program, Transportation Research Board of the National Academies, Washington, DC. 2004.

Pile Dynamics, Inc., GRLWEAP™: Wave Equation Analysis of Pile Driving. GRL Engineers Inc., Cleveland, Ohio. 2005.

Raghavendra, S., C.D. Ealy, A. F. Dimillio, and S.R. Kalaver. User Query Interface for the Deep Foundations Load Test Database. *Transportation Research Record: Journal of the Transportation Research Board*. Transportation Research Board of the National Academies, Washington, DC. Volume 1755. 2001.

Rausche, F., G. Thendean, H. Abou-matar, G.E. Likins, and G.G. Goble. *Determination of Pile Driveability and Capacity from Penetration Tests, Vol. 1-3*. Report No. FHWA-RD-96-179. Federal Highway Administration, Washington, DC. 1997.

Sabatini, P.J., R.C. Bachus, P.W. Mayne, J.A. Schneider, and T.E. Zettler. *Geotechnical Engineering Circular No. 5: Evaluation of Soil and Rock Properties*. FHWA-IF-02-034. Federal Highway Administration, Washington, DC. 2002.

Smith, T.D. and P. Dusicka. *Application of LRFD Geotechnical Principles for Pile Supported Bridges in Oregon: Phase 1*. OTREC Report TT-09-01. Oregon Transportation Research and Education Consortium. Portland State University. Portland. 2009.

Tomlinson, M. J. *Foundation Design and Construction*. 4<sup>th</sup> Ed. Pitman Advanced Publishing, Boston, MA. 1980.

William, J. L., E.P. Voytko, R.M. Barker, J.M. Duncan, B.C. Kelly, S.C. Musser, and V. Elias. *Load and Resistance Factor Design (LRFD) for Highway Bridge Substructures*. Report No. FHWA HI-98-032. Federal Highway Administration, Washington, DC. 1998.



## **APPENDICES**





**APPENDIX A:**

***FULL PSU MASTER DATABASE***



PSU Pile Number	Location	Pile Type	Pile Length - EIOD Embedded Length - BOR Length (ft)	Blowcounts		Set Up Ratio	Input Tier	Output Rank	Predominate Soil Condition		C/S/M	DRIVEN Capacity (Kips)	Davisson's Capacity (Kips)	GRLWEAP Capacity		Hammer Type	Comments
				EIOD (BPI)	BOR1 (BPI)				Side	Tip				EIOD (Kips)	BOR (Kips)		
<b>146 piles of BOR Final in PDLT2000 from WSDOT</b>																	
1	NE	HP - 10x42	75-73	2.83	8	2.83	2-a	1	CL	SP	Mix	302	304	297	408	Delmag D-30	
2	NE	PSC - 12"sq	65-65	5	5	1.00	2-a	1	CL	SP	Mix	525	358	391	437	Delmag D-30	
3	NE	PSC - 14"sq	65-66	9.17	6	0.65	2-a	3	CL	SP	Mix	687.15	378	517	487	Delmag D-30	
4	NE	CEP - 12.75"	70-66	2.5	5	2.00	2-a	1	CL	SP	Mix	404.5	292	287	405	Delmag D-30	
5	IA	HP - 14x89	120-118	3.33	10	3.00	2-a	1	SP-SC	SC	Sand	1881	928	372	536	Kobe K 25	
6	IA	CEP - 14"	100-95	5.83	10	1.72	1-a	1	SP-SC	SC	Sand	1210	650	390	443	Kobe K 25	
7	OK	CEP - 26"	63.3-61.3	4.58	3.75	0.82	2-b	1	CL	CL	Clay	743	598	744	657	MKT DE-110C	
8	OK	PSC - 24"oct	64.3-63.3	4.42	6	1.36	2-b	2	CL	CL	Sand	1000	760	733	978	MKT DE-110C	
9	OK	RC - 24"sq	63.3-57	25.3	14.8	0.58	2-b	3	CL	CL	Clay	868	1700	1843	1555	MKT DE-110C	
10	OR	PSC - 20"sq	135-126	9.58	92.8	9.69	2-b	2	SPSM	MH	Sand	6177	1360	1303	2270	Delmag D 46-23	
11	ME	CEP - 18"	120-100	1.42	3	2.11	1-a	1	SP	SW	Mix	809	440	349	518.00	Kobe K 45	
12	ME	CEP - 18"	80.5-71.5	1.42	3	2.11	1-a	1	SP	SP	Sand	758	408	358	575.00	Kobe K 45	
13	ME	CEP - 18"	60-52	1.33	2	1.50	1-a	1	SP	SP	Sand	476	342	329	453.00	Kobe K 45	
14	CO	CEP - 12.75"	NA-127.7	3.5	3.8	1.09	3							316		KC-25	(#1). Not in DFLID. Pile info needed
15	CO	CEP - 12.75"	NA-127.7	3.67	4	1.09	3							368		KC-25	(#1). Not in DFLID. Pile info needed
16	MO	CEP - 14"	87-83.5	3	7	2.33	2-b	1	SP	GP	Sand	518	330	327	429.00	ICE 640	
17	MO	CEP - 14"	65-61.75	1.42	3	2.11	2-b	1	SP	GP	Sand	247	209	186	323.00	ICE 640	
18	WA	CEP - 48"	160-34	19.7	16	0.81	1-c	3	ML	SP	Mix	4217	1300	1503.5	1443.00	CONMACO C300	
19	WA	CEP - 48"	158-16	26.75	17	0.64	1-c	3	SWSM	SP	Sand	3160	1000	1310	1229.00	CONMACO 300	
20	AL	PSC - 18"sq	67-65-67.5	1.5	7	4.67	1-a	2	SM/OL	SW	Sand	672	370	290	762.00	Kobe K 45	
21	AL	PSC - 18"sq	77-75	3.5	7	2.00	1-a	2	SM/OL	SM	Sand	2470	550	509	729.00	Kobe K 45	
22	AL	PSC - 24"sq	67-64-64.8	2.83	6	2.12	1-a	2	SM/OL	SM	Sand	1904	625	425	660.00	Kobe K 45	
23	AL	PSC - 24"sq	77-75-75.5	6.42	8	1.25	1-a	2	SM/OL	SM	Sand	4086	817	615	693.00	Kobe K 45	
24	AL	PSC - 36"sq	74-73-73.25	7.67	5	0.65	1-c	3	SM/OH	SM	Mix	5316	1140	990	937.00	Delmag D 62-22	
25	VT	HP - 14x73	95-75-75.75	4.17	9	2.16	1-a	2	GM	GP	Sand	1275	315	250	373.00	MKT DA 35B	
26	VT	HP - 14x73	95-90-90.4	2.67	3	1.12	1-a	2	GM	GP	Sand	1934	345	176	197.00	MKT DA 35B	
27	MN	HP - 14x73	100-96-96.1	1.83	25	13.66	2-b	1	ML	SC	Sand	655	765	460	880.00	ICE 90S	
28	PA	Monotube	37-23-23.67	5.42	13	2.40	2-b		SC	SP	Sand	116	243			Delmag D 12	
29	KT	PSC - 14"sq	75-34.67-34.75	15.5	30.5	1.97	1-c	2	CL	SC	Sand	222	378	384	450.00	LINKBELT LB 520	
30	LA	PSC - 24"sq	103-84-84.33	1.67	4	2.40	2-b	1	OL	CL	Clay	447	400	253	634.00	VULCAN Vul 020	
31	Ontario, Canada	CEP - 9.6"	NA-154.3-154.3	21.33	40	1.88	3							540		Birmingham B-400	(#1)
32	Ontario, Canada	CEP - 9.6"	NA-NA-101.1		14		3							366		Birmingham B-400	(#1), (#2), (#3)
33	Ontario, Canada	CEP - 10.24"	NA-NA-64.4		4.23		3							189		ICE 40S	(#1), (#2), (#3)
34	Ontario, Canada	CEP - 12.75"	NA-NA-38.6		50		3							242		Delmag D 12	(#1), (#2), (#3)
35	Ontario, Canada	CEP - 12.75"	NA-NA-54		8		3							660		Delmag D 30-13	(#1), (#2), (#3)
36	FL	PSC - 24"sq	50.4-37.2	9.33	9.33	1.00	1-a	2	SP	SP	Sand	1107	610	869	962	Delmag D 46-02	
37	FL	PSC - 24"sq	43.5-28-28.5	5	8	1.60	1-a	2	SP	SP	Sand	434	453	556	805.00	Delmag D 46-02	
38	FL	PSC - 30"sq	135-NA-128.6	5	6.67	1.33	1-a	2	SP	SP	Sand	2784	900	1796	2612.00	CONMACO 300E5	
39	FL	PSC - 30"sq	109-NA-110	3.3	5	1.52	1-a	2	SP	SP	Sand	2008	820	1310	2250.00	CONMACO 300E5	
40	Ontario, Canada	HP - 12x73	60-48.5-48.5	3.6	1.83	0.51	2-a	3	ML	SP	Mix	279	322	320	180.00	Birmingham B-400	Davison's at EIOD and BOR reported. Similar - EIOD used
41	Ontario, Canada	CEP - 12.75"	52.2-48.2-48.2	1.4	5.56	3.97	2-a	2	ML	SP	Mix	332	330	144	307.00	Birmingham B-400	Davison's at EIOD and BOR reported. Similar - EIOD used
42	Ontario, Canada	HP - 12x73	100.2-90.5-90.5	5.3	10.31	1.95	2-a	1	ML	SP	Mix	587	612	368	448.00	Birmingham B-400	Davison's at EIOD and BOR reported. Similar - EIOD used
43	Ontario, Canada	CEP - 12.75"	105.4-90-90.5	13.5	16.67	1.23	2-a	2	ML	SP	Mix	502	600	324	329.00	Birmingham B-400	Davison's at EIOD and BOR reported. Similar - EIOD used
44	Ontario, Canada	T-TIMBER	44.4-41.6	4.9	2.53	0.52	2-a	4	ML	SP	Mix	379	122			Birmingham B-225	No support of tapered timber piles in GRLWEAP
45	Ontario, Canada	PSC - 12"sq	50-48	4.1	6	1.46	2-a	3	ML	SP	Mix	446	402	269	365.00	Birmingham B-400	Davison's at EIOD and BOR reported. Similar - EIOD used
46	NC	PSC - 12"sq	NA-NA-44.5		10		3							415			(#1), (#2)
47	PA	HP - 12x53	70-NA-66	1.4	4.5	3.21	2-b	1	CH	CH	Clay	394	284	147	300.00	ICE 640	
48	NA	PSC - 20"sq	NA-NA-36		4		3							380			(#1), (#2)
49	NA	PSC - 20"sq	NA-NA-55		8		3							580			(#1), (#2)
50	NA	PSC - 20"sq	NA-NA-86		7		3							620			(#1), (#2)

(#1) – Incomplete or missing soil data

(#2) – Incomplete or missing hammer data

(#3) – Incomplete or missing blow count data

Output Rank 4 does not qualify for recalibration

C/S/M – Major soil contribution. Clay, sand, or mix.

All lines in **bold** represent Input Tier 1 & 2

PSI Pile Number	Location	Pile Type	File Length - EOID Embedded Length - BOR Length (ft)	Blowcounts		Set Up Ratio	Input Tier	Output Rank	Predominate Soil Condition		C/S/M	DRIVEN Capacity (Kips)	Davisson's Capacity (Kips)	GRIWEAP Capacity		Hammer Type	Comments
				EOID (BPI)	BOR1 (BPI)				Side	Tp				EOID (Kips)	BOR (Kips)		
51	NA	PSC - 20"sq	NA-NA-94		10		3					600					(#1), (#2)
52	NA	PSC - 10"sq	NA-NA-50		10		3					250					(#1), (#2)
53	NA	PSC - 10"sq	NA-NA-58		5.5		3					270					(#1), (#2)
54	VA	PSC - 54"sq	NA-NA-109		7.86		3					920					(#1), (#2)
55	VT	CEP - 12.75"	NA-NA-99.5		12		3					360					(#1), (#2)
56	Australia	RC - 10.8"sq	NA-NA-67.6	3.63	18.14	5.00	3					652					(#1), (#2)
57	Australia	RC - 10.8"sq	NA-NA-67.6	1.95	6.68	3.43	3					558					(#1), (#2)
58	Ottawa, Canada	CEP - 9.625"	NA-68.9	14	6	0.43	2-b	4	CL	Glacial Till		271				Delmag D 30-32	(#1)
59	FL	VC - 24"sq	98-93.2	3.42	4	1.17	2-b	1	OH/ML	SW	Sand	1173	958	512	756.00	Vulcan 020	
60	FL	VC - 24"sq	83.9-56.03-58.83	3.3	3	0.91	2-a	1	SM	SW	Sand	935	870	747	890.00	Conmco 300	
61	FL	VC - 24"sq	66.3-54.6	5	8	1.60	1-a	1	SM	SW	Sand	900	715	645	1056.00	Vulcan 020	
62	FL	PSC - 18"sq	65.2-61	3.17	6	1.89	2-b	1	SM	SW	Mix	147	315	245	491.00	VULCAN 010	
63	FL	VC - 24"sq	69.17-62	4	8	2.00	2-b	1	SM	SW	Mix	774	524	550	1018.00	Vulcan 020	
64	FL	VC - 24"sq	98-62	2.91	6	2.06	1-a	2	SC	SC	Sand	405	812	422	967.00	VULCAN Val 020	
65	FL	VC - 24"sq	123.67-103.6	5.1	12	2.35	2-b	1	CH	MH	Clay	639	808	785	1400.00	Vulcan 020	
66	FL	VC - 24"sq	121.5-103	6	12	2.00	2-b	1	SC	CL	Sand	678	976	815	1336.00	Vulcan 020	
67	FL	PSC - 24"sq	84-NA-84.3	1	10	10.00	2-b	1	SP	SC	Sand	771	500	190	1195.00	VULCAN Val 020	
68	FL	VC - 30"sq	71.1-54	12	12	1.00	2-b	1	SW	SP	Sand	1322	1250	1064	1193.00	ICE 200S	
69	FL	VC - 30"sq	106.2-NA-87.7	2	2	1.00	2-b	2	SC	CH	Sand	1703	1435	521	570.00	ICE 200S	
70	FL	VC - 30"sq	102-78.4	16	15.33	0.96	2-b	1	SM	ML/CL	Sand	1305	1515	1474	1755.00	ICE 200S	
71	FL	VC - 30"sq	101-83.4	3	8	2.67	2-b	1	SM	ML/CL	Sand	1361	643	637	1345.00	ICE 200S	
72	FL	VC - 30"sq	106-84.7	4.6	8	1.74	2-b	1	SW	ML/CL	Sand	1556	917	780	1306.00	ICE 200S	
73	FL	VC - 30"sq	102-72.9	8.75	20	2.29	2-b	1	SW	ML/CL	Sand	1450	1463	1130	1871.00	ICE 200S	
74	FL	VC - 30"sq	106-80	15.17	24	1.58	2-b	1	SPSC	CL	Sand	1371	1410	1615	2467.00	ICE 200S	
75	FL	PSC - 24"sq	80-70.7	5.42	10	1.85	1-b	1	SM/SP	ML	Sand	958	960	800	1350.00	VULCAN Val 020	
76	Ontario, Canada	HP - 12x73	120.6-114.4	12	16	1.33	1-c	2	CL/ML	SM/ML	Mix	659	800	455	477.00	Birmingham B-400	EOID hammer not confirmed. Assumed same as BOR
77	Ontario, Canada	CEP - 12.75"	108.2-107.2	39	76	1.95	1-c	2	ML	SM/ML	Mix	412	490	337	345.00	Birmingham B-400	EOID hammer not confirmed. Assumed same as BOR
78	Ontario, Canada	HP - 12x74	NA-20.1	30	20	0.67	3					354					(#1), (#2)
79	Ontario, Canada	HP - 12x74	NA-25.7	22	10	0.45	3					556					(#1), (#2)
80	Ontario, Canada	HP - 12x53	NA-25.2	38	25	0.66	3					410					(#1), (#2)
81	Ontario, Canada	CEP - 7.063"	NA-NA		4		3					140					(#1), (#2)
82	Brunswick	HP - 12x89	NA-NA-126				3					730					(#1), (#2)
83	Brunswick	CEP - 12.75"	NA-NA-104		4.67		3					340					(#1), (#2)
84	WI	CEP - 12.75"	140.4-123	20.2	48	2.38	1-c	2	OL/MH/CH	SW	Clay	682	654	343	360.00	VULCAN Val 200C	
85	WI	HP - 12x63	NA-155.5	0.75	2.5	3.33	1-a	1	OL/MH/CH	SW	Mix	1097.4	302	100	267.00	Vulcan 010	
86	WI	CEP - 9.63"	165.92-142	0.83	5	6.02	2-b	1	CL-ML	SW	Clay	696	360	90	262.00	VULCAN Val 010	
87	WI	CEP - 9.63"	145-142	0.83	16	19.28	2-b	1	CL-ML	SW	Clay	696	660	90	324.00	VULCAN Val 010	
88	WI	CEP - 9.63"	154.58-144	0.5	11.36	22.72	1-b	1	CL-ML	SW	Mix	474	376	60	332.00	VULCAN Val 010	
89	WI	CEP - 9.63"	NA-139	1.17	10	8.55	2-b	1	CL-ML	SW	Clay	347	556	120	308.00	VULCAN Val 010	
90	WI	CEP - 9.63"	NA-NA-140	4.58	32	6.99	2-b	1	CL-ML	SW	Clay	678	596	256	347.00	VULCAN Val 010	
91	WI	CEP - 9.63"	NA-NA-156	1.5	30	20.00	2-b	1	CL-ML	SW	Mix	826	600	167	376.00	VULCAN Val 010	
92	FL	PSC - 18"sq	32.78-19.33-20.63	7.6	5.33	0.70	1-c	3	SW	SW	Sand	212	274	496	410.00	ICE 640	
93	FL	PSC - 18"sq	34.25-17.4-17.6	9.17	20	2.18	1-c	2	SW	SW	Sand	132	230	537	758.00	ICE 640	
94	FL	PSC - 24"sq	92-NA-85.8	7	7.29	1.04	2-b	3	SW	SW	Sand	1710	855	1178	1400.00	Delmag D 46-32	
95	FL	PSC - 24"sq	65-NA-61.3	16.7	10.35	0.62	2-b	3	SPGP	SC	Sand	846	1671	1678	1793.00	Delmag D 46-32	
96	FL	VC - 30"sq	121-92.8-94.5	3.36	5.21	1.55	2-b	3	CL	SP	Mix	2795	1006	1025	1676.00	CONMACO 300E5	
97	FL	VC - 30"sq	116.9-88.3-89.3	3	3.7	1.23	2-b	3	SP	SP	Sand	2106	1162	935	1356.00	CONMACO 300E5	
98	FL	VC - 30"sq	110.6-80.22-81	5.75	6.25	1.09	2-b	1	SP	CL	Sand	1244	1114	1775.5	2423.50	CONMACO 300E5	
99	FL	VC - 30"sq	104.5-71.6-78.6	5.083	5.33	1.05	2-b	2	SP	SP	Sand	4035	1136	1394	1800.00	CONMACO 300E5	
100	FL	PSC - 24"sq	67.57.25-58.5	5	4	0.80	2-b	3	MH	SP	Mix	792	752	844	689.00	Delmag D 46-32	

(#1) – Incomplete or missing soil data

(#2) – Incomplete or missing hammer data

(#3) – Incomplete or missing blow count data

Output Rank 4 does not qualify for recalibration

C/S/M – Major soil contribution. Clay, sand, or mix.

All lines in **bold** represent Input Tier 1 & 2

PSU Pile Number	Location	Pile Type	Pile Length - EIOD Embedded Length - BOR Length (ft)	Blowcounts		Set Up Ratio	Input Tier	Output Rank	Predominate Soil Condition		C/S/M	DRIVEN Capacity (Kips)	Davisson's Capacity (Kips)	GRLWEAP Capacity		Hammer Type	Comments
				EIOD (BPI)	BORI (BPI)				Side	Tip				EIOD (Kips)	BOR (Kips)		
101	FL	PSC - 24"sq	62-46.1	7	18.75	2.68	2-b	4	SC/Limestone	CL		1827	1066			Delmag D 46-32	Limestone dampening factors unknown
102	FL	PSC - 24"sq	39-NA-36	9	9.17	1.02	2-b	4	ML/OH	CL			566			Delmag D 46-32	Limestone dampening factors unknown
103	SC	PSC - 24"oct	66.5-61	6	5	0.83	1-c	1	SC	GW	Sand	1276	1140	771	1094.00	VULCAN Val 320 & 520	
104	SC	PSC - 16"sq	NA-62-63	1.75	5.58	3.19	3						807				(#1), (#2)
105	SC	HP - 14x89	NA-NA-66				3						897				(#1), (#2)
106	SC	OEP - 16"	NA-NA-66				3						932				(#1), (#2)
107	SC	OEP - 24"	85-81	3.75	12.5	3.33	2-b	1	SW	SP	Mix	649.47	596	638	937	VULCAN Val 512	
108	SC	HP - 14x73	85-78-79	1.42	0.67	0.47	2-b	2	SW	SP	Mix	544	318	300	584.00	VULCAN Val 512	
109	FL	PSC - 14"sq	115-90-91	5.67	6.5	1.15	2-b	2	SM-SC	SC	Sand	2023	842	226	551.00	VULCAN Val 80C	BOR Hammer - VULCAN Val 010
110	FL	CEP - 12.75"	90-83-88-33	2.25	4	1.78	2-b	2	SM-SC	SC	Sand	439	496	125	236.00	VULCAN Val 80C	BOR Hammer - VULCAN Val 010
111	LA	PSC - 24"sq	NA-81.5	0.83	1.75	2.11	3						414				(#1), (#2)
112	LA	PSC - 30"sq	NA-82-83	1.17	1.92	1.64	3						511				(#1), (#2)
113	LA	PSC - 30"sq	NA-82-83	1.82	4.92	2.70	3										(#1), (#2)
114	LA	PSC - 36"cyt	NA-81-82	1.25	2.83	2.26	3						542				(#1), (#2)
115	LA	PSC - 36"cyt	NA-81	3.93	2.67	0.68	3						540				(#1), (#2)
116	VA	PSC - 24"sq	110-NA-105	0.6	6	10.00	2-b	4	SM	SW	Sand	3642	508	222	1283.00	Delmag D 46-32	CAPWAP less than 1/2 of BOR Capacity. No Davisson's criteria
117	OH	CEP - 12"	40-NA-30	3.8	3.6	0.95	2-b	3	CL-ML	CL-ML	Sand	121	152	164	160.00	FEC 1500	
118	MS	HP - 14x73	40-40	3	6	2.00	1-a	1	SM-SC	SC	Sand	182	500	213	350.00	Delmag D 19-32	No load test result known
119	SC	PSC - 24"sq	90-90	3	83.3	27.77	2-b	2	CL	CL	Sand	1097	1066	667	2385.00	VULCAN Val 520	
120	SC	HP - 14x73	90-91	0.5	83.3	166.60	1-c	2	CL-CH	CL-CH	Clay	364	619	128	852.00	VULCAN Val 520	
121	SC	PSC - 12"sq	91-88	2.6	26	10.00	2-b	2	CL-CH	CL-CH	Clay	210	360	334	531.00	ICE 640	
122	AZ	HP - 14x117	51.3-50.5	20.4	15	0.74	2-b	3	SC	GW	Sand	481	1460	836	765.00	MKT DE 70B	
123	AZ	HP - 14x117	65.6-50-51	25.6	6	0.23	2-b	3	CL-SC	SC	Sand	797	1281	737	455.00	MKT DE 70B	
124	AZ	CEP - 14"	30.75-22.4	65.3	13	0.20	2-b	3	CL-SC	SC	Sand	344	721	793	635.00	MKT DE 70B	
125	AZ	CEP - 14"	42.5-NA-24.8	34.5	16	0.46	2-b	3	SC	GP	Clay	391	668	585	525.00	MKT DE 70B	
126	AZ	PSC - 16"sq	32-NA-23	24.3	29	1.19	2-b	2	CL-SC	SC	Sand	639	952	696	908.00	MKT DE 70B	
127	AZ	PSC - 16"sq	41.6-19	56.3	12	0.21	2-b	3	SC	GP	Sand	538	1006	715	623.00	MKT DE 70B	
128	WI	CEP - 12.75"	161.25-NA-95.1	18	14	0.78	2-b	2	CL-ML	SP	Sand	74.41	438	266	322.00	Vulcan 010	BOR Hammer - Conmaco 100E5
129	Hong Kong	PSC - 19.69"cyt	NA-74.5	3.63	9.07	2.50	3						980				(#1), (#2)
130	Hong Kong	HP - 12x120	NA-97.44	4.38	10.58	2.42	3						1065				(#1), (#2)
131	CA	OEP - 24"	50-40.3	0.92	1.25	1.36	1-a	1	SP	CL	Mix	687.74	685	365	480.00	Delmag D 62-22	
132	CA	CEP - 24"	64-60	1.5	2.5	1.67	1-a	1	SP	CL	Mix	1120	726	234	667.00	Delmag D 30-32	
133	CA	CEP - 24"	64-60	1.25	10.33	8.26	1-b	1	SP	CL	Mix	1120	885	200	1155.00	Delmag D 30-32	
134	NY	HP - 10x42	NA-109.9	13	34	2.62	3						312				(#1), (#2)
135	FL	PSC - 24"sq	68.8-49.2	8	38	4.75	2-b	3	SP	CL-ML	Clay	1866	786	1093	1892.00	CONMACO C300	
136	FL	PSC - 20"sq	68-47.29	3.08	28	9.09	2-b	2	SP	CL-ML	Clay	1301	587	401	1124.00	CONMACO 160	
137	FL	PSC - 24"sq	60.5-27.4-27.9	11	26	2.36	2-b	3	SP	CL-ML	Sand	2473	1148	1135	1650.00	CONMACO C300	
138	FL	PSC - 24"cyt	43.5-26.7	14	16	1.14	2-b	4	SP/Limestone	SP		3029	623		CONMACO C300	Define ASCON cap block properties. Predominant soil is	
139	FL	PSC - 20"sq	55-45.75-46.2	8	13	1.63	2-b	2	SM	SP	Sand	1636	583	695	1085.00	Vulcan 510	EIOD hammer not confirmed. Assumed same as BOR
140	FL	PSC - 20"sq	37-NA-36.4	3.92	7	1.79	2-a	1	SP	SW	Sand	570	368	480	853.00	Vulcan 510	EIOD hammer not confirmed. Assumed same as BOR
141	FL	PSC - 30"sq	101.75-72.6-73.5	4.75	5	1.05	2-a	2	SP	SP	Sand	3782	754	1105	1480.00	CONMACO C300	
142	FL	PSC - 30"sq	75-64.4-69	8.3	11.4	1.37	2-a	1	SP-ML	SP	Sand	3579	908	984	1382.00	ICE 200S	EIOD hammer not confirmed. Assumed same as BOR
143	FL	PSC - 30"sq	65-53.4-59	4.33	5.3	1.22	1-b	2	SM	SM	Sand	2269	778	732	933.00	ICE 200S	EIOD hammer not confirmed. Assumed same as BOR
144	FL	PSC - 18"sq	53.1-53.1	7.7	9	1.17	2-b	2	SP-SM	SP-SM	Sand	1201	312	481	563.00	ICE 640	EIOD hammer not confirmed. Assumed same as BOR
145	FL	PSC - 14"sq	76-76	2	10	5.00	2-a	2	SP	SM	Sand	700	398	210	592.00	ICE 640	EIOD hammer not confirmed. Assumed same as BOR
146	FL	PSC - 14"sq	69.65-69.5	5.55	13	2.34	2-b	2	CL-ML	SM	Clay	1734.73	360	354	564.00	ICE 640	EIOD hammer not confirmed. Assumed same as BOR
<b>10 additional piles of multiple BORs in PDL T2000 from WSDOT</b>																	
147	NY	CEP - 11.73"	NA-NA-65.6		11		3						468				(#1), (#2)
148	Brunswick	HP - 12x89	NA-NA-102.1		25		3						325				(#1), (#2)
149	WI	HP - 12x63	NA-155.5	1	2	2.00	1-a	4	SP	SM		1240.9	200				(#1), (#2)
150	WI	CEP - 14"	NA-155.2	1.75	2.08	1.19	1-a	4	SP	SM		1962.19	188				(#1), (#2)

- (#1) – Incomplete or missing soil data
- (#2) – Incomplete or missing hammer data
- (#3) – Incomplete or missing blow count data

Output Rank 4 does not qualify for recalibration  
C/S/M – Major soil contribution. Clay, sand, or mix.  
All lines in **bold** represent Input Tier 1 & 2

PSU Pile Number	Location	Pile Type	Pile Length - EOD Embedded Length - BOR Length (ft)	Blowcounts		Set Up Ratio	Input Tier	Output Rank	Predominate Soil Condition		C/S/M	DRIVEN Capacity (Kips)	Davisson's Capacity (Kips)	GRLWEAP Capacity		Hammer Type	Comments
				EOD (BPI)	BORI (BPI)				Side	Tip				EOD (Kips)	BOR (Kips)		
151	FL	PSC - 24"sq	NA-NA-36				3						566				(#1), (#2)
152	SC	PSC - 24" oct	81.5-78	2.75	2	0.73	1-b	2	SP-SC	Limestone	Sand	1382	512	472	546.00	VULCAN Vul 320 & 520	
153	DelR, Holland	PSC - 9.7"sq	NA-NA-35.8		2.4		3						68				(#1), (#2)
154	DelR, Holland	PSC - 9.7"sq	NA-NA-60		3.14		3						226				(#1), (#2)
155	DelR, Holland	PSC - 9.7"sq	NA-NA-60		6.35		3						236				(#1), (#2)
156	CA	CEP - 24"	60-56	2.17	1.11	0.51	1-c	3	SP	CL	Mix	766	694	487	370.00	Delmag D 46-32	BOR Hammer - Delmag D 62-22
<b>5 piles from TTI (Texas Transportation Institute) in 1973</b>																	
157	TX	CEP - 16"	67-63.75-68.42	1.33	6	4.50	1-b	1	ML	CH	Clay	105.49	194	95	252.00	LINKBELT LB 520	Report recommended use Davison's at BOR
158	TX	CEP - 16"	7874-79.5	1.5	16.67	11.11	1-b	2	ML	CH	Clay	182	218	102	295.00	LINKBELT LB 520	Report recommended use Davison's at BOR
159	TX	PSC - 16"sq	38-33.7-38	4	7	1.75	1-b	1	SP	SP	Sand	238.72	248	220	315.00	Delmag D 22	Report recommended use Davison's at BOR
160	TX	PSC - 16"sq	20-19.85-21.77	7.08	10	1.41	1-b	2	SP-CL	SP	Mix	120.47	356	286	330.00	LINKBELT LB 520	Report recommended use Davison's at BOR
161	TX	PSC - 16"sq	24-21.1-24.3	3.58	4	1.12	1-b	1	CL	SP	Mix	448.05	230	199.5	226.00	LINKBELT LB 520	Report recommended use Davison's at BOR
<b>25 piles from Prof. Jim Long's FHWA database matched with DFLTDI</b>																	
162	MA	PSC - 14"sq	97-87.4	29	27	0.93	2-b	1	SC-ML	GC	Clay	990	520	622	669.00	ICE 660	
163	ME	HP - 14x117	150.25-135.4	13.6	28	2.06	2-b	1	SP-SC	GW	Sand	2082.34	900	794	906.00	Kobe K 45	
164	AL	OEP - 12.75"	50-48	4	7	1.75	2-b	2	SP	SP	Mix	453.13	270	190.3	262.00	Kobe K 13	
165	AL	OEP - 12.75"	140-86	2.8	3.4	1.21	2-b	2	SP	SP	Mix	1147.64	760	477	510.00	Delmag D 46-13	
166	IA	HP - 14x89	115-93	3.6	9	2.50	1-b	2	SP	SP	Mix	1989.69	509	326	454.00	Kobe K 25	
167	IA	CEP - 14"	80-80	4.2	8	1.90	1-b	2	SP	SM	Mix	1300.21	375	340	416.50	Kobe K 25	
168	OH	HP - 14x89	120-103	30	22	0.73	2-b	3	CL	CL	Mix	887.34	601	757	731.00	Vulcan 512	
169	OH	OEP - 18"	120-104	15	35	2.33	2-b	1	CL	CL	Mix	1684	720	703	787.00	Vulcan 512	
170	OH	HP - 12x53	121-105	4.3	20	4.65	1-b	1	SM	CL	Sand	536.8	315	351	474.00	Vulcan 506	
171	TN	PSC - 14"sq	45-26	12	19	1.58	2-b	1	SM	SC	Sand	62	267	513	738.00	Delmag D 19-32	
172	TX	OEP - 24"	140-133	3.3	210	63.64	2-b	3	SM	CH	Clay	1007	1514	542	986.00	Raymond R 5/0	
173	TX	PSC - 20"sq	101.5-98	4.7	52	11.06	2-b	1	SM	CH	Mix	865	987	708	1294.00	Raymond R 5/0	
174	Annacis, Canada	PSC - 24" oct	96.79-75.6	8.1	9	1.11	2-b	3	SM	SM	Sand	1484.64	400	1300	1380.00	Menck MH 96	
175	SC	PSC - 16"sq	80-79.7	1.2	15	12.50	1-b	2	CL	CL	Mix	480.1	590	320	1123.00	Vulcan 520	
176	FL	PSC - 24"sq	85.55-49.5-54.8	7.9	10	1.27	1-a	1	SP	SP	Sand	2023.04	967	858	1168.00	Vulcan 020	
177	WI	CEP - 12.75"	161-143	30.8	80	2.60	2-b		ML-CL	CL				656		Vulcan 010	
178	WI	CEP - 9.625"	166.17-120	1.2	9.8	8.17	2-b	3	ML-CL	CL	Clay	244.45	580	155	322.50	Vulcan 012	
179	WI	CEP - 9.625"	155.42-142	0.9	20.8	23.11	2-b	3	ML-CL	CL	Mix	726	600	94	329.00	Vulcan 010	
180	PA	HP - 12x74	70-61	100	26	0.26	2-b	3	SM	SP	Sand	412	580	571	524.00	ICE 640	
181	PA	HP - 12x75	34-28	15	28	1.87	2-b	1	SM	SP	Sand	78	305	419	460.00	LINKBELT LB 520	
182	PA	HP - 10x57	35-31.25	15	39	2.60	2-b	3	SM	SP	Sand	75	340	393	344.00	LINKBELT LB 520	
183	PA	HP - 12x74	50-32.75	39	8	0.21	2-b	3	SM	SP	Sand	111	240	463	362.00	LINKBELT LB 520	
184	PA	HP - 10x57	36-33.85	39	7	0.18	2-b	3	SM	SP	Sand	86	310	460	416.00	LINKBELT LB 520	
185	PA	HP - 10x57	50-34.84-35.5	48	26	0.54	2-b	3	GM	SP	Sand	155	367	567	552.00	ICE 640	
186	PA	HP - 12x74	50-35.58	23	35	1.52	2-b	1	GM	SP	Sand	212	480	611	633.00	ICE 640	
<b>11 piles from SC reports sent from Jeffrey Sizemore</b>																	
187	SC	OEP - 54"	90-80	8.5	6	0.71	1-c	3	SW	SM	Sand	5545.8	2950	3184	3352.00	APE 400u	
188	SC	OEP - 54"	90-81	2.83	10	3.53	1-a	3	SW-ML	SM	Sand	1957.67	2460	2890	4406.00	APE 400u	
189	SC	PSC - 24" oct	90-82.5	3.75	2.25	0.60	2-b	4	SP-CL	SP	Sand	2713		614	571.00	Vulcan 520	No load test result known. Relaxation shown at BOR
190	SC	PSC - 24"sq	77-63.5	26.17	3	0.11	2-b	4	SP-CL	SP		1333		1172	473.00	Vulcan 520	No load test result known. Relaxation shown at BOR
191	SC	OEP - 24"	85-80.5				3									VULCAN Vul 512	(#1)
192	Se	PSC - 24" oct	90-79				3									VULCAN Vul 512	(#1)
193	SC	HP - 14x89	80-66	80		0.00	3		SC	MH			950			CONMACO 100E5	(#3)
194	SC	PSC - 16"sq	80-62	1.75	6	3.43	1-a	2	SC	MH	Sand	368.25	560	237	683.00	CONMACO 100E5	
195	SC	OEP - 16"	80-66	80			3		SC	MH			970			CONMACO 100E5	(#3)
196	SC	HP - 14x73	80-66	3.67	23	6.27	1-b	4	SC	MH	Sand	199.47		425	617.00	CONMACO 100E5	No load test result known
197	SC	HP - 14x73	80-66	1	7	7.00	3		SC	MH						CONMACO 100E5	Not analyzed due to being a reaction pile
<b>21 piles from Prof. Jim Long's FHWA data only</b>																	
198	Los Angeles, CA	PSC - 24" oct	95-95	19.8	20	1.01	2-b	4	CL-ML	SM						Delmag D 46-02	No load test result known
199	Boston, MA	HP - 12x74	90.54-90.54	7	24	3.43	3									CONMACO 160	(#1)
200	Kontich, Belgium	HP - 14x142	196.86-196.86	30.7	95.3	3.10	3									Delmag D 36	(#1)

(#1) – Incomplete or missing soil data

(#2) – Incomplete or missing hammer data

(#3) – Incomplete or missing blow count data

Output Rank 4 does not qualify for recalibration

C/S/M – Major soil contribution. Clay, sand, or mix.

All lines in **bold** represent Input Tier 1 & 2

PSU File Number	Location	Pile Type	Pile Length - EOID Embedded Length - BOR Length (ft)	Blowcounts		Set Up Ratio	Input Tier	Output Rank	Predominate Soil Condition		C/S/M	DRIVEN Capacity (Kips)	Davisson's Capacity (Kips)	GRLWEAP Capacity		Hammer Type	Comments	
				EOID (BPI)	BOR (BPI)				Side	Tip				EOID (Kips)	BOR (Kips)			
201	Kontich, Belgium	HP - 14x143	65.62-65.62	3.2			3									Delmag D 36	(#1)	
202	Kontich, Belgium	HP - 14x144	55.78-55.78	2.9	5.3	1.83	3									Delmag D 36	(#1)	
203	Kontich, Belgium	HP - 14x145	65.62-65.62	5.4			3									Delmag D 36	(#1)	
204	China	PSC - 31.5" cyl	59.06-59.06	0.6	3.8	6.33	3									Delmag D 62	(#1)	
205	Duluth, MN	OEP - 9.625"	145.33-145.33	1.5	5	3.33	3									Delmag D 36-32	(#1)	
206	New Orleans, LA	CEP - 12.75"	70-70	0.5	3	6.00	3									Vulcan 06	(#3)	
207	New Orleans, LA	T - 16.5/8.5	70-70	0.5	4	8.00	3									Vulcan 06	(#3)	
208	New Orleans, LA	PSC - 14" sq	70-70	0.7	9	12.86	3									Vulcan 06	(#3)	
209	New Orleans, LA	CEP - 12.75"	70-70	0.5	3	6.00	3									Vulcan 06	(#3)	
210	Jakarta, Indonesia	PSC - 15.75" sq	NA-65.62-47.57	13.5	12.8	0.95	3									IHI 35	(#3)	
211	Mobile, AL	G - 12x0.075	48-48	3.9	5.8	1.49	2-b	4	MH	SP		180				CONMACO 65	G pile classification unknown	
212	Mobile, AL	CEP - 12.75"	65-65	3.7	7.1	1.92	2-b	1	MH	SP	Mix	456	340	189	226.00	CONMACO 65		
213	Mobile, AL	Monotube	60-60	4.5	21	4.67	2-b		MH	SP			240			CONMACO 65	Monotube pile not analyzable	
214	Luling Bridge, LA	PSC - 24" sq	84-84	0.8	4	5.00	3									Delmag D 46-13	(#1)	
215	Luling Bridge, LA	PSC - 30" sq	84-84	1.2	2	1.67	3									Delmag D 46-13	(#1)	
216	Luling Bridge, LA	PSC - 30" sq	84-84	1.9	4.9	2.58	3									Delmag D 46-13	(#1)	
217	Luling Bridge, LA	PSC - 36" cyl	84-84	1.3	2.8	2.15	3									Delmag D 46-13	(#1)	
218	Luling Bridge, LA	PSC - 36" cyl	84-84	3.8	2.7	0.71	3									Delmag D 46-13	(#1)	
<b>8 piles from Development of Resistance Factors for Axial Capacity of Driven Piles in North Carolina (2002) by Kim, Kyung #un</b>																		
219	Martin Bertie, NC	PSC - 20" sq	62-57	3.33			3		SP	SW		400					Kobe K 22	(#3)
220	Carteret, NC	PSC - 24" sq	80-73				3		SP-CL	SP		386					CONMACO 160	(#3)
221	Carteret, NC	PSC - 20" sq	65-41				3		SP-CL	SP		330					CONMACO 160	(#3)
222	Dare, NC	PSC - 30" sq	95-70				3		SW-CL	ML		650					Delmag D 100-13	(#3)
223	Bertie/Chowan, NC	PSC - 30" sq	119-66				3		ML	SW		1860					Raymond R 60x	(#3)
224	Bertie/Chowan, NC	PSC - 20" sq	46-32				3		SW	SP		510					Commco 300	(#3)
225	Sampson, NC	HP - 12x53	55-51				3					320					MKT DE 30B	(#3)
226	Dare, NC	PSC - 20" sq	66-54				3		SM	SM		390					Vulcan 512	(#3)
<b>1 pile from "Static or Dynamic Test - Which to Trust?" by Ede, Robert D. and Fellenius, Bengt H. Geotechnical News, Vol. 8, No. 4, December 1990, p. 28.</b>																		
227	OTTAWA	CEP - 9.625"	NA-62.3	6	18	3.00	2-b	4	CL	SW		502					Delmag D 30-32	(#1)
<b>1 pile from "LRFD: Case Studies for ODOT Bridge Pile Foundations" Jackson, Bethany</b>																		
228	OR	HP - 14x89	96-61-71	5.17	5.58	1.08	2-b	4	MH	SP							Vulcan 010	(#1)
<b>4 piles from "Design and Construction of Driven Pile Foundations: Lessons Learned on the Central Artery/Tunnel Project" FHWA June 2006</b>																		
229	Boston, MA	PSC - 16" sq	NA-142.71	7	11	1.57	2-a	1	ML	CL	Mix	3183.09	876	688	770.00		ICE 1070	
230	Boston, MA	PSC - 16" sq	NA-122	4	5	1.25	2-a	2	ML	CL	Mix	3192.05	1034	550	610.00		ICE 1070	
231	Charlestown, MA	CEP - 12.25"	NA-64	5	7	1.40	2-a	2	GW	GP	Sand	897.74	640	326	360.00		Delmag D 19-42	
232	Charlestown, MA	CEP - 12.25"	NA-74.1	5	8	1.60	2-a	2	GW	GP	Sand	979.46	607	464	516.00		Delmag D 30-32	
<b>2 piles from GRL Report "Determination of Pile Driveability and Capacity from Penetration Tests" Vol. 1.2.3 May 1997 FHWA</b>																		
233	Delaware	PSC - 24" sq	75-66	4.08	10.7	2.62	1-b	1	SM	SM	Sand	1824.3	1150	782	1598.00		Delmag D 46-32	
234	Delaware	PSC - 24" sq	75-72	2.83	10.4	3.67	1-b	1	SM	SM	Sand	1158.89	1300	540	1700.00		Delmag D 46-32	
<b>1 pile from "Static Loading Test on a 45 m Long Pipe Pile in Sandpoint, Idaho" Canadian Geotechnical Journal 2003.</b>																		
235	Sandpoint, ID	CEP - 16"	150.6-148	0.25	2	8.00	2-a	1	SM	CL	Mix	611.3	430	65	360.00		APE D36-32	
<b>5 piles from "Offshore and onshore loading tests for the Ford Island Bridge, Hawaii" Seki, Mimura, and Smith DFI-98, Vienna, 1998</b>																		
236	Pearl Harbor, HA	PSC - 24" oct	95-95	3.17	13	4.10	2-a	1	CH	CH	Clay	969.9	895	303	959.00		HPSI 1000	
237	Pearl Harbor, HA	PSC - 24" oct	106-105	2.5			2-a	4	CH	CH	Clay	1161	900	267			HPSI 1000	(#3). No hammer cushion data
238	Pearl Harbor, HA	PSC - 24" oct	99-98	2.17			2-a	4	CH	CH	Clay	1403	900	241			HPSI 1000	(#3). No hammer cushion data
239	Pearl Harbor, HA	PSC - 16.8" oct	66-65.6	3.75	50	13.33	2-a	3	CH	CH	Clay	515	450	375	892.00		HPSI 1000	
240	Pearl Harbor, HA	PSC - 24" oct	67-65.6	3.17	30	9.46	2-a	1	CH	CH	Clay	683.14	415	320	1132.00		HPSI 1000	
<b>2 piles from "Installation and Loading Tests of Deep Piles in Shanghai Alluvium" Pump, Korista, and Scott DFI-1998, Vienna</b>																		
241	Shanghai, China	OEP - 36"	262-259	3	50	16.67	2-a	2	CL	CH	Sand	13400	3440	1838	2900.00		BSP HA-30	
242	Shanghai, China	OEP - 36"	262-259	3	50	16.67	2-a	2	CL	CH	Sand	13400	3777	1838	2900.00		BSP HA-30	
<b>9 piles from "Measured Pile Setup During Load Testing and Production Piling" Atwood, Holloway, Rollins, Esrig, Sakhi and Hemenway Transportation Research Record 1663 Paper No. 99-1140</b>																		
243	Salt Lake City, UT	CEP - 12.75"	NA-NA-114	0.83	26.66	32.12	2-b		CH	CH		599					Junttan HHK6A	(#1)
244	Salt Lake City, UT	CEP - 12.75"	NA-88	0.33	15.84	48.00	2-b		CH	CH		610					Junttan HHK6A	(#1)
245	Salt Lake City, UT	CEP - 24"	NA-108.5	1.833	33.79	18.43	2-b		CH	CH		842					Junttan HHK6A	(#1)
246	Salt Lake City, UT	CEP - 12.75"	NA-76	1	6.02	6.02	2-b		CH	CH		468					Junttan HHK6A	(#1)
247	Salt Lake City, UT	CEP - 16"	NA-75	6.833	20.52	3.00	2-b		TBD	TBD		880					Junttan HHK6A	(#1)
248	Salt Lake City, UT	CEP - 12.75"	NA-89.25	8.33	62.03	7.45	2-b		TBD	TBD		675					Junttan HHK6A	(#1)
249	Salt Lake City, UT	CEP - 12.75"	NA-91	5.95	18.09	3.04	2-b		TBD	TBD		650					Junttan HHK6A	(#1)
250	Salt Lake City, UT	CEP - 16"	NA-66	4.5	36.65	8.14	2-b		TBD	TBD		700					Junttan HHK6A	(#1)

(#1) – Incomplete or missing soil data

(#2) – Incomplete or missing hammer data

(#3) – Incomplete or missing blow count data

Output Rank 4 does not qualify for recalibration

C/S/M – Major soil contribution. Clay, sand, or mix.

All lines in **bold** represent Input Tier 1 & 2



PSU File Number	Location	Pile Type	Pile Length - EOID Embedded Length - BOR Length (ft)	Blowcounts		Set Up Ratio	Input Tier	Output Rank	Predominate Soil Condition		C/S/M	DRIVEN Capacity (Kips)	Davisson's Capacity (Kips)	GRLWEAP Capacity		Hammer Type	Comments
				EOID (BPI)	BOR (BPI)				Side	Tip				EOID (Kips)	BOR (Kips)		
251	Salt Lake City, UT	CEP-12.75"	NA-35	5.67	8.64	1.52	2-b		TBD	TBD			740			Junntan HHK6A	(#1)
2 piles from Ministry of Transportation, Ontario, Canada																	
252	Ontario, Canada	OEP-12.75"	40-40-41	0.92	1.83	1.99	2-b	4	SW	SW		185	154			Drop 1.81T	Drop hammer used. Not in GRLWEAP library
253	Ontario, Canada	HP-12x53	45-44-45	1.33	2.08	1.56	2-b	4	SW	SW		177.43	155			Drop 1.81T	Drop hammer used. Not in GRLWEAP library
11 piles from "Performance Evaluation of a Large Scale Pile Load Testing Program in Light of Newly Developed LRFD Parameters" Thibodeau and Paikowsky Geo Frontiers 2005 GSP 1310																	
254	New Haven, CT	PSC-14"sq	105-98.5	3.25	42	12.92	2-b	2	SP	MH	Sand	615	490	556	1073.00	HPSI 2000	
255	New Haven, CT	PSC-16"sq	120-114.5	3.75	46	12.27	2-b	2	SP	MH	Sand	1045	600	649	1462.00	HPSI 2000	
256	New Haven, CT	CEP-18"	125.5-119	15.25	12	0.79	2-b	3	SP	MH	Sand	858.5	680	971	907.00	HMC 86	
257	New Haven, CT	Monotube	100-94.5	2	5	2.50	2-b		SP	MH			623			HMC 86	Unknown pile type
258	New Haven, CT	CEP-12.75"	126-120.25	1.75	4	2.29	2-b	1	SP	MH	Sand	422	358	138	209.00	HMC 86	
259	New Haven, CT	CEP-18"	153-141	2.5	2	0.80	2-b	3	SC-CL	SC-CL	Sand	1468	510	589	534.00	HPSI 2000	
260	New Haven, CT	PSC-16"sq	105-100	1.75	2	1.14	2-b	2	SC-CL	SC-CL	Sand	1030	640	424	566.00	HPSI 2000	
261	New Haven, CT	Monotube	100-90-90.8	1	5	5.00	2-b		SC-CL	SC-CL			450			HPSI 2000	Unknown pile type
262	New Haven, CT	CEP-24"	166-156.9	2.5	3	1.20	2-b	3	SC-CL	SC-CL	Sand	2654	828	650	700.00	HPSI 2000	
263	New Haven, CT	PSC-16"sq	120-115	2	3	1.50	2-b	2	SC-CL	SC-CL	Sand	1342	633	480	734.00	HPSI 2000	
264	New Haven, CT	CEP-18"	127-120-121.3	1	4	4.00	2-b	3	SC-CL	SC-CL	Sand	1096	440	290	833.00	HPSI 2000	
7 piles from Jim Long's additional FHWA data not matched to either PDLT200 or DFLTD																	
265	Choctawhatchee, FL	PSC-24"sq	125-87.2	3	11	3.67	2-b	2	ML	SC	Sand	1237	807	776	1953.00	Delmag D 62-12	
266	Orlando, FL	CEP-12.75"	175-NA-NA	10.17			3						784			Delmag 80C	(#1). BOR Hammer - Vulcan 010
267	Cimarron, OK	HP-14x117	113-NA-NA	16.67			3						770			MKT DE-110C	(#1)
268	Socastee, SC	PSC-24"sq	85-NA-NA	19.17	83.3	4.35	3						1095			Vulcan 520	(#1)
269	Unknown	HP-12x53	75-NA-NA	7.5	10	1.33	3						374			ICE 640	(#1)
270	Unknown	HP-12x54	40-NA-NA	10	30	3.00	3						521			ICE 640	(#1)
271	Unknown	HP-12x55	80-NA-NA	12.67	20	1.58	3						378			ICE 640	(#1)
1 pile from "Friction Bearing Design of Steel H-Piles" by James H. Long and Massimo Maniaci IDOT ITRC 1-5-38911 December 28, 2000																	
272	Jacksonville, IL	HP-12x53	NA-34.94-42.65	3	5	1.67	1-a	1	CL	SM	Mix	224	570	218	299.00	Delmag D 19-32	Used reported BOR Davisson's based on chronology
2 piles from "Design and Construction of Driven Pile Foundations: Lessons Learned on the Central Artery/Tunnel Project" FHWA June 2006																	
273	Boston, MA	PSC-16"sq	NA-107.9	7	8	1.14	2-b	3	CL	ML	Clay	738	899	833	989.00	HPSI 2000	
274	Boston, MA	PSC-16"sq	NA-149	16	21	1.31	2-b	1	CL	ML	Clay	1088.9	854	860	911.00	ICE 1070	
1 pile from "Pile Load Test for W.R. Bennett Bridge" by Naesgaard, Uthayakumar, Esroy and Gillespie																	
275	Kelowna, B.C., Canada	CEP-24"	170-144.7-146	13	19	1.46	2-b	4	ML	ML	Mix	2655	786		1104.00	Delmag D 62	EOID utilized 3855 kg drop hammer, not in library.
1 pile from "Axial and Lateral Load Performance of Two Composite Piles and One Prestressed Concrete Pile" by Miguel Pando, George Filz, Carl Ealy and Edward Hoppe Transportation Research Record 1849 Paper No. 03-2912																	
276	Hampton, VA	PSC-24"	591-55				3		SW-ML	CH			696			ICE 80S	(#3)
6 piles from "On the Prediction of Long Term Pile Capacity from End-of-Driving Information" by Frank Rausche, Brent Robinson, and Garland Likins ASCE GSP 125 2004																	
277	LA	OEP-24"	109.9-53.15	2.17	9	4.15	3						302			Delmag D 46-32	(#1)
278	LA	PSC-24"sq	67.9-39	1.67	16	9.58	3						720			Delmag D 46-32	(#1)
279	LA	PSC-16"sq	77-32.5	0.75	8.33	11.11	3						224			ICE 60S	(#1)
280	LA	PSC-16"sq	55.1-36.1	0.583	16.67	28.59	3						216			ICE 60S	(#1)
281	LA	PSC-14"sq	59-43.3	0.83	5	6.02	3						224			ICE 60S	(#1)
282	LA	PSC-16"sq	70-23	15.8	67	4.24	3						595			ICE 60S	(#1)
3 piles from Florida Deep Foundations Database																	
283	Appalachicola Bay, FL	PSC-18"sq	68.2-64	4.17	12.5	3.00	2-b	2	CL	CH	Clay	179.3	400	360	719.00	CONMACO 115	
284	Appalachicola Bay, FL	PSC-24"sq	69-64.6	5.42	12.92	2.38	2-b	2	SC	CL	Sand	539.4	860	811	1504.00	Vulcan 020	
285	Dodge Island, FL	PSC-30"sq	110-39.8	11	20	1.82	2-b	4	SM	Sandstone		1118.2	1260		Conmaco 300	Sandstone properties required	
1 pile from "Correlation of CAPWAP with instrumented static load test on a steel H pile" Paraiso, S.C., Costa, C.M.C., and Alexio, L. The application of stress-wave theory to piles: science, technology and practice, pg 637																	
286	Sao Paulo, Brazil	HP-12x93	183-177.16-178.13	5			3		CH	CH						Free Fall Hammer	(#2), (#3)
2 piles from "Dynamic Pile Monitoring and Pile Load Tests in Unconsolidated Sands and Gravels, Wyoming" Schulte, Michael P. Proceedings of the 37th Annual Highway Geology Symposium, Helena, Montana, August 20-22 1986.																	
287	North Platte River, WY	HP-12x53	NA-70-72	13.17	12.75	0.97	2-b	3	SW	SW	Sand	283.6	280	392	387.00	Mitsubishi MH 15	
288	North Platte River, WY	HP-14x73	NA-85-86	13.75	15	1.09	2-b	2	SW	SW	Sand	677.3	430	491	504.00	Mitsubishi MH 15	
1 pile from "Comparison Between Static and Dynamic Pile Capacity. A Case Study From Norway" Tsetel, J., Torum, E., Rønning, S., Alstad, M., Vik, A., Schram Simonsen, A.																	
289	Elkem Mosjøen, Norway	PSC-14"sq	128.6-125.7	1.5	11.5	7.67	2-b	4	SP	SP	Sand		742			Banutt Superram rig	Hammer not in GRLWEAP library
1 pile from "Load Testing of a Closed-Ended Pipe Pile Driven in Multilayered Soil" Kim, Daehyeon; Bica, Adriano Virgilio Damiani; Salgado, Rodrigo; Prezzi, Monica; Lee, Wonje Journal of Geotechnical and Geoenvironmental Engineering April 2009 pp 463-473																	
290	Jasper County, IN	CEP-14"	NA-57.1	4.23	12.7	3.00	3		OH	ML			309			ICE 42 S	(#2). SLT performed on adjacent pile. Length of pile unknown
1 pile from Louisiana DOT for Highland Road Job #06-CS-HC-0026 Pile TP-1, Station 57+03.56																	
291	Baton Rouge, LA	PSC-24"sq	45-40.5-41.17	4.7	3	0.64	2-a	3	CL	CH	Clay	484.7	460			PILECO D36-32	(#2)
2 piles from "Load Capacity of Pipe Piles in Cohesive Ground" Dyaljee, Vishnu; Parifi, Murthy. Deep Foundations 2002 pp 1318-1334.																	
292	Alberta, Canada	CEP-12.75"	NA-66.44	4	2.5	0.63	3						207			Hera 1500	(#1), (#2), (#3)
293	Alberta, Canada	CEP-12.75"	53.4	4	2	0.50	3						187			Hera 1500	(#1), (#2), (#3)

(#1) – Incomplete or missing soil data

(#2) – Incomplete or missing hammer data

(#3) – Incomplete or missing blow count data

Output Rank 4 does not qualify for recalibration

C/S/M – Major soil contribution. Clay, sand, or mix.

All lines in **bold** represent Input Tier 1 & 2

PSU Pile Number	Location	Pile Type	Pile Length - EOID Embedded Length - BOR Length (ft)	Blowcounts		Set Up Ratio	Input Tier	Output Rank	Predominate Soil Condition		C/S/M	DRIVEN Capacity (Kips)	Davisson's Capacity (Kips)	GRLWEAP Capacity		Hammer Type	Comments
				EOID (BPI)	BOR1 (BPI)				Side	Tip				EOID (Kips)	BOR (Kips)		
<b>5 piles from Michigan DOT</b>																	
294	MI	HP - 12x53	61-53.4	7	9	1.29	1-b	1	CH	CH	Clay	279	418	184	201.00	Vulcan 50C	
295	MI	HP - 12x54	60-53.2	6	13	2.17	1-b	1	CH	CH	Clay	279	418	174	222.00	Vulcan 50C	
296	MI	HP - 12x55	61-53	4	7	1.75	1-b	1	CH	CH	Clay	279	418	131	181.00	McKiernan-Terry DE-30	
297	MI	CEP - 12"	80-65.4	3.5	5	1.43	1-b		CH	CH			775			Delmag D 12	???
298	MI	OEP - 12"	72.75-56.4-NA	3	4	1.33	1-b		CH	CH			100				(#2)
<b>24 piles from Rollins Brown's M.S. Thesis, Appendix B, 2006.</b>																	
299	Oakland, CA	CEP - 24"	78.5-70.7				3		SP-CL	ML			1000			Delmag D 46-32	(#3)
300	Oakland, CA	CEP - 24"	64-53				3		CH	CL			756			Delmag D 46-32	(#3)
301	Oakland, CA	CEP - 24"	75.4-66.5				3		CH	CL			668			Delmag D 46-32	(#3)
302	Oakland, CA	OEP - 40"	85.4-73.3				3		SP	CL			1176			Delmag D 62-22	(#3)
303	Oakland, CA	OEP - 40"	98-83				3		CH	CH			1225			HPSI 2005	(#3)
304	Oakland, CA	OEP - 40"	105-91				3		ML-SP	GP-CL			1031			HPSI 2005	(#3)
305	Oakland, CA	OEP - 40"	101-86				3		CL-GP	CL			710			HPSI 2005	(#3)
306	Oakland, CA	CEP - 24"	64-60				3		CL-SP	CL-SP			998			Delmag D 30-32	(#3)
307	Oakland, CA	CEP - 24"	45-40				3		CL-SP	CL			1000			HPSI 2005	(#3). BOR hammer - Delmag D62-22
308	Oakland, CA	OEP - 24"	64-60				3		CL-GP	CL			401			Delmag D 46-32	(#3). BOR hammer - Delmag D 436-32 & D 62-22
309	Oakland, CA	CEP - 24"	33.3-28.3				3		SM	SP-SM			552			Delmag D 62-22	(#3)
310	Los Angeles, CA	PSC - 14"sq	43-40				3		CL	SC			363			Delmag D 36-32	(#3)
311	Oakland, CA	OEP - 24"	43-43				3		SP	CH			568			MKT 11B3	(#3)
312	San Diego, CA	PSC - 14"sq	34-34				3		SP	CH			252			Delmag D 36-32	(#3)
313	San Diego, CA	PSC - 14"sq	24-24				3		SP	CH			228			Delmag D 36-32	(#3)
314	San Diego, CA	PSC - 14"sq	17-17				3		SP	CH			251			Delmag D 36-32	(#3)
315	San Jose, CA	CEP - 14"	55-49				3		SP	CH			340			Vulcan 80 C	(#3)
316	Castroville, CA	OEP - 72"	114-114				3		SP	CH			1513			Delmag D80-23	(#3)
317	San Francisco, CA	OEP - 24"	64.5-47.5				3		SP	CH			1007			Menck MHF5-10	(#3)
318	San Francisco, CA	OEP - 24"	70.5-51.5				3		SP	CH			999			Menck MHF5-10	(#3)
319	San Francisco, CA	OEP - 16"	66.5-52.5				3		SP	CH			954			Menck MHF5-10	(#3)
320	San Francisco, CA	OEP - 24"	70-53				3		SP	CH			997			Menck MHF5-10	(#3)
321	San Francisco, CA	OEP - 24"	100-79				3		SP	CH			209			Menck MHF5-10	(#3)
322	San Francisco, CA	OEP - 24"	74-49				3		SP	CH			901			Menck MHF5-10	(#3)

- (#1) – Incomplete or missing soil data  
 (#2) – Incomplete or missing hammer data  
 (#3) – Incomplete or missing blow count data

Output Rank 4 does not qualify for recalibration  
 C/S/M – Major soil contribution. Clay, sand, or mix.  
 All lines in **bold** represent Input Tier 1 & 2



**APPENDIX B:**

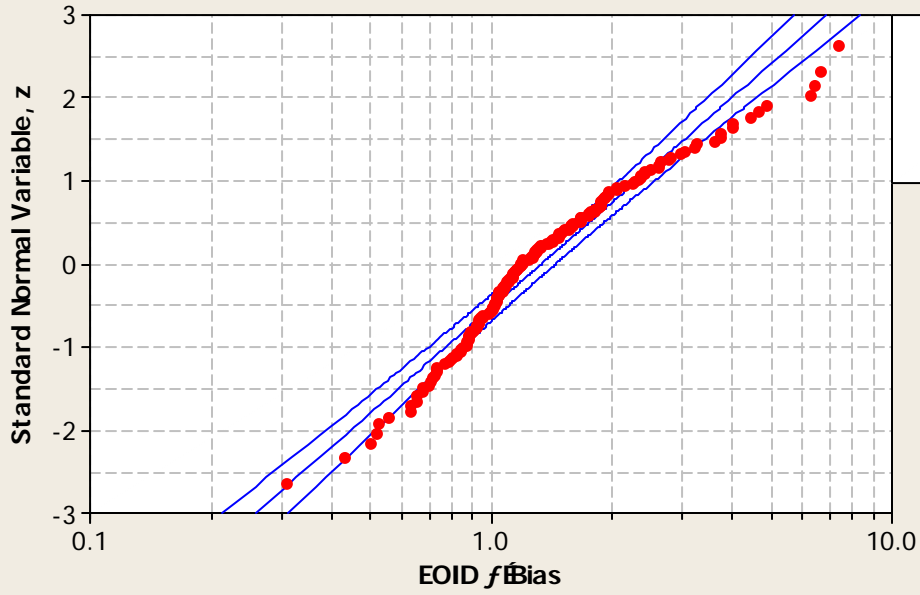
**LOGNORMAL DISTRIBUTION EOID/BOR STATISTICAL  
CHECKS FOR SCENARIO A, F, G, AND I (BOR)**



### Lognormal Probability Plot for EOID $f_{Bias}$

Scenario A

95% Confidence Interval

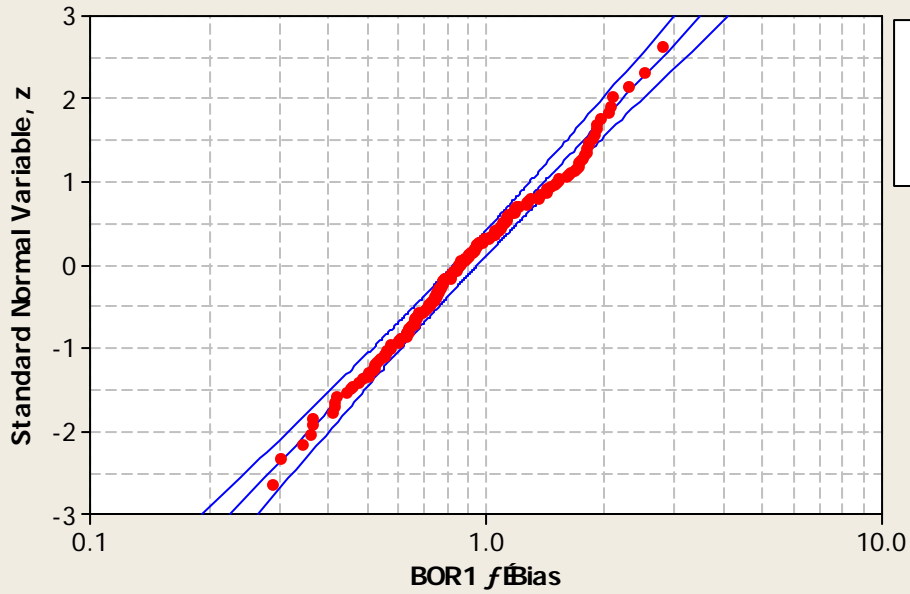


Loc	0.2884
Scale	0.5469
N	172
AD	2.298
P-Value	<0.005

### Lognormal Probability Plot for BOR1 $f_{Bias}$

Scenario A

95% Confidence Interval

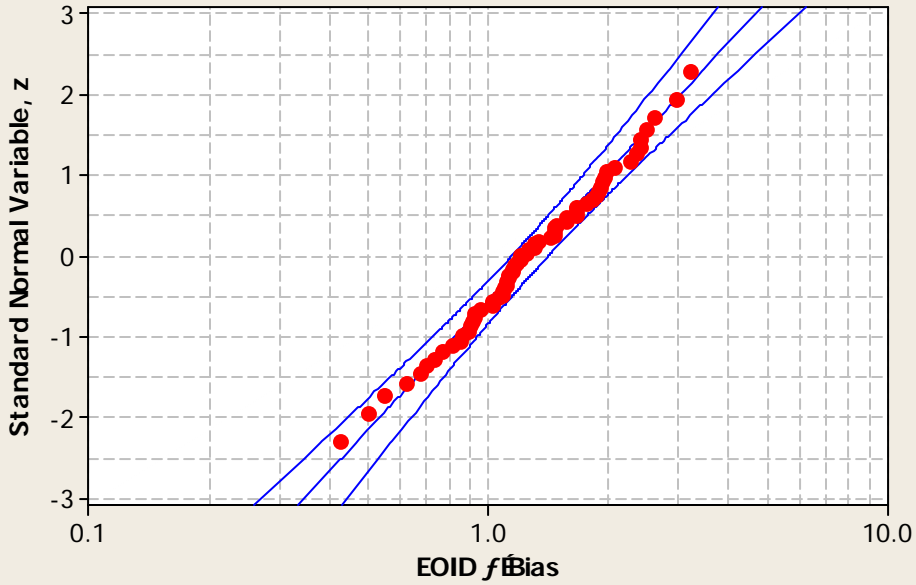


Loc	-0.1130
Scale	0.4570
N	172
AD	0.548
P-Value	0.156

### Lognormal Probability Plot for EOID $f\bar{E}$

Scenario F

95% Confidence Interva

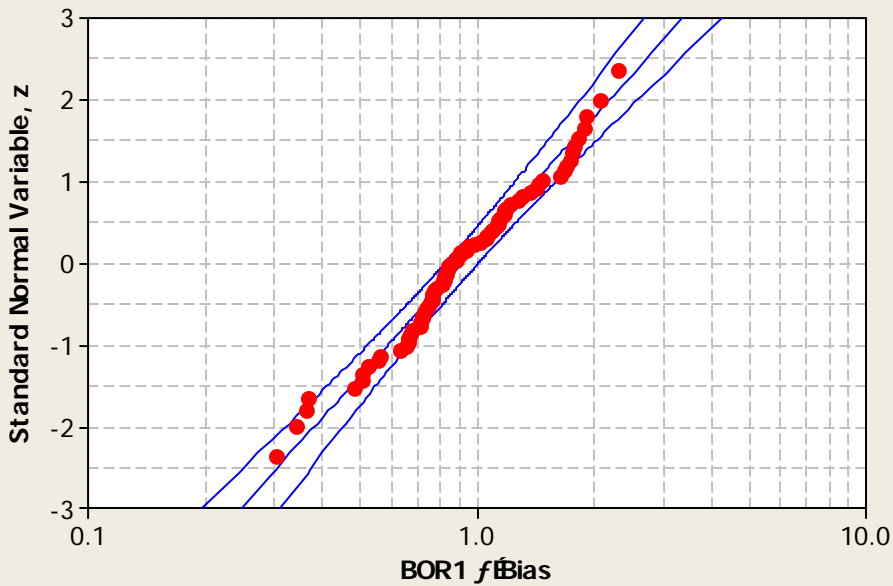


Loc	0.2418
Scale	0.4324
N	65
AD	0.193
P-Value	0.890

### Lognormal Probability Plot for BOR1 $f\bar{E}$

Scenario F

95% Confidence Interva

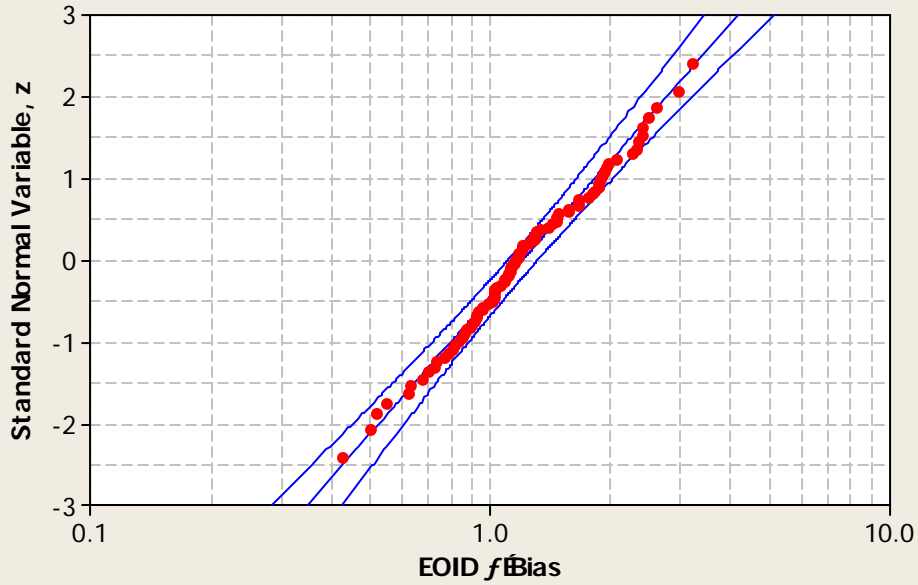


Loc	-0.08930
Scale	0.4357
N	75
AD	0.507
P-Value	0.195

### Lognormal Probability Plot for EOID $f_{\text{Bias}}$

Scenario G

95% Confidence Interval

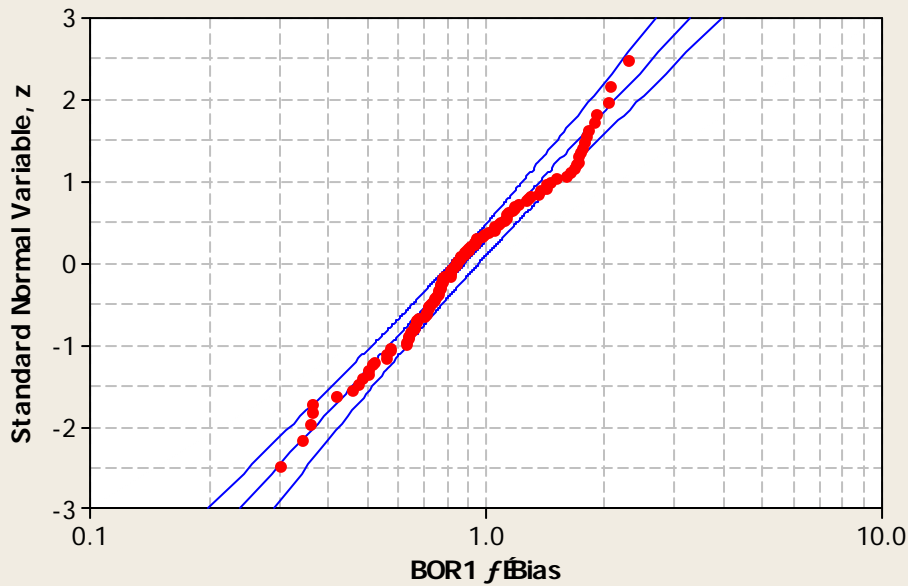


Loc	0.1890
Scale	0.4140
N	90
AD	0.388
P-Value	0.380

### Lognormal Probability Plot for BOR1 $f_{\text{Bias}}$

Scenario G

95% Confidence Interval



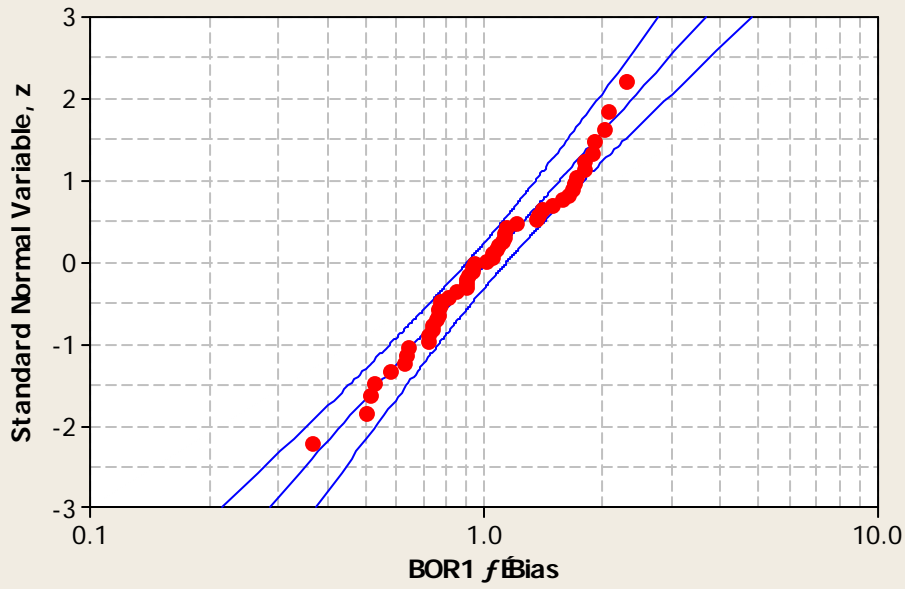
Loc	-0.1163
Scale	0.4362
N	110
AD	0.670
P-Value	0.078



### Lognormal Probability Plot for BOR1 $f_{Bias}$

Scenario I

95% Confidence Interval

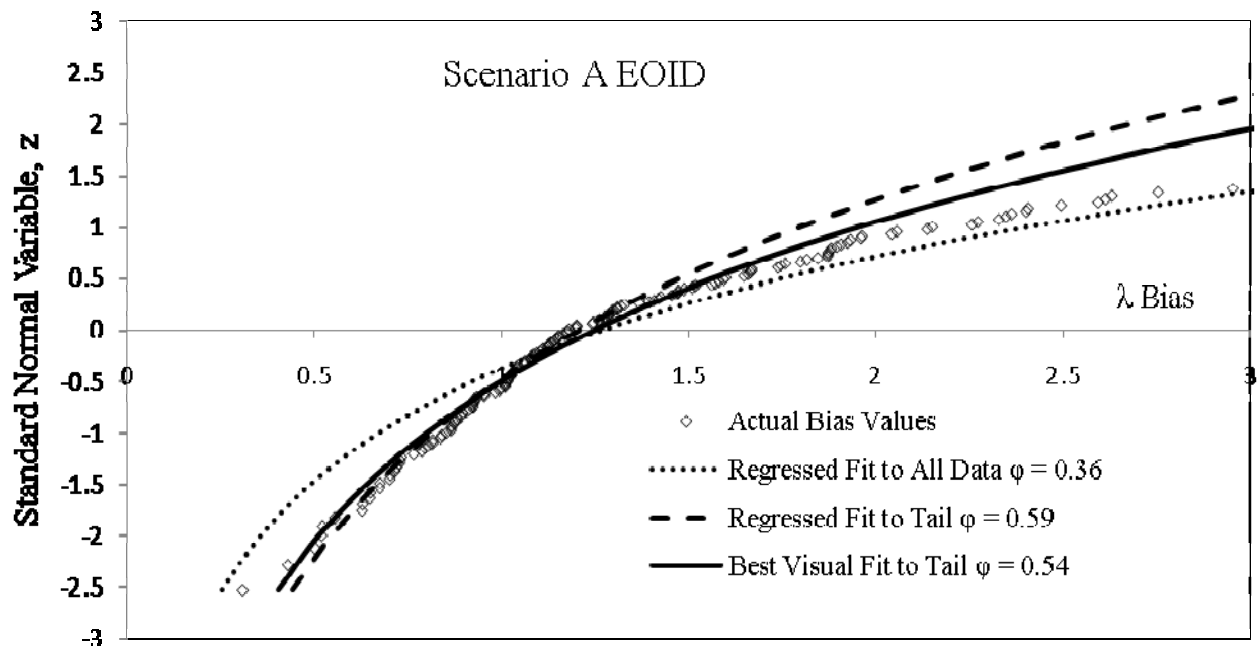
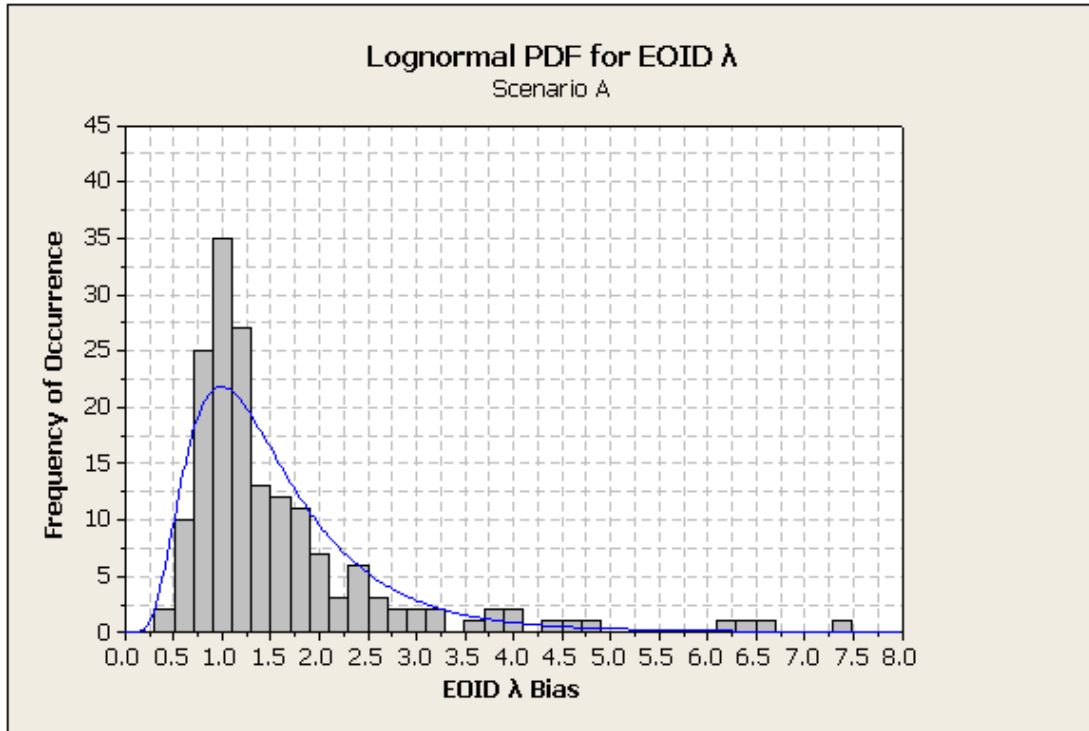


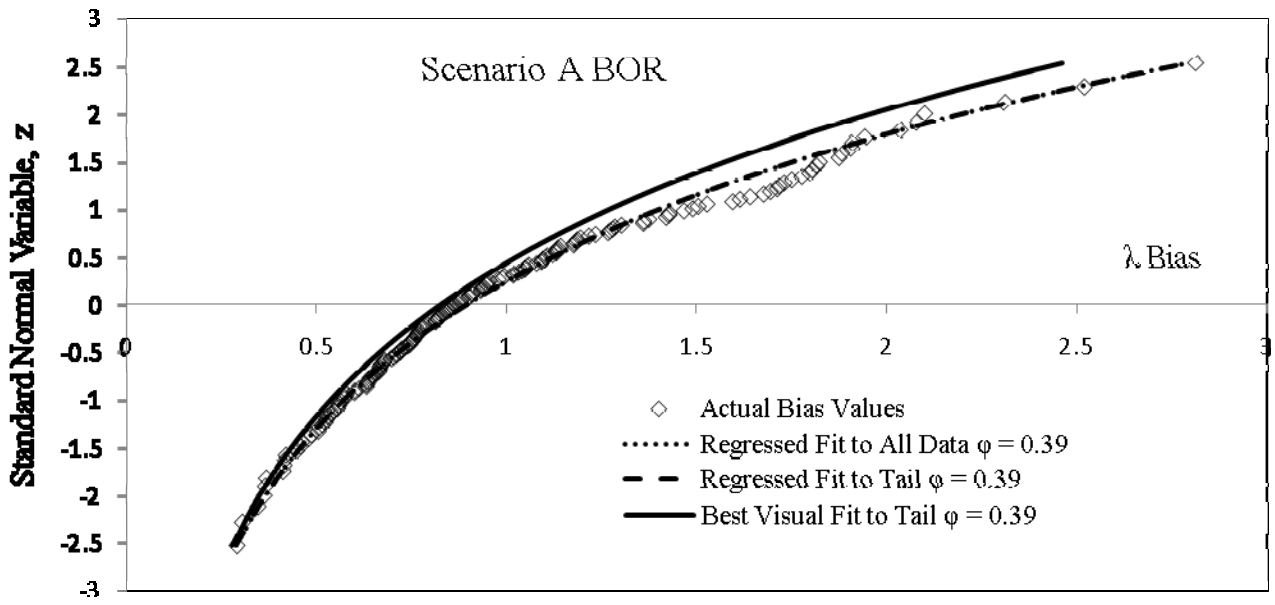
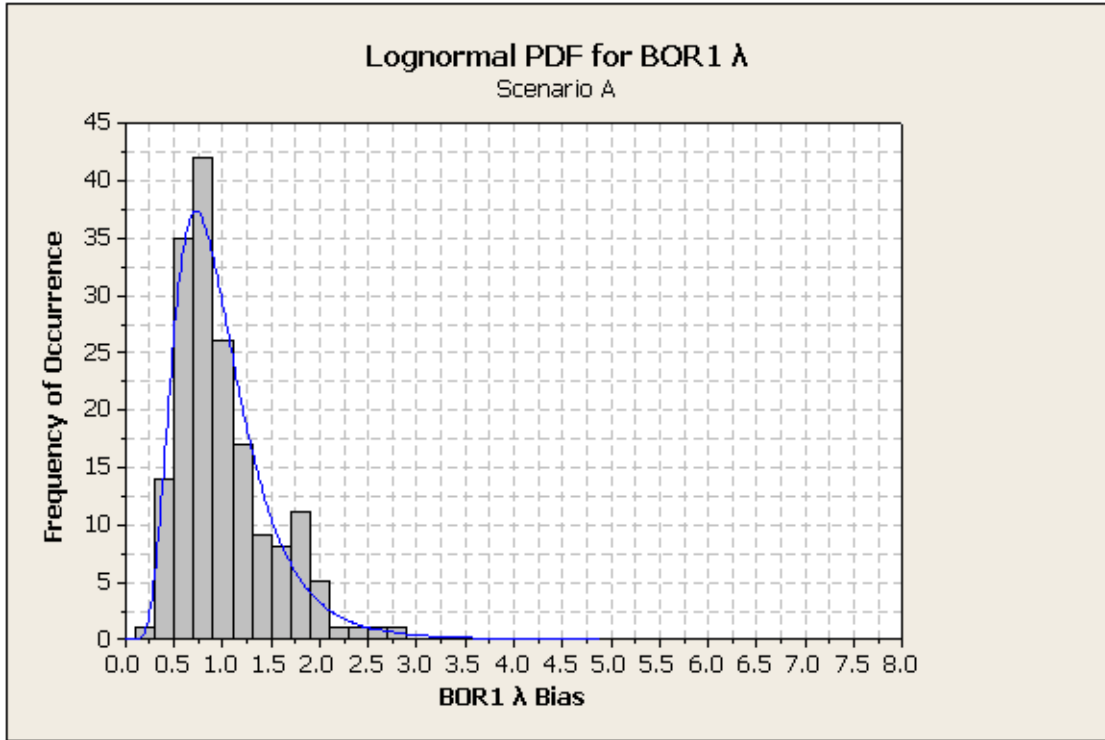
Loc	0.02450
Scale	0.4255
N	52
AD	0.399
P-Value	0.353

**APPENDIX C:**

**SCENARIO A STATISTICAL EOID/BOR PDF AND CDF PLOTS**



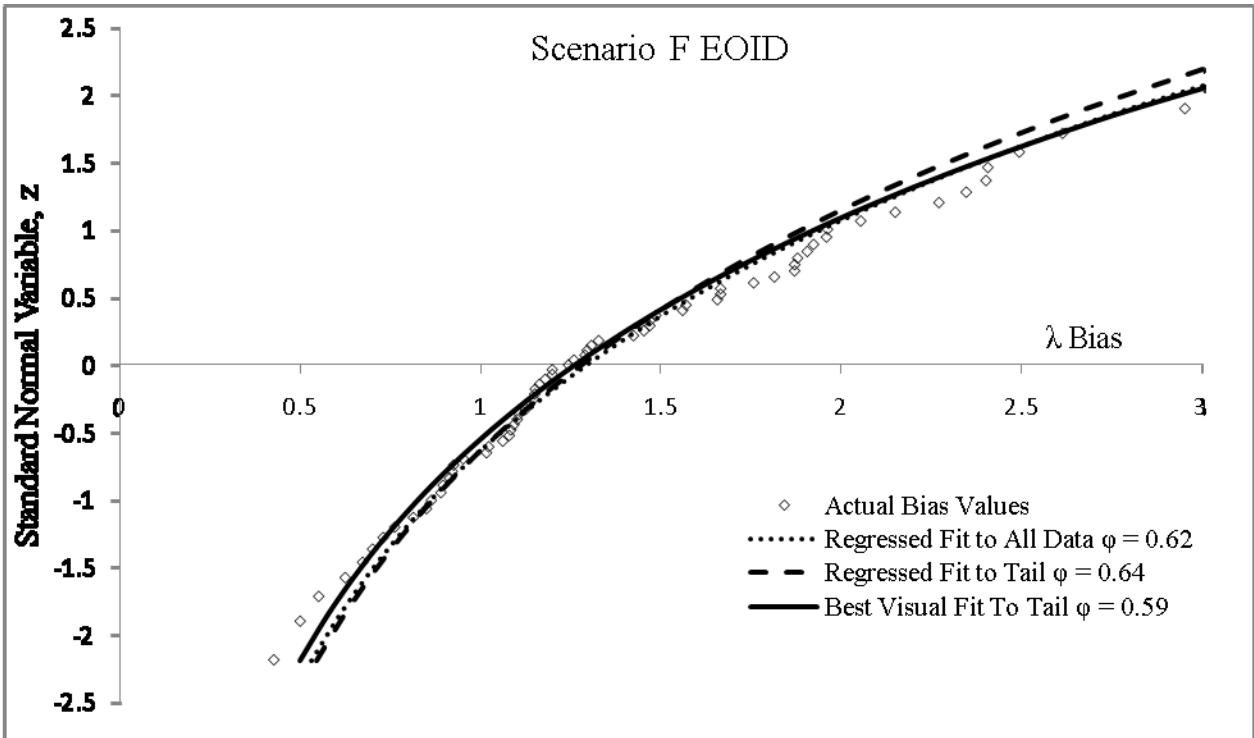
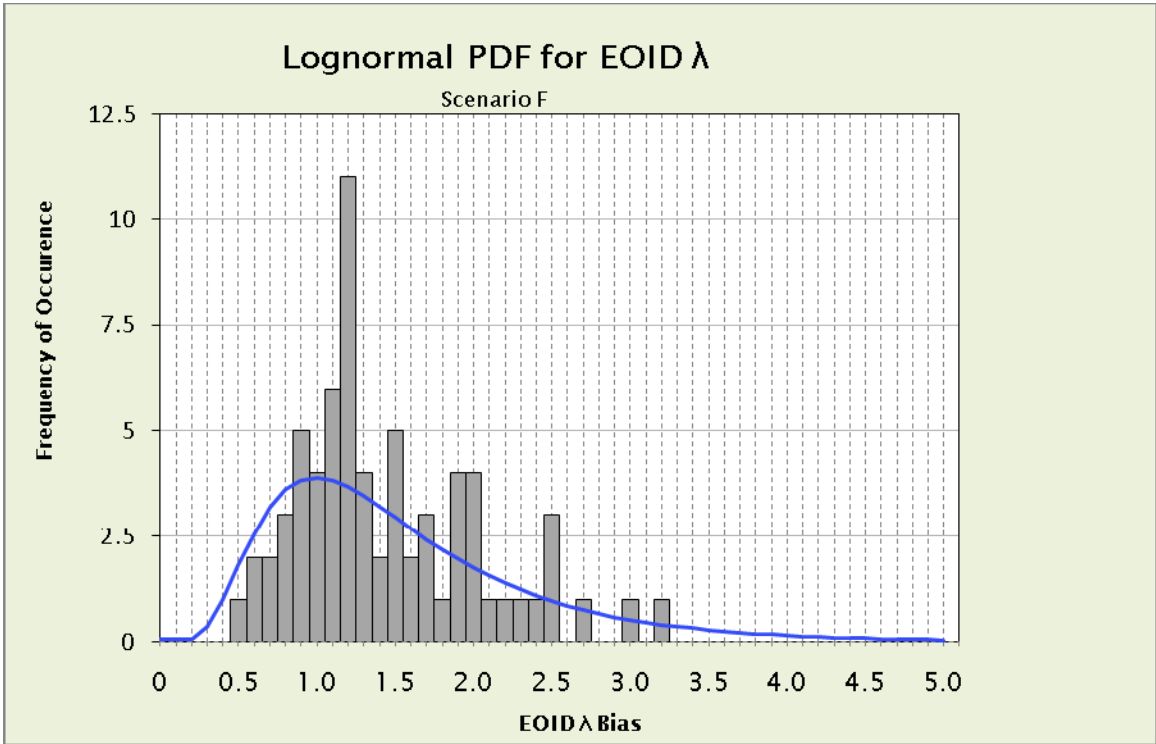




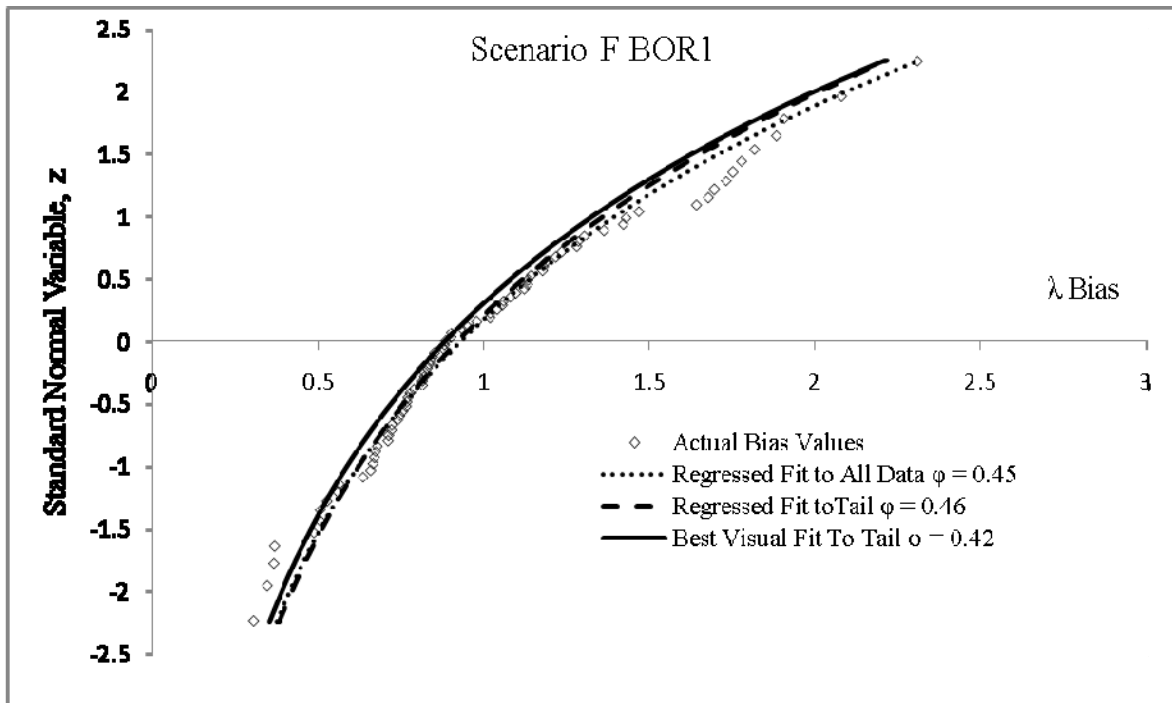
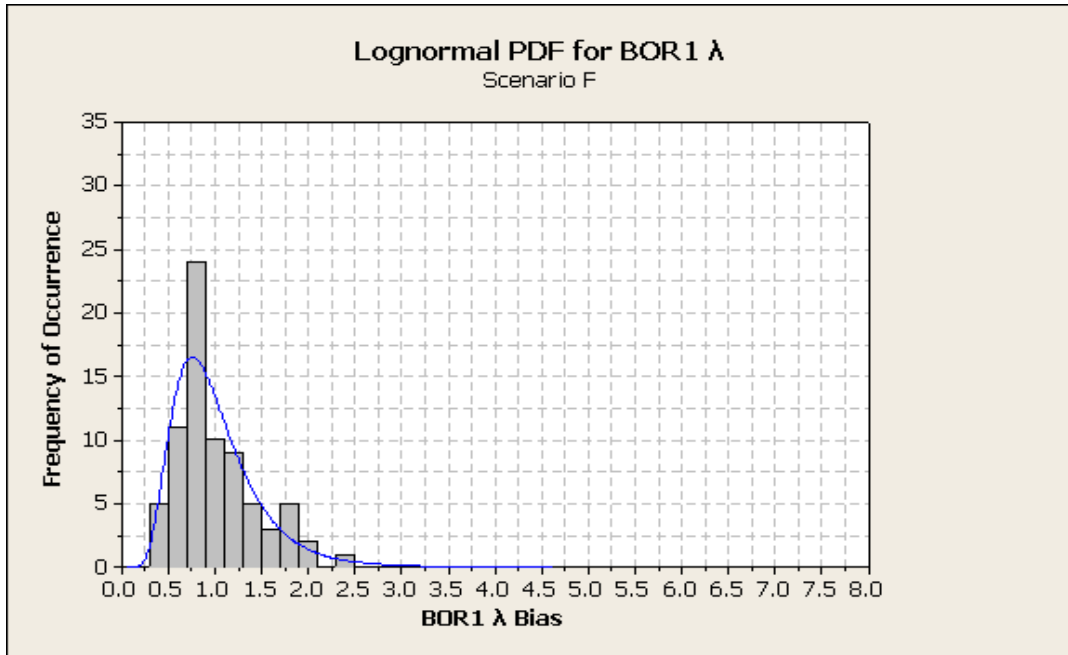
**APPENDIX D:**

**SCENARIO F STATISTICAL EOID/BOR PDF AND CDF PLOTS**





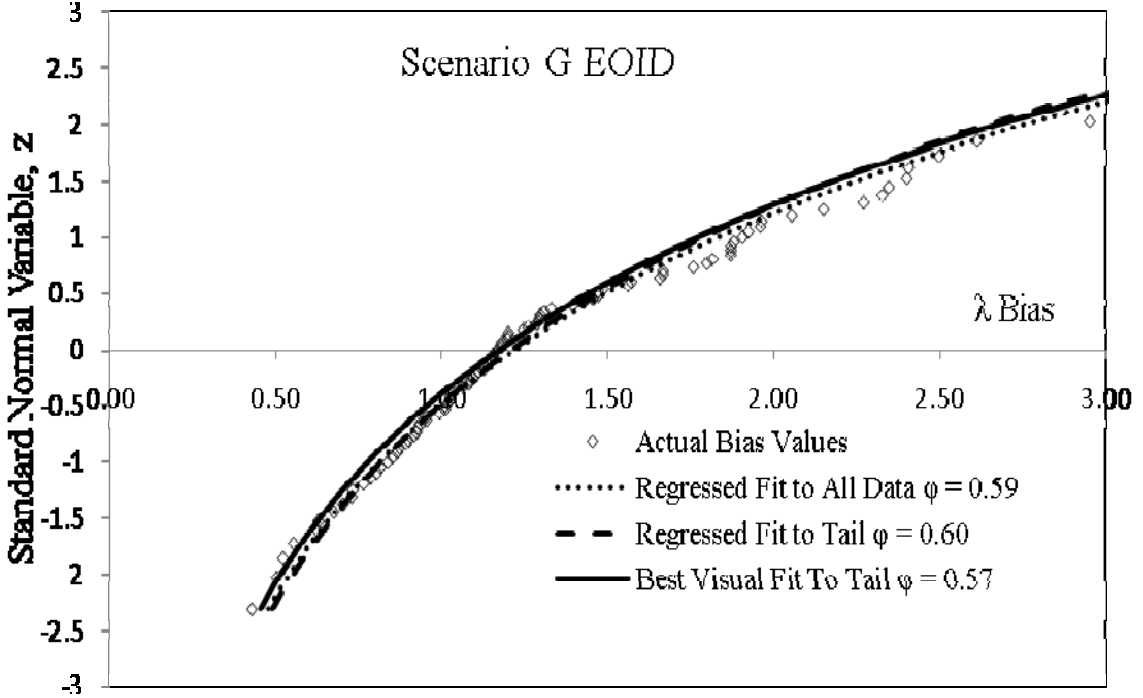
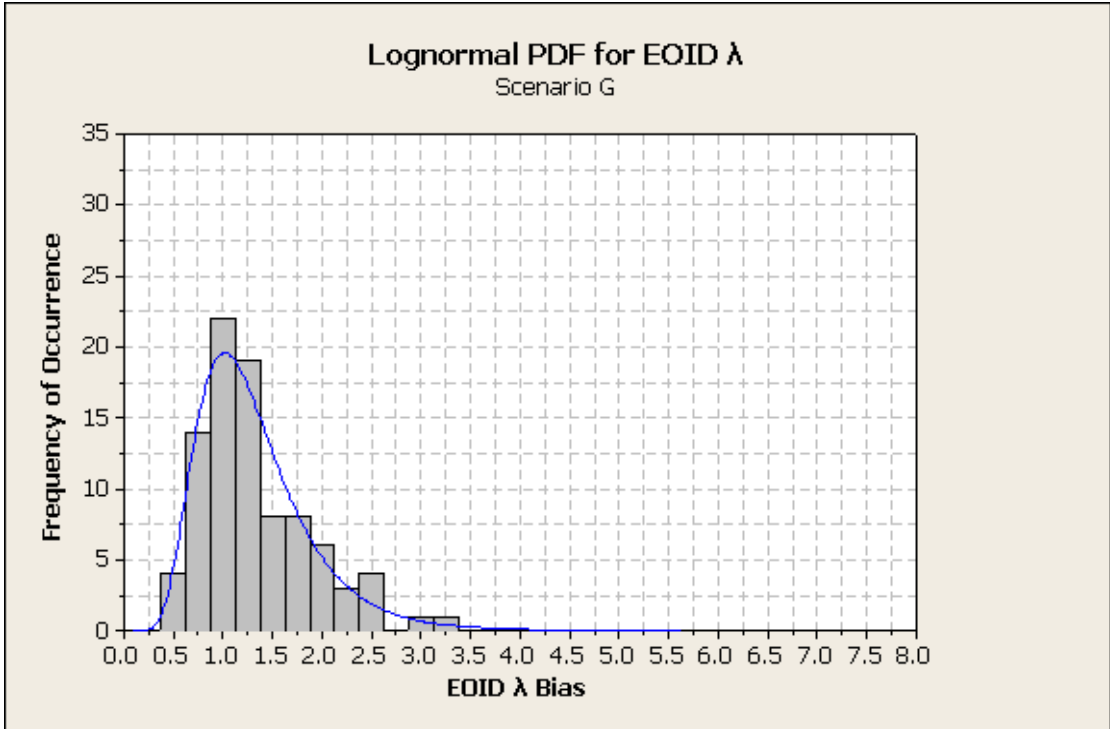


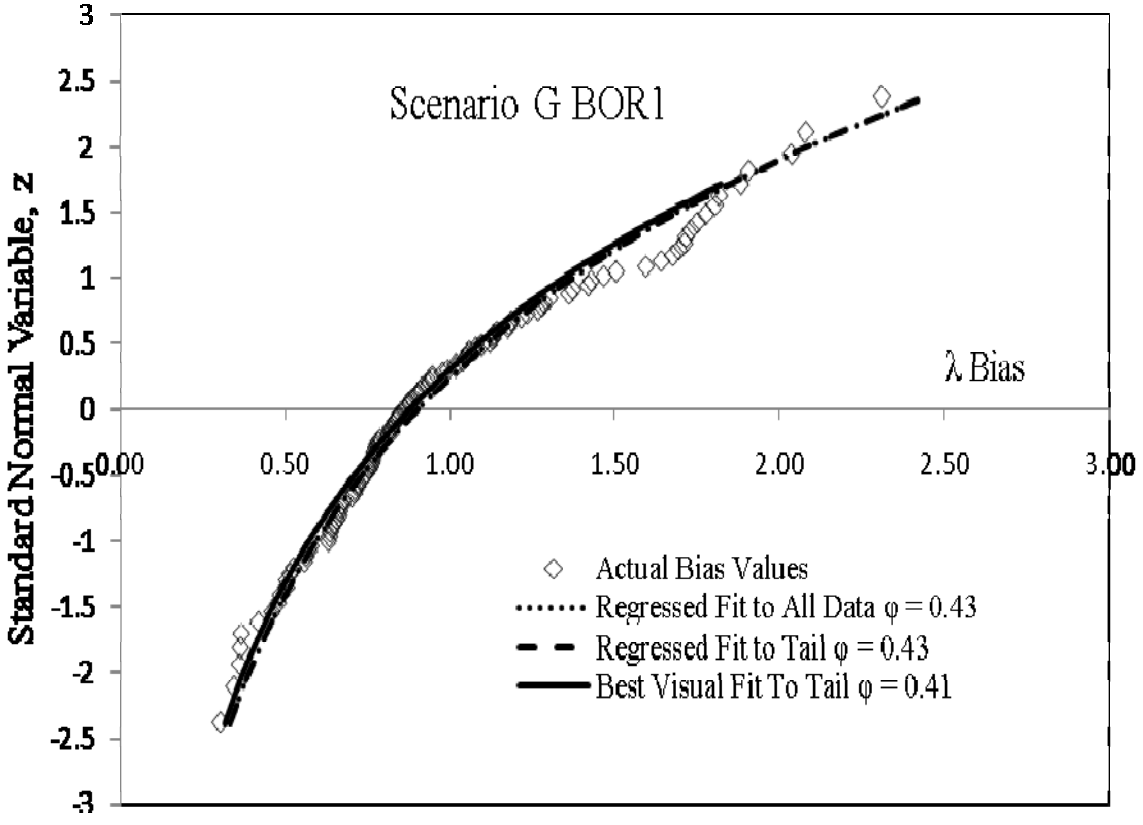
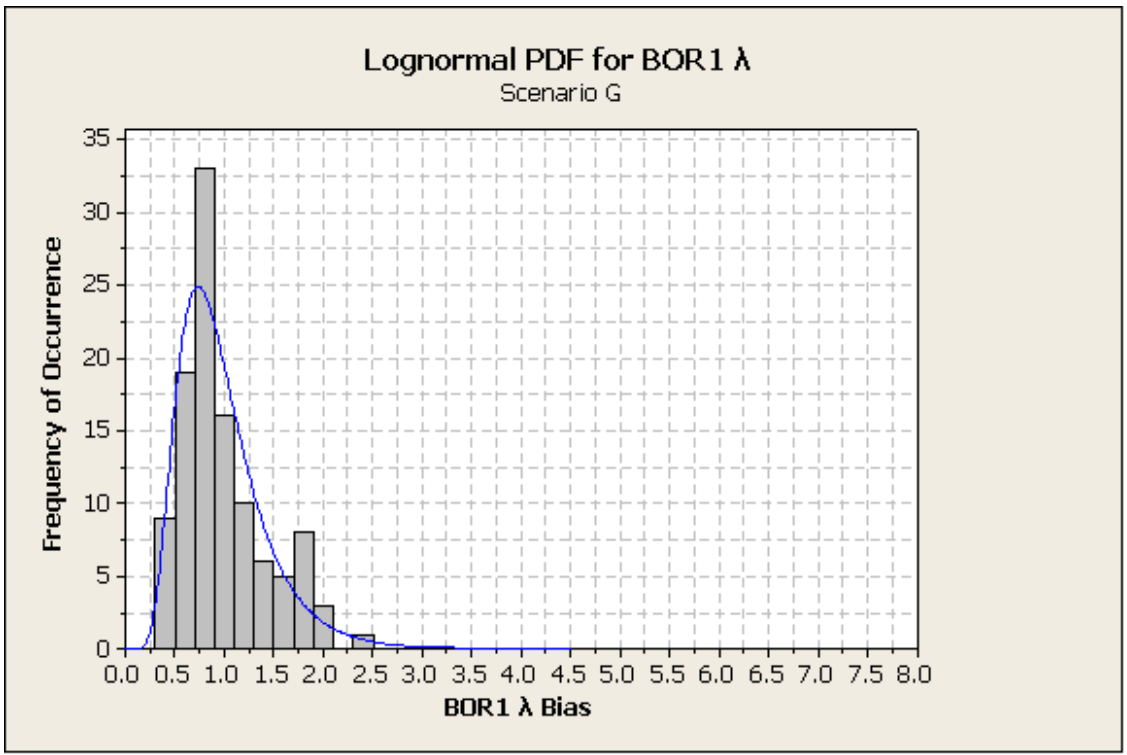


**APPENDIX E:**

**SCENARIO G STATISTICAL EOID/BOR PDF AND CDF PLOTS**







**APPENDIX F:**

**SCENARIO I STATISTICAL EOID/BOR PDF AND CDF PLOTS**



